



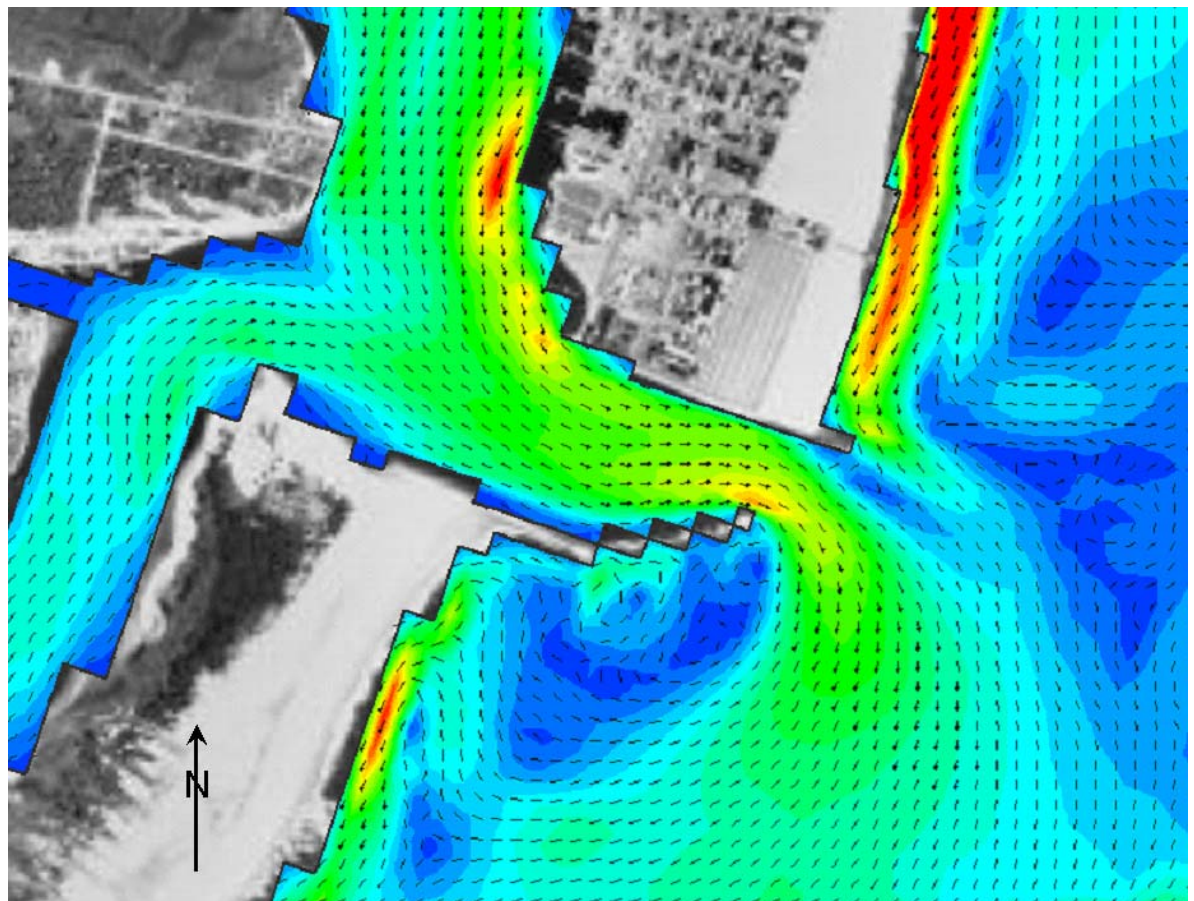
**US Army Corps  
of Engineers®**  
Engineer Research and  
Development Center

*Coastal Inlets Research Program*

## **Two-Dimensional Depth-Averaged Circulation Model M2D: Version 2.0, Report 1, Technical Documentation and User's Guide**

Adele Militello, Christopher W. Reed,  
Alan K. Zundel, and Nicholas C. Kraus

May 2004



# Two-Dimensional Depth-Averaged Circulation Model M2D: Version 2.0, Report 1, Technical Documentation and User's Guide

Adele Militello

*Coastal Analysis LLC  
Eureka, CA 95503*

Christopher W. Reed

*URS Corporation  
Tallahassee, FL 32303*

Alan K. Zundel

*Environmental Modeling Research Laboratory  
Brigham Young University  
Provo, UT 84602*

Nicholas C. Kraus

*Coastal and Hydraulics Laboratory  
U.S. Army Engineer Research and Development Center  
3909 Halls Ferry Road  
Vicksburg, MS 39180-6199*

Final report

Approved for public release; distribution is unlimited

**ABSTRACT:** The two-dimensional (2-D) circulation model M2D, developed under the Coastal Inlets Research Program conducted at the U.S. Army Engineer Research and Development Center, Coastal and Hydraulics Laboratory, has been designed for local applications, primarily at inlets, the nearshore, and bays. M2D is computationally efficient, easy to set up, and has features required for many coastal engineering applications including robust flooding and drying, wind-speed dependent (time-varying) wind-drag coefficient, variably-spaced bottom-friction coefficient, time- and space-varying wave-stress forcing, efficient grid storage in memory, two hot-start options, and the convenience, through control statements, of independently turning on or off the advective terms and mixing terms. If wave information is available, such as through coupling with the STeady state spectral WAVE model STWAVE, M2D will calculate wave friction and wave mixing. M2D can be coupled to regional circulation models through boundary conditions providing flexibility for large-scale applications and connectivity between models.

A graphical interface for M2D has been implemented within the Surface-Water Modeling System (SMS) Versions 8.1 and higher. Features of the M2D interface are grid development, control file specification, model runs, post-processing of results, and visualization. M2D can be driven by larger-domain circulation models, such as ADCIRC, through boundary specification capabilities contained within the SMS. The Steering Module in SMS provides an automated means of coupling of M2D with STWAVE, which is convenient for projects that require wave-stress forcing for M2D as well as wave friction and mixing owing to breaking waves. The Steering Module allows the user to choose from seven possible coupling combinations, providing flexibility in conducting simulations of wave-driven currents and wave-current interaction.

**DISCLAIMER:** The contents of this report are not to be used for advertising, publication, or promotional purposes. Citation of trade names does not constitute an official endorsement or approval of the use of such commercial products. All product names and trademarks cited are the property of their respective owners. The findings of this report are not to be construed as an official Department of the Army position unless so designated by other authorized documents.

**DESTROY THIS REPORT WHEN IT IS NO LONGER NEEDED. DO NOT RETURN TO ORIGINATOR.**

# Contents

---

Preface.....	viii
1—Introduction to M2D.....	1
Scope of Model .....	2
Implementation within Surface-Water Modeling System .....	2
Studies with M2D.....	3
Report Contents.....	4
2—Governing Equations.....	5
3—Numerical Implementation of Governing Equations.....	13
Rectilinear Grid .....	13
Momentum Equations .....	14
x-momentum equation.....	15
y-momentum equation.....	17
Bottom-friction coefficient.....	20
Wind stress .....	23
Eddy viscosity coefficient.....	24
Wave stress scaling for shallow water.....	26
Continuity Equation .....	26
Cell Numbering.....	27
Courant Condition .....	29
4—Boundary Conditions.....	30
Water Level Forcing Boundary Conditions .....	30
Tidal-constituent forcing .....	31
Time series water level forcing .....	31
Time Series Water Level and Velocity Forcing Boundary Condition .....	32
Time Series Flow Rate Forcing Boundary Condition .....	32
Closed, Reflective Boundary Condition.....	33
Wave-Adjusted Water Level and Velocity Forcing .....	33

5—Model Features .....	36
Flooding and Drying .....	36
Hot-Start Capabilities .....	38
Model Spin-Up: Ramp Function .....	38
Coupling with Larger-Domain Model.....	38
Coupling with STWAVE .....	40
Output Options .....	43
Observation cell time series.....	43
Global field output.....	44
6—Surface-Water Modeling System Interface for M2D .....	45
Required Information .....	45
Grid Generation from M2D Coverage .....	46
Grid frame creation and editing.....	47
Grid generation.....	48
Cartesian Grid Module .....	50
M2D Menu .....	52
Delete Simulation.....	52
Assign BC .....	52
Delete BC .....	54
Assign Cell Attributes .....	54
Merge Cells .....	55
Model Check .....	55
Model Control .....	56
Run M2D.....	58
Steering Module .....	58
7—Model Setup and File Structure .....	61
Input Files.....	61
Grid file .....	61
Model control .....	63
Initial conditions.....	66
Water level forcing data files .....	66
Velocity forcing data files .....	68
Flow rate forcing data files.....	69
Wind speed and direction.....	70
Tidal constituents .....	70
Wave stresses .....	70
Selected cell output specification file.....	71
Global output time specification files.....	71
Output Files .....	71
Time series at station locations.....	72
Global output time specification files.....	72
References .....	73

Appendix A: Example Input and Output Files .....	A1
Appendix B: M2D Citations.....	B1
Appendix C: Slosh Tests .....	C1
Appendix D: Wind Setup Tests.....	D1
Appendix E: Advection Test .....	E1
Appendix F: Wetting and Drying Tests.....	F1
Test 1: Channel with Sloping Bottom .....	F1
Test 2: Depression in Square Grid.....	F3
Appendix G: Wave-Adjusted Boundary Condition Test.....	G1
Appendix H: Surf Zone Verification Tests .....	H1

SF 298

## List of Figures

---

Figure 1.	Comparison of longshore current speed values for Visser Case 4 .....	11
Figure 2.	Cell and variable definitions for M2D .....	14
Figure 3.	Control volume definition for $x$ -momentum equation .....	15
Figure 4.	Control volume definition for $y$ -momentum equation .....	18
Figure 5.	Bottom-friction coefficient adjustment versus total water depth .....	23
Figure 6.	Control volume definition for continuity equation .....	27
Figure 7.	Cell numbering system .....	28
Figure 8.	M2D grid and ADCIRC mesh for Shinnecock Inlet, NY .....	39
Figure 9.	Time discretization of a sinusoidal water level curve .....	40
Figure 10.	Example M2D and STWAVE grid orientations .....	41
Figure 11.	Example M2D and STWAVE grid spacing .....	42
Figure 12.	Grid frame around scattered data points .....	46
Figure 13.	<i>Map-&gt; 2D Grid and Refine Point</i> dialogs .....	48
Figure 14.	SMS generated grid .....	49
Figure 15.	Arc options for generating coastlines .....	50
Figure 16.	<i>M2D Boundary Conditions</i> dialog .....	53
Figure 17.	<i>Assign Cell Attributes</i> dialog .....	55
Figure 18.	<i>M2D Model Control</i> dialog .....	56
Figure 19.	<i>Steering Module</i> dialog .....	60

## List of Tables

---

Table 1.	Boundary Condition Types .....	30
Table 2.	Criteria for Flooding and Drying Algorithms.....	36
Table 3.	Definitions of Parameters in Grid File .....	62
Table 4.	Cell Types and their Function in M2D.....	63
Table 5.	Model Control File Specifications .....	64

# Preface

---

Development of the tidal and nearshore circulation model M2D was conducted as part of activities of the Coastal Inlets Research Program (CIRP), Inlet Modeling System (IMS) work unit. CIRP is administered at the U.S. Army Engineer Research and Development Center (ERDC), Coastal and Hydraulics Laboratory (CHL) under the Navigation Systems Program for Headquarters, U.S. Army Corps of Engineers (HQUSACE). Mr. Barry W. Holliday is HQUSACE lead technical monitor for CIRP. Dr. Sandra K. Knight, CHL, is Technical Director for the Navigation Systems Program. Dr. Nicholas C. Kraus, Senior Scientists Group, CHL, is CIRP Program Manager, and Ms. Mary A. Cialone, Coastal Processes Branch, CHL, is IMS work unit Principal Investigator.

The mission of CIRP is to conduct applied research to improve USACE capability to manage federally maintained inlets, which exist on all coasts of the United States (including the Atlantic Ocean, Gulf of Mexico, Pacific Ocean, and Great Lakes regions). CIRP objectives are to (a) make management of channels – the design, maintenance, and operation – more effective to reduce the cost of dredging, and (b) preserve the adjacent beaches in a systems approach that treats the inlet and beach together. To achieve these objectives, CIRP is organized in work units conducting research and development in hydrodynamic, sediment transport, and morphology change modeling; navigation channels and adjacent beaches; inlet scour and jetties; laboratory and field investigations; and technology transfer.

This report was prepared by Dr. Adele Militello, Coastal Analysis LLC, Dr. Christopher W. Reed, URS Corporation, Dr. Alan K. Zundel, Environmental Modeling Research Laboratory, Brigham Young University, and Dr. Nicholas C. Kraus, CHL. Dr. Militello was Principal Investigator for M2D model development. Dr. Frank Buonaiuto, State University of New York at Stony Brook, Marine Sciences Research Institute, contributed to model development and testing for wave radiation-stress implementation. Work was performed under the general administrative supervision of Mr. Thomas W. Richardson, Director, CHL, and Dr. William D. Martin, Deputy Director, CHL

At the time of publication of this report, Dr. James R. Houston was Director of ERDC, and COL James R. Rowan, EN, was Commander and Executive Director.

# 1 Introduction to M2D

---

At coastal inlets, water and sediment undergo complex motions by forcing at many temporal and spatial scales, and with constraints imposed by the sea bottom morphology, jetties, training structures, and dredging. Forcing can involve combinations of the astronomical and meteorological tide, waves, wind, and rivers. Interactions also occur among waves, currents, sediment, and the bottom morphology, which also changes through time. Advances in numerical modeling, increased speed of desktop computers, and reliable and powerful interfaces now make calculation of morphology change at inlets feasible. Simulation of morphology change at inlets is an emerging area of applied research of interest to the U.S. Army Corps of Engineers (USACE) and its navigation mission at coastal inlets.

Because of the wide range of problems to be addressed, both basic and applied, success in simulation of coastal inlet processes is expected to be an outcome of exchange of information among interdisciplinary teams. These teams are composed of coastal engineers and scientists working in government, private industry, and academia. A system approach is required that is based on a comprehensive numerical model with a code accessible to a wide range of researchers. At the same time, the model should be efficient in calculation so that it may be exercised in addressing practical problems. Experience with a variety of coastal inlets and engineering problems will, in turn, call for improvements and advances in model development.

The model M2D was developed under the Coastal Inlets Research Program (CIRP) conducted at the U.S. Army Engineer Research and Development Center (ERDC), Coastal and Hydraulics Laboratory (CHL) as one such simulation model with which to support multidisciplinary research teams and conduct practical projects at coastal inlets. M2D is a hydrodynamic model intended for local applications, primarily at inlets, the nearshore, and bays. M2D is computationally efficient, easy to set up, and has features required for many coastal engineering applications. M2D can be coupled to regional circulation models, such as the ADvanced CIRCulation (ADCIRC) model (Luettich et al. 1992), through boundary conditions (Militello and Zundel 2002a, 2002b), providing flexibility for large-scale applications and connectivity between models. At the same time, the code is accessible to CIRP researchers with expertise in areas other than computational fluid dynamics, as expected in interdisciplinary teams.

## Scope of Model

M2D is a finite-difference numerical representation of the two-dimensional (2-D) depth-integrated continuity and momentum equations of water motion. The governing equations, finite-difference approximation, representation of bottom and surface stresses, grid scheme, boundary conditions, other model features, and graphical interface are documented in this report. Cells are defined on a staggered, rectilinear grid and can have constant or variable side lengths. Momentum equations are solved in a time-stepping manner first, followed by solution of the continuity equation, in which the updated velocities calculated by the momentum equations are applied.

For support of engineering applications, features of the model M2D include flooding and drying, wind-speed dependent (time-varying) wind-drag coefficient, variably-spaced bottom-friction coefficient, time-and space-varying wave-stress forcing, efficient grid storage in memory, two hot-start options, and the convenience, through control statements, of independently turning on or off the advective terms, mixing terms, and flooding and drying calculations. Additionally, model output is written in formats convenient for importing into commercially available plotting packages. For researchers, the code is readily understandable for implementation of supplemental algorithms for the wave-current interaction, and for calculating sediment transport and morphology change.

M2D has been designed as a local-scale model that can be easily and quickly applied to engineering projects. The model has been developed to maximize flexibility in grid specifications and model forcing. For example, if forcing by a water surface elevation time series is prescribed as a boundary condition, the time interval between values in the time series does not have to be constant. Thus, if values were being supplied from a water level gauge and the sampling rate was modified, the measurements could be prescribed as forcing without subsampling the data set.

## Implementation within Surface-Water Modeling System

A graphical interface for M2D has been implemented within the Surface-Water Modeling System (SMS) Versions 8.1 and higher (Zundel 2000). Features of the M2D interface are grid development, control file specification, model runs, post-processing of results, and visualization. SMS provides flexibility in grid generation and modification by providing tools to assign bathymetric data sets for interpolation to the M2D grid, manually modify depths and friction coefficients, adjust cell sizes, and insert or delete cells. Variably spaced grids can be easily developed by applying tools that spatially scale the cell sizes over user-defined extents. SMS provides dialogs for specification of boundary conditions. For some boundary types, forcing information can be input manually from within SMS, or predefined information can be read in from files. A model

control dialog provides the user with a convenient interface for specifying timing control, model options, wind and wave forcing, and output options.

M2D can be driven by larger-domain circulation models, such as ADCIRC, through boundary specification capabilities contained within the SMS. The boundary conditions dialog provides access to solutions from larger-domain models that can be extracted and mapped to M2D boundaries. The user can decide whether to specify water surface elevation or a combination of water surface elevation and velocity as boundary forcing for M2D. This capability provides M2D with boundary conditions that preserve tidal phase and other variations calculated by the larger-scale model.

SMS also provides an automated means of coupling of M2D with the STeady state spectral WAVE model STWAVE (Smith et al. 1999, 2001) through the Steering Module, which is convenient for projects that require wave-stress forcing for M2D. The Steering Module allows the user to choose from seven possible coupling combinations, providing flexibility in conducting simulations of wave-driven currents and wave-current interaction.

## **Studies with M2D**

M2D was developed and tested in basic and applied studies covering a wide range of bathymetric configurations, forcing, and project goals. Summaries of selected applications are provided to familiarize users with model capabilities and to establish model history.

M2D was first applied to investigate hydrodynamic responses to proposed engineering projects on the Texas coast. Changes in circulation patterns in the Upper Laguna Madre and exchange of water with the Gulf of Mexico were calculated for proposed causeway modifications designed to improve evacuation safety (Brown et al. 1995a, 1995b, 1995c). In an investigation of a proposed new inlet called the Southwest Corner Cut that would connect East Matagorda Bay to the Colorado River Navigation Channel (CRNC), M2D was applied to calculate velocity changes in the CRNC and Gulf Intracoastal Waterway and to determine whether the new inlet would promote closure of Mitchell's Cut (Kraus and Militello 1996; Militello and Kraus 1998; Kraus and Militello 1999).

In a scientific study of the hydrodynamics of Baffin Bay, TX, M2D was applied to calculate the wind-driven circulation and setup/setdown in the non-tidal bay (Militello 1998, 2000). Model calculations also determined the contributions of nonlinear terms in the governing equations to harmonics of the oscillatory wind (sea breeze) forcing in Baffin Bay (Militello 1998; Militello and Kraus 2001).

In a channel infilling study for Bay Center, WA, M2D calculated current velocity over a 1-month time interval from which bed elevation changes were computed (Militello 2002; Militello et al. 2002). The Bay Center application also demonstrated successful coupling of M2D with ADCIRC. This success,

combined with CIRP goals, led to the development of the automated M2D and ADCIRC (or other larger-domain model) coupling capability within the SMS (Militello and Zundel 2002a; Militello and Zundel 2002b).

As part of the CIRP program to assure model reliability, M2D calculated tide and wave-driven currents at an idealized inlet and ebb shoal for fair weather and storm waves (Militello and Kraus 2003). Interactions between wave-driven currents and the ebb jet varied, depending on the relative strength of the two current sources. For storm waves, calculated alongshore velocities were stronger and the surf zone was wider and further from shore, as compared to the fair weather waves. This study demonstrated coupling of M2D and STWAVE, formally described in this volume and Militello and Zundel (2003), and correct trends in sediment transport and morphology change that are presently under testing in M2D.

## Report Contents

This report provides documentation for M2D and instruction on development of an M2D project within the SMS. Description of the model consists of hydrodynamics only; sediment transport and morphology change are under development and will be described in future M2D technical reports. Chapter 2 gives the governing equations solved in the model. Chapter 3 describes the finite-difference approximations and defines the cell numbering method. Chapter 4 describes the types of boundary conditions available in M2D. Chapter 5 provides descriptions of model features. Chapter 6 describes the SMS interface for M2D and provides guidance for project development. Chapter 7 provides information on model setup and file structure.

Appendices supplement the main text and contain more detailed and auxiliary information. Appendix A gives example input and output files. Appendix B provides references for M2D development and applications. Appendices C through F describe results of numerical model integrity tests. Appendix G demonstrates the wave-adjusted boundary condition, which modifies prescribed boundary condition values for the presence of wave forcing. Appendix H compares calculated and measured longshore currents from laboratory experiments.

## 2 Governing Equations

---

M2D solves the 2-D, depth-integrated continuity and momentum equations by applying a flux-based finite-difference method. Velocity components in two horizontal dimensions are calculated. This chapter introduces the governing equations and describes the respective terms and variables. Wind and bottom stress formulations are presented, as well as implementation of wave stresses.

The 2-D, depth-integrated continuity and momentum equations solved by M2D are

$$\frac{\partial(h+\eta)}{\partial t} + \frac{\partial q_x}{\partial x} + \frac{\partial q_y}{\partial y} = 0 \quad (1)$$

$$\begin{aligned} \frac{\partial q_x}{\partial t} + \frac{\partial u q_x}{\partial x} + \frac{\partial v q_x}{\partial y} + \frac{1}{2} g \frac{\partial(h+\eta)^2}{\partial x} = \frac{\partial}{\partial x} D^x \frac{\partial q_x}{\partial x} + \frac{\partial}{\partial y} D^y \frac{\partial q_x}{\partial y} \\ + f q_y - \tau_{bx} + \tau_{wx} + \tau_{sx} \end{aligned} \quad (2)$$

$$\begin{aligned} \frac{\partial q_y}{\partial t} + \frac{\partial u q_y}{\partial x} + \frac{\partial v q_y}{\partial y} + \frac{1}{2} g \frac{\partial(h+\eta)^2}{\partial y} = \frac{\partial}{\partial x} D^x \frac{\partial q_y}{\partial x} + \frac{\partial}{\partial y} D^y \frac{\partial q_y}{\partial y} \\ - f q_x - \tau_{by} + \tau_{wy} + \tau_{sy} \end{aligned} \quad (3)$$

where

$h$  = still-water depth

$\eta$  = deviation of the water-surface elevation from the still-water level

$t$  = time

$q_x$  = flow per unit width parallel to the x-axis

$q_y$  = flow per unit width parallel to the y-axis

$u$  = depth-averaged current velocity parallel to the x-axis

$v$  = depth-averaged current velocity parallel to the y-axis

$g$  = acceleration due to gravity

$D_x$  = diffusion coefficient for the x direction

$D_y$  = diffusion coefficient for the y direction

$f$  = Coriolis parameter

$\tau_{bx}$  = bottom stress parallel to the x-axis

$\tau_{by}$  = bottom stress parallel to the y-axis

$\tau_{wx}$  = surface stress parallel to the x-axis

$\tau_{wy}$  = surface stress parallel to the y-axis

$\tau_{sx}$  = wave stress parallel to the x-axis

$\tau_{sy}$  = wave stress parallel to the y-axis

Component velocities are related to the flow rate per unit width as

$$u = \frac{q_x}{h + \eta} \quad (4)$$

$$v = \frac{q_y}{h + \eta} \quad (5)$$

For the situation without waves, bottom stresses are given by

$$\tau_{bx} = C_b u |U| \quad (6)$$

$$\tau_{by} = C_b v |U| \quad (7)$$

where  $U$  is the total current speed and  $C_b$  is an empirical bottom-stress coefficient. The total current speed is

$$|U| = \sqrt{u^2 + v^2} \quad (8)$$

and the bottom-friction coefficient is calculated by

$$C_b = \frac{g}{C^2} \quad (9)$$

where  $C$  is the Chezy coefficient given by

$$C = \frac{R^{1/6}}{n} \quad (10)$$

in which  $R$  is the hydraulic radius, and  $n$  is the Manning roughness coefficient.

In the presence of waves, the bottom stress contains contributions from both the quasi-steady current (as from tide, wind, and surface waves) and the bottom orbital motion of the waves. Assessment of an average bottom stress over the period of a surface wave, which requires numerical integration, would need to be performed at every grid point at every time-step, a computation-intensive operation. Instead, here a square wave approximation for the wave is applied, which allows analytic estimation of the time average. It is given by the following approximation for the time-averaged bottom stress under combined currents and waves (Nishimura 1988)

$$\tau_{bx} = C_b \left\{ \left( U_{wc} + \frac{\omega_b^2}{U_{wc}} \cos^2 \alpha \right) u + \left( \frac{\omega_b^2}{U_{wc}} \cos \alpha \sin \alpha \right) v \right\} \quad (11)$$

$$\tau_{by} = C_b \left\{ \left( \frac{\omega_b^2}{U_{wc}} \cos \alpha \sin \alpha \right) u + \left( U_{wc} + \frac{\omega_b^2}{U_{wc}} \sin^2 \alpha \right) v \right\} \quad (12)$$

in which  $\alpha$  is the wave angle relative to the x-axis, and  $U_{wc}$  and  $\omega_b$  are given by

$$U_{wc} = \frac{1}{2} \left\{ \sqrt{u^2 + v^2 + \omega_b^2 + 2(u \cos \alpha + v \sin \alpha) \omega_b} + \sqrt{u^2 + v^2 + \omega_b^2 - 2(u \cos \alpha + v \sin \alpha) \omega_b} \right\} \quad (13)$$

$$\omega_b = \frac{\sigma H}{\pi \sinh[k(h + \eta)]} \quad (14)$$

where  $\sigma$  is the wave angular frequency,  $H$  is wave height, and  $k$  is wave number.

Surface wind stresses are given by

$$\tau_{wx} = C_d \frac{\rho_a}{\rho_w} W^2 \sin(\theta) \quad (15)$$

$$\tau_{wy} = C_d \frac{\rho_a}{\rho_w} W^2 \cos(\theta) \quad (16)$$

where

$C_d$  = wind drag coefficient

$\rho_a$  = density of air

$\rho_w$  = density of water

$W$  = wind speed

$\theta$  = wind direction

The convention for wind direction is specified to be 0 deg for wind from the east with angle increasing counterclockwise.

Wave stresses are calculated from spatial gradients in radiation stresses as

$$\tau_{Sx} = -\frac{1}{\rho_w} \left( \frac{\partial S_{xx}}{\partial x} + \frac{\partial S_{xy}}{\partial y} \right) \quad (17)$$

$$\tau_{Sy} = -\frac{1}{\rho_w} \left( \frac{\partial S_{xy}}{\partial x} + \frac{\partial S_{yy}}{\partial y} \right) \quad (18)$$

where  $S_{xx}$ ,  $S_{xy}$ , and  $S_{yy}$  are wave-driven radiation stresses. Radiation-stress tensor calculations are based on linear wave theory and computed within STWAVE or other wave model. They represent the summation of standard tensor formulations across the defined spectrum. For a coordinate system with the x-axis oriented normal to the shoreline, the tensor components are (Smith et al. 2001)

$$S_{xx} = \iint E(\omega, \alpha) \left[ 0.5 \left( 1 + \frac{2k(h+\eta)}{\sinh 2k(h+\eta)} \right) (\cos^2 \alpha + 1) - 0.5 \right] d\omega d\alpha \quad (19)$$

$$S_{xy} = \iint \frac{E(\omega, \alpha)}{2} \left[ 0.5 \left( 1 + \frac{2k(h+\eta)}{\sinh 2k(h+\eta)} \right) \sin 2\alpha \right] d\omega d\alpha \quad (20)$$

$$S_{yy} = \iint E(\omega, \alpha) \left[ 0.5 \left( 1 + \frac{2k(h+\eta)}{\sinh 2k(h+\eta)} \right) (\sin^2 \alpha + 1) - 0.5 \right] d\omega d\alpha \quad (21)$$

where

$S_{xx}$ , = flux of shore-normal momentum

$S_{xy}$  = of shore-parallel momentum, or the shear component of the radiation stress

$S_{yy}$  = flux of momentum alongshore

$E$  = wave energy density

Details of the spectral wave calculations conducted by STWAVE are described in the STWAVE User's Guide (Smith et al. 2001).

Wave models, such as STWAVE, generally define their coordinate systems such that the x-axis is normal to the shoreline (positive x directed toward the shore) and the y-axis is parallel to the shoreline. For M2D applications, the radiation-stress tensor is rotated from the STWAVE grid and mapped onto the M2D grid by the SMS.

The Coriolis parameter is given by

$$f = 2\Omega \sin(\varphi) \quad (22)$$

where  $\Omega$  is the angular frequency of the Earth's rotation and  $\varphi$  is latitude.

The depth-mean horizontal eddy viscosity coefficient,  $D$ , is dependent on the strength of mixing in the water column which is a function of the acting processes at a location. If waves do not contribute significantly to mixing,  $D$  can be calculated as a function of the total water depth, current speed, and bottom roughness as (Falconer 1980)

$$D_o = \frac{1}{2} \left[ 1.156g (h + \eta) \frac{|U|}{C^2} \right] \quad (23)$$

where the subscript  $o$  denotes oceanic mixing. The form of the eddy viscosity coefficient given by Equation 23 results in mixing terms that are weakly nonlinear.

In the surf zone, waves contribute significantly to lateral mixing, and the eddy viscosity coefficient is expected to be a function of the wave properties. Here, surf zone mixing is given by

$$D_w = \varepsilon_L \quad (24)$$

where  $\varepsilon_L$  describes the lateral mixing below trough level (Smith et al. 1993) and is expressed as (Kraus and Larson 1991)

$$\varepsilon_L = \Lambda u_m H \quad (25)$$

where  $\Lambda$  is an empirical coefficient representing the lateral mixing strength, and  $u_m$  is the amplitude of the horizontal component of the wave orbital velocity at the bottom given by

$$u_m = \frac{gHT}{\left[ 2\lambda \cosh\left(\frac{2\pi(h+\eta)}{\lambda}\right) \right]} \quad (26)$$

where  $T$  is the wave period.

Mixing is a vigorous three-dimensional (3-D) process in the surf zone and cannot be represented directly in a depth-averaged model. Such vertical processes cannot be directly described in a depth-average model; the mixing coefficient in Equation 25 should be considered as a surrogate. Streaming from undertow advects turbulent eddies or mixing offshore, and this mixing can support a strong current seaward of the wave breakpoint (Putrevu and Svendsen 1992). With further distance seaward, the vertical current decreases as the volume of water increases, weakening the mixing and the longshore current.

The transition between surf zone mixing and oceanic mixing seaward of the breakpoint is represented in M2D by a weighted mixing coefficient specified as

$$D = (1 - \theta)D_o + \theta D_w \quad (27)$$

where the weighting parameter  $\theta$  is

$$\theta = \left( \frac{H}{h + \eta} \right)^3 \quad (28)$$

The method of weighting and the weighting parameter are ad hoc and must be validated by comparison to data. Intuitively, a cubic dependence on water depth introduces the fluid volume.

To illustrate the control on the cross-shore distribution of the longshore current by wave friction and representation of mixing, four simulations corresponding to Visser (1982) Case 4 were conducted. Details of the Visser laboratory data and M2D grid and parameter values are given in Appendix H with one difference being that the Manning's  $n$  value for velocities discussed in this section was 0.013. The four simulations consisted of combinations of wave friction specification and mixing coefficient. Simulations denoted as "No Wave Friction" did not include waves as a source of friction, whereas "Wave Friction" denoted the bottom stress as defined by Equations 11 and 12. Mixing coefficients were calculated as "Wave Mixing," which indicated application of Equation 24, and "Weighted Mixing," which denoted the combined oceanic and surf zone mixing described by Equation 27.

Calculated and measured longshore current for Visser's Case 4 are compared in Figure 1. Values of distance increase toward the offshore direction. Peak calculated current speed varies between 0.37 and 0.40 m/s and the measured peak speed is 0.39 m/s. Thus, combinations of both wave friction to the bottom stress and representation of the mixing coefficient exert control on the maximum current speed. The area of greatest variation among the calculated speeds is located between the peak current and the weakening of the current with distance offshore. Calculation with the weighted mixing coefficient and wave friction produced a curve in which the magnitude and slope compare well with measurements. All of the remaining calculations show deviation in magnitude and curvature from the measured values in the offshore tail.

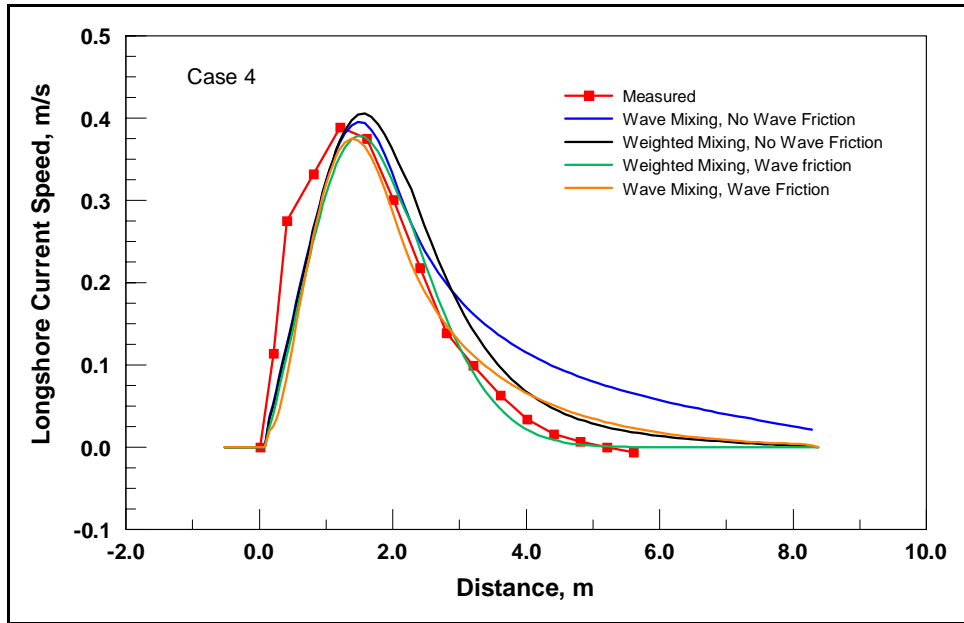


Figure 1. Comparison of longshore current speed values for Visser Case 4

Accurate estimation of the wind-stress coefficient is necessary for calculating wind-induced flow in shallow water ( $\approx < 5$  m). A short review describing the development of the variable wind-stress coefficient implemented in M2D is presented here.

The flux of momentum into the water column from the wind is specified as a function of the wind speed and wind-stress coefficient. Anemometer height above the water or land surface must be considered for accurate estimation of the wind-stress coefficient because wind speed varies logarithmically in the vertical direction for unstratified atmospheric conditions. A general law for the vertical wind profile is given by (Charnock 1955; Hsu 1988)

$$W_z = \frac{W_*}{\kappa} \ln \frac{Z}{Z_0} \quad (29)$$

where

$W_z$  = wind speed at height  $Z$  above the surface

$Z_0$  = surface roughness

$W_*$  = friction velocity

$\kappa$  = von Kármán constant

The friction velocity is defined in terms of the surface wind stress  $\tau_0$  as (Hsu 1988)

$$\tau_0 = \rho_a W_*^2 = \rho_a K_m \frac{\partial W}{\partial z} \quad (30)$$

where  $K_m$  is an eddy viscosity coefficient and  $z$  is the vertical dimension.

Under the assumption of nearly neutral atmospheric stability, the wind-stress coefficient over water at a height 10 m above the water surface,  $C_{10}$ , can be expressed as (Hsu 1988)

$$C_{10} = \left( \frac{\kappa}{14.56 - 2 \ln W_{10}} \right)^2 \quad (31)$$

where  $W_{10}$  is the wind speed in m/s at 10 m above the surface. Development of Equation 31 includes the assumption of fully developed seas. For measurements of wind speed made at heights other than 10 m, an approximation for the 10-m wind speed is (*Shore Protection Manual* 1984)

$$W_{10} = W_z \left( \frac{10}{Z} \right)^{1/7} \quad (32)$$

The surface wind-stress Equations 15 and 16, as implemented in M2D, apply the 10-m wind-drag coefficient and wind speed to compute the surface stress. Thus, values of  $C_{10}$  and  $W_{10}$  defined by Equations 31 and 32 are specified as  $C_d$  and  $W$  in Equations 15 and 16.

Equations 31 and 32 have been successfully applied in modeling studies investigating motion in strong wind-forced shallow embayments with typical depths ranging from 1 to 4 m (Brown et al. 1995a; Kraus and Militello 1999; Militello 2000). Calculated water level and current compared well with measurements, indicating that these formulations are satisfactory for estimation of the vertical wind profile and wind stress in shallow-water systems.

# 3 Numerical Implementation of Governing Equations

---

Grid definition and discretization of the governing equations are described in this chapter. The governing equations are solved numerically on a staggered rectilinear grid by a finite-volume calculation approach. All spatial derivatives are approximated with central differences with the exception of the advection terms, for which an upwind algorithm is applied. The solution method implemented is a flux-based approach in which M2D solves the momentum equations first, followed by the continuity equation wherein updated velocity values are applied.

To maximize efficiency of memory for domains with complex shorelines, the M2D grid is stored in a 1-dimensional (1-D) array rather than a 2-D matrix. The cell numbering convention is described in this chapter. Information is also provided on the Courant stability criterion, which provides the user with an initial approximation of an appropriate model time-step.

## Rectilinear Grid

The governing equations are solved on a discretized domain where cells are defined on a rectilinear grid (which can be regular or irregular) as shown in Figure 2. Each cell has indices  $i$  and  $j$  that correspond to its position along the  $x$ - and  $y$ -axes of the grid domain, respectively. Water-surface elevation is calculated at the cell center, whereas the  $x$ - and  $y$ -components of the velocity are calculated on the left face center and bottom face center of the cell, respectively. Values of flow rate per unit width,  $q_x$  and  $q_y$ , are calculated at the same locations as  $u$  and  $v$ , respectively. Because the best orientation of the grid may be such that the  $x$ - and  $y$ -axes do not correspond to geographical coordinates (N-S and E-W), cells in the grid are defined in a local (or grid) coordinate system. The local coordinate system is referenced to geographic coordinates by specification of the angle between the  $y$ -axis and true north. A positive value of this angle denotes clockwise rotation and the maximum rotation angle should not exceed 45 deg to retain an orientation as close to geographic as possible.

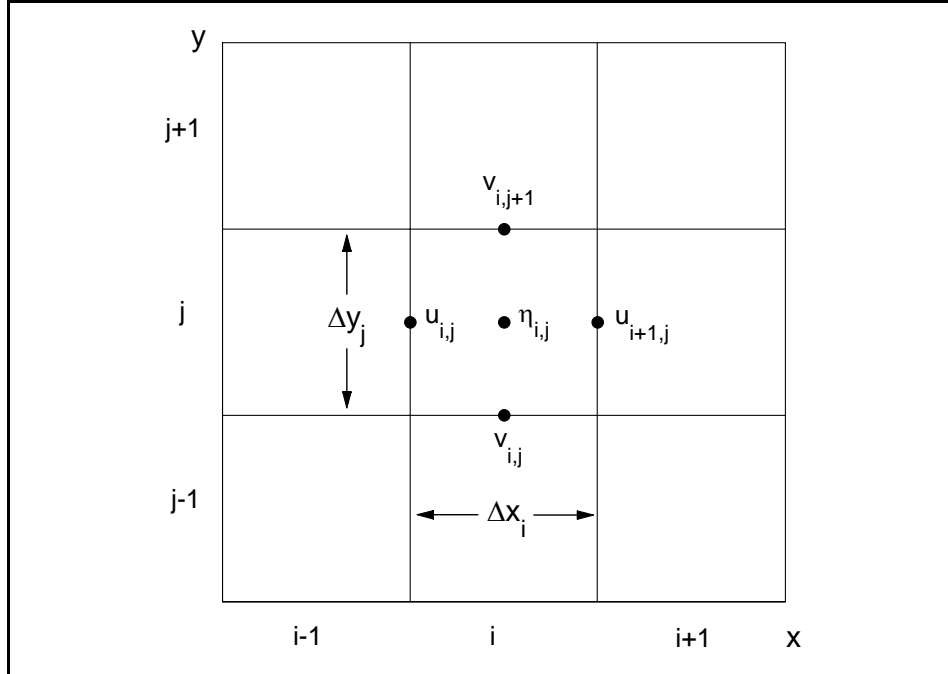


Figure 2. Cell and variable definitions for M2D

The 2-D array format for referencing cell locations is retained here to facilitate the presentation of the finite-volume approximations. Mapping of the cell indices from a 2-D array to a 1-D array is conducted primarily to reduce computer memory requirements. Details of the 1-D indexing of cells are discussed later in this section.

## Momentum Equations

The finite-difference scheme for the *x-momentum equation* will be given first, followed by that for the *y-momentum equation*. Calculation of the bottom stress coefficient, wind stress, eddy viscosity coefficient, and adjustment to the wave stress for shallow water follow the finite-difference approximation of the *y-momentum equation* because their descriptions are common for both *x-* and *y-momentum equations*.

Solution of the momentum equations is conducted to calculate the *x-* and *y-* components of velocity *u* and *v*, respectively. The explicit approach implemented in M2D solves each momentum equation for the corresponding flow rate per unit width  $q_{x_{i,j}}^{k+1}$  or  $q_{y_{i,j}}^{k+1}$  at the present time-step  $k+1$  from values calculated at time-step  $k$ . Velocity components  $u_{i,j}^{k+1}$  and  $v_{i,j}^{k+1}$  are then calculated from the values of  $q_{x_{i,j}}^{k+1}$  and  $q_{y_{i,j}}^{k+1}$ , respectively.

### x-momentum equation

The  $x$ -momentum equation is solved explicitly by a finite-volume approximation for the control volume shown in Figure 3. The control volume is indicated by the dashed blue line. Surface and bottom stresses (i.e., wind and friction) are approximated on the upper and lower surfaces and momentum fluxes are approximated at each cell face.

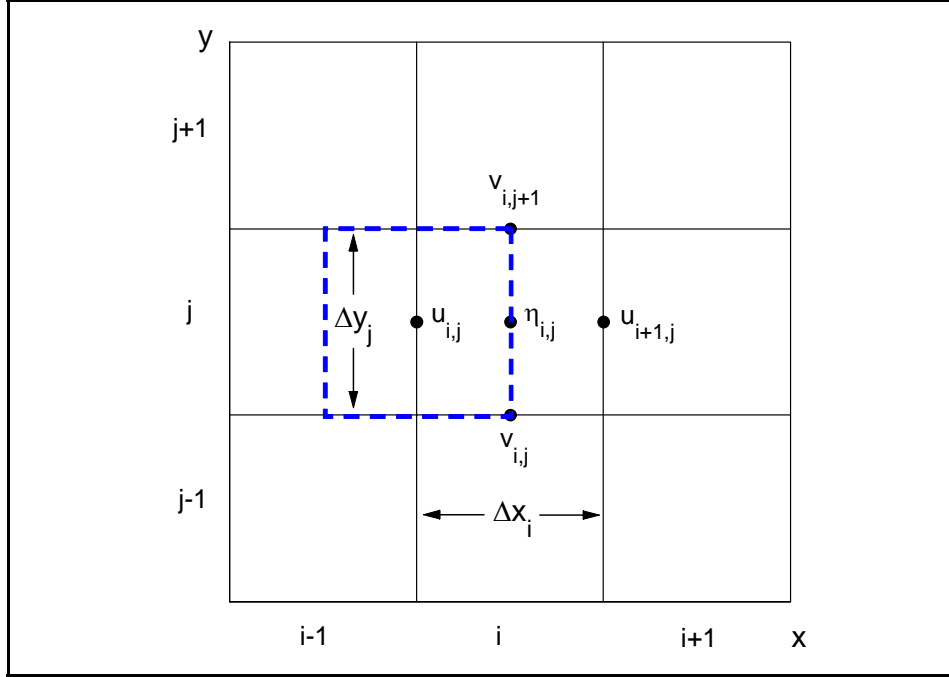


Figure 3. Control volume definition for  $x$ -momentum equation

The  $x$ -momentum equation in finite volume form is given by

$$\begin{aligned}
 & \frac{\Delta q_{x_{i,j}}}{\Delta t} \Delta x_{i,j} \Delta y_{i,j} + \left( F_{x_{i+1/2,j}}^k - F_{x_{i-1/2,j}}^k \right) \Delta y_{i,j} + \left( G_{y_{i,j+1}}^k - G_{y_{i,j-1}}^k \right) \Delta x_{i,j} \\
 & + \frac{1}{2} g \left[ \left( h_{i,j} + \eta_{i,j}^k \right)^2 - \left( h_{i-1,j} + \eta_{i-1,j}^k \right)^2 \right] \Delta y_{i,j} = \\
 & \left[ \frac{D_{x_{i+1/2,j}}^k \left( q_{x_{i+1,j}}^k - q_{x_{i,j}}^k \right)}{\Delta x_{i,j}} - \frac{D_{x_{i-1/2,j}}^k \left( q_{x_{i,j}}^k - q_{x_{i-1,j}}^k \right)}{\Delta x_{i-1,j}} \right] \Delta y_{i,j} \\
 & + \frac{f}{4} \left( q_{y_{i,j}}^k + q_{y_{i-1,j-1}}^k + q_{y_{i,j+1}}^k + q_{y_{i-1,j+1}}^k \right) \Delta x_{i,j} \Delta y_{i,j} \\
 & - \left( C_b \right)_{i,j}^k u_{i,j}^k |U_{i,j}^k| \Delta x_{i,j} \Delta y_{i,j} + \tau_{wx_{i,j}}^k \Delta x_{i,j} \Delta y_{i,j} \\
 & + \left( \tau_{sx} \right)_{i,j}^{k+1} \Delta x_{i,j} \Delta y_{i,j}
 \end{aligned} \tag{33}$$

where

$$\Delta q_{x_i,j} = q_{x_i,j}^{k+1} - q_{x_i,j}^k$$

$i, j$  = cell location on the grid

$k$  = time-step

$\Delta x_{i,j}$  = cell-side length parallel to the x-axis

$\Delta y_{i,j}$  = cell-side length parallel to the y-axis

and

$$F_{x_{i+1/2},j}^k = \bar{u}_{i+1/2,j}^k q_x', \quad \bar{u}_{i+1/2,j}^k = \frac{q_{x_i,j}^k + q_{x_{i+1},j}^k}{2(h_{i,j} + \eta_{i,j}^k)},$$

$$q_x' = q_{x_i,j}^k \quad \text{if } \bar{u}_{i+1/2,j}^k > 0$$

$$q_x' = q_{x_{i+1},j}^k \quad \text{if } \bar{u}_{i+1/2,j}^k < 0$$
(34)

$$F_{x_{i-1/2},j}^k = \bar{u}_{i-1/2,j}^k q_x', \quad \bar{u}_{i-1/2,j}^k = \frac{q_{x_i,j}^k - q_{x_{i-1},j}^k}{2(h_{i-1,j} + \eta_{i-1,j}^k)},$$

$$q_x' = q_{x_{i-1},j}^k \quad \text{if } \bar{u}_{i-1/2,j}^k > 0$$

$$q_x' = q_{x_i,j}^k \quad \text{if } \bar{u}_{i-1/2,j}^k < 0$$
(35)

$$G_{y_{i,j+1}}^k = \bar{v}_{i,j+1}^k q_x',$$

$$\bar{v}_{i,j+1}^k = \frac{q_{y_{i,j+1}}^k}{(h_{i,j} + \eta_{i,j} + h_{i,j+1} + \eta_{i,j+1})} + \frac{q_{y_{i-1,j+1}}^k}{(h_{i-1,j} + \eta_{i-1,j} + h_{i-1,j+1} + \eta_{i-1,j+1})}$$

$$q_x' = q_{x_i,j}^k \quad \text{if } \bar{v}_{i,j+1}^k > 0$$

$$q_x' = q_{x_{i,j+1}}^k \quad \text{if } \bar{v}_{i,j+1}^k < 0$$
(36)

$$\begin{aligned}
G_{y,i,j}^k &= \bar{v}_{i,j}^k q_x', \\
\bar{v}_{i,j}^k &= \frac{q_{y,i,j}^k}{\left(h_{i,j} + \eta_{i,j} + h_{i,j-1} + \eta_{i,j-1}\right)} \\
&\quad + \frac{q_{y,i-1,j}^k}{\left(h_{i-1,j} + \eta_{i-1,j} + h_{i-1,j-1} + \eta_{i-1,j-1}\right)} \\
q_x' &= q_{x,i,j-1}^k \quad \text{if } \bar{v}_{i,j-1}^k > 0 \\
q_x' &= q_{x,i,j}^k \quad \text{if } \bar{v}_{i,j-1}^k > 0
\end{aligned} \tag{37}$$

The x-directed current velocity is given by

$$u_{i,j}^k = 2 \frac{q_{x,i,j}^k}{\left(h_{i,j} + \eta_{i,j}^k + h_{i-1,j} + \eta_{i-1,j}^k\right)} \tag{38}$$

and the current speed for the  $x$ -momentum equation is

$$|U_{i,j}^k| = \sqrt{\left(u_{i,j}^k\right)^2 + \left(v_*^k\right)^2} \quad \text{where } v_*^k = \frac{\left(v_{i,j}^k + v_{i-1,j}^k + v_{i,j+1}^k + v_{i-1,j+1}^k\right)}{4} \tag{39}$$

Wave stress for the  $x$ -momentum equation  $\tau_{sx}$  is given by

$$\left(\tau_{sx}\right)_{i,j}^{k+1} = \frac{1}{\rho_w} \left[ \left(\frac{\partial \mathcal{S}_{xx}}{\partial x}\right)_{i,j}^{k+1} + \left(\frac{\partial \mathcal{S}_{xy}}{\partial y}\right)_{i,j}^{k+1} \right] \tag{40}$$

### **y-momentum equation**

The  $y$ -momentum equation is solved explicitly with a finite volume approximation for a control volume as shown in Figure 4. The control volume is indicated by the dashed blue line. Surface and bottom stresses (i.e., wind and friction) are approximated on the upper and lower surfaces and momentum fluxes are approximated at each cell face.

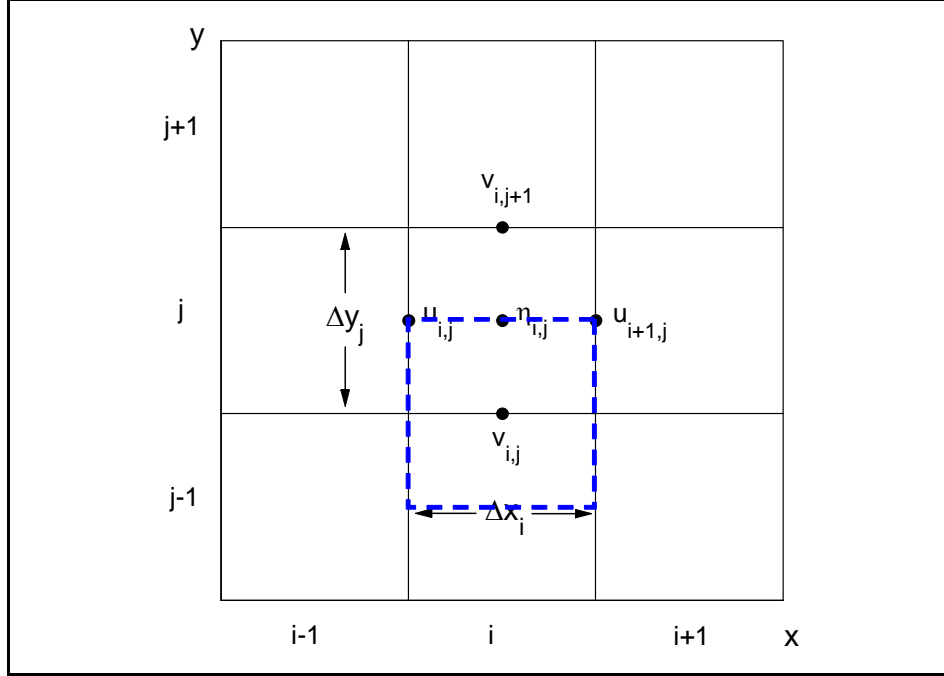


Figure 4. Control volume definition for  $y$ -momentum equation

The  $y$ -momentum equation in finite volume form is given by

$$\begin{aligned}
 & \frac{\Delta q_{y_{i,j}}}{\Delta t} \Delta x_{i,j} \Delta y_{i,j} + \left( F_{y_{i,j+1/2}}^k - F_{y_{i,j-1/2}}^k \right) \Delta x_{i,j} + \left( G_{x_{i+1,j}}^k - G_{x_{i,j}}^k \right) \Delta y_{i,j} \\
 & + \frac{1}{2} g \left[ \left( h_{i,j} + \eta_{i,j}^k \right)^2 - \left( h_{i,j-1} + \eta_{i,j-1}^k \right)^2 \right] \Delta x_{i,j} = \\
 & \left[ \frac{D_{y_{i,j+1/2}}^k \left( q_{y_{i,j+1}}^k - q_{y_{i,j}}^k \right)}{\Delta y_{i,j}} - \frac{D_{y_{i,j-1/2}}^k \left( q_{y_{i,j}}^k - q_{y_{i,j-1}}^k \right)}{\Delta y_{i,j-1}} \right] \Delta y_{i,j} \\
 & + \frac{f}{4} \left( q_{x_{i,j}}^k + q_{x_{i+1,j}}^k + q_{x_{i,j-1}}^k + q_{x_{i+1,j-1}}^k \right) \Delta x_{i,j} \Delta y_{i,j} \\
 & - \left( C_b \right)_{i,j}^k v_{i,j}^k \left| V_{i,j}^k \right| \Delta x_{i,j} \Delta y_{i,j} + \tau_{wy_{i,j}}^k \Delta x_{i,j} \Delta y_{i,j} \\
 & + \left( \tau_{Sy} \right)_{i,j}^{k+1} \Delta x_{i,j} \Delta y_{i,j}
 \end{aligned} \tag{41}$$

where  $\Delta q_{y_{i,j}} = q_{y_{i,j}}^{k+1} - q_{y_{i,j}}^k$  and

$$F_{y_{i,j+1/2}}^k = \bar{v}_{i,j+1/2}^k q_y', \quad \bar{v}_{i,j+1/2}^k = \frac{q_{y_{i,j}}^k + q_{y_{i,j+1}}^k}{2(h_{i,j} + \eta_{i,j}^k)},$$

$$q_y' = q_{y_{i,j}}^k \quad \text{if } \bar{v}_{i,j+1}^k > 0$$

$$q_y' = q_{y_{i,j+1}}^k \quad \text{if } \bar{v}_{i,j+1}^k < 0$$
(42)

$$F_{y_{i,j-1/2}}^k = \bar{v}_{i,j-1/2}^k q_y', \quad \bar{v}_{i,j-1/2}^k = \frac{q_{y_{i,j}}^k + q_{y_{i,j-1}}^k}{2(h_{i,j-1} + \eta_{i,j-1}^k)},$$

$$q_y' = q_{y_{i,j-1}}^k \quad \text{if } \bar{v}_{i,j-1}^k > 0$$

$$q_y' = q_{y_{i,j}}^k \quad \text{if } \bar{v}_{i,j-1}^k < 0$$
(43)

$$G_{x_{i+1,j}}^k = \bar{u}_{i+1,j}^k q_y',$$

$$\bar{u}_{i+1,j}^k = \frac{q_{x_{i+1,j}}^k}{(h_{i,j} + \eta_{i,j} + h_{i+1,j} + \eta_{i+1,j})} + \frac{q_{x_{i+1,j-1}}^k}{(h_{i,j-1} + \eta_{i,j-1} + h_{i+1,j-1} + \eta_{i+1,j-1})}$$

$$q_y' = q_{y_{i,j}}^k \quad \text{if } \bar{u}_{i+1,j}^k > 0$$

$$q_y' = q_{y_{i+1,j}}^k \quad \text{if } \bar{u}_{i+1,j}^k < 0$$
(44)

$$G_{x_{i-1,j}}^k = \bar{u}_{i-1,j}^k q_y',$$

$$\bar{u}_{i-1,j}^k = \frac{q_{x_{i,j}}^k}{(h_{i,j} + \eta_{i,j} + h_{i-1,j} + \eta_{i-1,j})} + \frac{q_{x_{i,j-1}}^k}{(h_{i,j-1} + \eta_{i,j-1} + h_{i-1,j-1} + \eta_{i-1,j-1})}$$

$$q_y' = q_{y_{i-1,j}}^k \quad \text{if } \bar{u}_{i-1,j}^k > 0$$

$$q_y' = q_{y_{i,j}}^k \quad \text{if } \bar{u}_{i-1,j}^k < 0$$
(45)

The y-directed current velocity is given by

$$v_{i,j}^k = 2 \frac{q_{y_{i,j}}^k}{(h_{i,j} + \eta_{i,j}^k + h_{i,j-1} + \eta_{i,j-1}^k)}$$
(46)

and the current speed for the y-momentum equation is

$$|V_{i,j}^k| = \sqrt{(u_*^k)^2 + (v_{i,j}^k)^2} \quad \text{where } u_*^k = \frac{(u_{i,j}^k + u_{i+1,j}^k + u_{i,j-1}^k + u_{i+1,j-1}^k)}{4} \quad (47)$$

Wave stress for the y-momentum equation  $\tau_{sy}$  is given by

$$(\tau_{sy})_{i,j}^{k+1} = \frac{1}{\rho_w} \left[ \left( \frac{\partial S_{xy}}{\partial x} \right)_{i,j}^{k+1} + \left( \frac{\partial S_{yy}}{\partial y} \right)_{i,j}^{k+1} \right] \quad (48)$$

### Bottom-friction coefficient

The bottom-friction coefficient  $(C_b)_{i,j}^k$  is given by

$$(C_b)_{i,j}^k = \frac{g}{(C_{i,j}^k)^2} \quad (49)$$

where  $C_{i,j}$  is the Chezy coefficient calculated as

$$C_{i,j}^k = \frac{(R_{i,j}^k)^{1/6}}{n_{i,j}} \quad (50)$$

where  $R_{i,j}$  is the hydraulic radius, which is dependent on the cell dimension  $\Delta s$ , in the corresponding flow direction. The hydraulic radius for a given cell is calculated by

$$R_{i,j}^k = \frac{(h_{i,j} + \eta_{i,j}^k) \Delta s_{i,j}}{P_{i,j}^k} \quad (51)$$

where  $P_{i,j}$  is the wetted perimeter of the cell, and  $\Delta s$  denotes  $\Delta x$  or  $\Delta y$  for application of Equation 51 to the x- or y-momentum equation, respectively. The wetted perimeter is taken to be equal to  $\Delta s$  if a cell has no impermeable walls. If walls are present, the wetted perimeter is calculated by

$$P_{i,j}^k = \Delta s_{i,j} + m(h_{i,j} + \eta_{i,j}^k) \quad (52)$$

where  $m$  is the number of wall boundaries on sides parallel to the component of flow corresponding to  $s$ . For example, in the case of flow along a one-cell-wide channel aligned with the x-axis, the wetted perimeter would be calculated as  $P = \Delta x + 2(h + \eta)$  at all cells in the channel. If the channel is two cells wide, then the wetted perimeter for the x-momentum equation would be calculated as

$P = \Delta x + (h + \eta)$ . The formulation of the bottom-friction coefficient takes into account wall friction, but does not distinguish it from friction along the channel bottom. In addition, calculation of the wetted perimeter does not account for changes in depth between adjacent cells (increase in wetted surface area).

Inclusion of waves in the bottom stress is implemented by representing the combined wave and current terms of Equations 11 and 12, respectively, as

$$\left[ \left( U_{wc} + \frac{\omega_b^2}{U_{wc}} \cos^2 \alpha \right) u + \left( \frac{\omega_b^2}{U_{wc}} \cos \alpha \sin \alpha \right) v \right]_{i,j}^k = \left( U_{wcx} + \frac{\omega_{bx}^2}{U_{wcx}} \cos^2 \alpha_x \right)_{i,j}^k u_{i,j}^k + \left( \frac{\omega_{bx}^2}{U_{wcx}} \cos \alpha_x \sin \alpha_x \right)_{i,j}^k v_{i,j}^k \quad (53)$$

$$\left[ \left( \frac{\omega_b^2}{U_{wc}} \cos \alpha \sin \alpha \right) u + \left( U_{wc} + \frac{\omega_b^2}{U_{wc}} \sin^2 \alpha \right) v \right]_{i,j}^k = \left( \frac{\omega_{by}^2}{U_{wcy}} \cos \alpha_y \sin \alpha_y \right)_{i,j}^k u_{i,j}^k + \left( U_{wcy} + \frac{\omega_{by}^2}{U_{wcy}} \sin^2 \alpha_y \right)_{i,j}^k v_{i,j}^k \quad (54)$$

where

$$U_{wcx,i,j}^k = \frac{1}{2} \left\{ \sqrt{u^2 + v_*^2 + \omega_{bx}^2 + 2(u \cos \alpha_x + v_* \sin \alpha_x) \omega_{bx}} + \sqrt{u^2 + v_*^2 + \omega_{bx}^2 - 2(u \cos \alpha_x + v_* \sin \alpha_x) \omega_{bx}} \right\}_{i,j}^k \quad (55)$$

$$U_{wcy,i,j}^k = \frac{1}{2} \left\{ \sqrt{u_*^2 + v^2 + \omega_{by}^2 + 2(u_* \cos \alpha_y + v \sin \alpha_y) \omega_{by}} + \sqrt{u_*^2 + v^2 + \omega_{by}^2 - 2(u_* \cos \alpha_y + v \sin \alpha_y) \omega_{by}} \right\}_{i,j}^k \quad (56)$$

$$\omega_{bx,i,j}^k = \left\{ \frac{\sigma_x H_x}{\pi \sinh [k_x (h + \eta)]} \right\}_{i,j}^k \quad (57)$$

$$\omega_{by,i,j}^k = \left\{ \frac{\sigma_y H_y}{\pi \sinh [k_y (h + \eta)]} \right\}_{i,j}^k \quad (58)$$

$$(\alpha_x)_{i,j}^k = \frac{1}{2}(\alpha_{i,j}^k + \alpha_{i-1,j}^k) \quad (59)$$

$$(\alpha_y)_{i,j}^k = \frac{1}{2}(\alpha_{i,j}^k + \alpha_{i,j-1}^k) \quad (60)$$

$$(\sigma_x)_{i,j}^k = \frac{1}{2}(\sigma_{i,j}^k + \sigma_{i-1,j}^k) \quad (61)$$

$$(\sigma_y)_{i,j}^k = \frac{1}{2}(\sigma_{i,j}^k + \sigma_{i,j-1}^k) \quad (62)$$

$$(H_x)_{i,j}^k = \frac{1}{2}(H_{i,j}^k + H_{i-1,j}^k) \quad (63)$$

$$(H_y)_{i,j}^k = \frac{1}{2}(H_{i,j}^k + H_{i,j-1}^k) \quad (64)$$

$$(k_x)_{i,j}^k = \frac{1}{2}(k_{i,j}^k + k_{i-1,j}^k) \quad (65)$$

$$(k_y)_{i,j}^k = \frac{1}{2}(k_{i,j}^k + k_{i,j-1}^k) \quad (66)$$

Because the wave properties are scalar values, they are located at cell centers and must be face-averaged for application in the bottom stress calculation.

If water in a cell approaches a thin layer, numerical instability may arise and unrealistically large values of water level and current speed can be calculated. This numerical problem is more apparent than real because water creeping onto a dry surface is expected to experience large frictional resistance. Stability in shallow water is enhanced within M2D by adjustment of the bottom-friction coefficient by the following formulation

$$\left[ (C_b)_{adjusted} \right]_{i,j}^k = (C_b)_{i,j}^k \left( 1 + \exp^{-\alpha(h_{i,j} + \eta_{i,j}^k)} \right) \quad (67)$$

where the subscript *adjusted* denotes the modified bottom-friction coefficient, and  $\alpha$  is a parameter that controls the gradient of the increase of the bottom-friction coefficient as the water depth approaches zero. The bottom-friction coefficient can vary within the range  $C_b$  to  $2C_b$  with the adjustment scaled by the exponential expression given within Equation 67. Figure 5 shows the depth-dependent adjustment of the bottom-friction coefficient as given by the exponential formulation with the parameter  $\alpha$  set to 10. Significant increases in the bottom-friction coefficient occur for small water depth, particularly less than

0.1 m because of the presence of large roughness elements relative to the water depth. Thus, modification of the bottom-friction coefficient from its normal value is restricted to small water depth. For depths greater than approximately 0.2 m, modification of the bottom-friction coefficient is small.

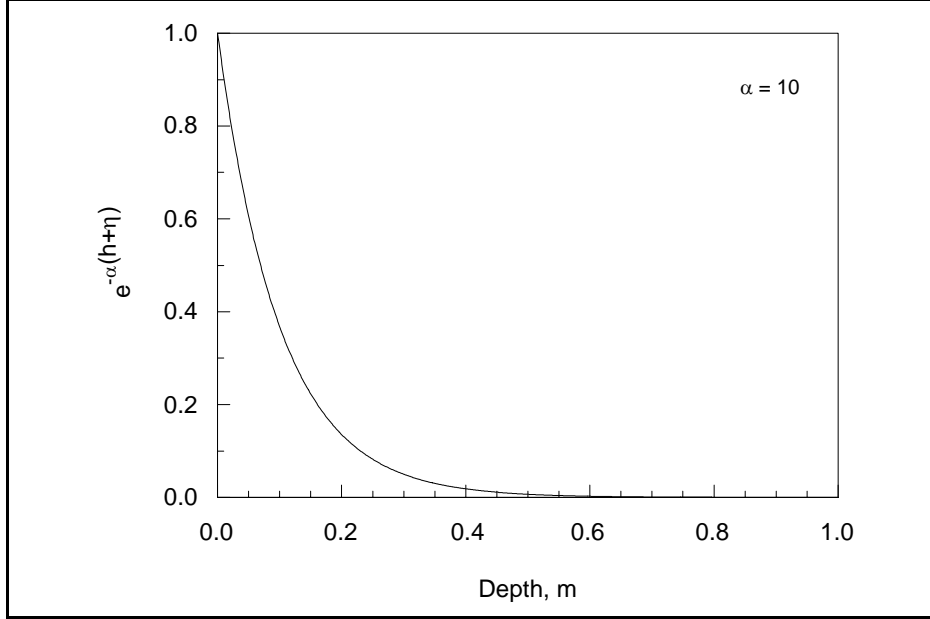


Figure 5. Bottom-friction coefficient adjustment versus total water depth

### Wind stress

Wind-stress terms are calculated by

$$\tau_{wx} = C_d \frac{\rho_a}{\rho_w} (W_{10}^{k+1})^2 \cos(\theta^{k+1}) \quad (68)$$

$$\tau_{wy} = C_d \frac{\rho_a}{\rho_w} (W_{10}^{k+1})^2 \sin(\theta^{k+1}) \quad (69)$$

where  $C_d$  is calculated by Equation 31 and  $W_{10}$  has been calculated from  $W$ . Height of the anemometer is specified in an input file. Wind forcing in M2D can vary over time, but is homogenous over space.

## Eddy viscosity coefficient

Two formulations for calculation of the eddy viscosity coefficient are implemented in M2D, one for oceanic mixing and one for surf zone mixing. If waves are not present, the oceanic coefficient of eddy viscosity is calculated as

$$(D_o)_{i+1/2,j}^k = \frac{1}{2} \left[ 1.156g (h_{i,j} + \eta_{i,j}^k) \frac{|\bar{U}_{i,j}^k|}{C_{i,j}^k{}^2} \right] \quad (70)$$

$$(D_o)_{i-1/2,j}^k = \frac{1}{2} \left[ 1.156g (h_{i-1,j} + \eta_{i-1,j}^k) \frac{|\bar{U}_{i-1,j}^k|}{C_{i-1,j}^k{}^2} \right] \quad (71)$$

$$(D_o)_{i,j+1/2}^k = \frac{1}{2} \left[ 1.156g (h_{i,j} + \eta_{i,j}^k) \frac{|\bar{U}_{i,j}^k|}{C_{i,j}^k{}^2} \right] \quad (72)$$

$$(D_o)_{i,j-1/2}^k = \frac{1}{2} \left[ 1.156g (h_{i,j-1} + \eta_{i,j-1}^k) \frac{|\bar{U}_{i,j-1}^k|}{C_{i,j-1}^k{}^2} \right] \quad (73)$$

where

$$|\bar{U}_{i,j}^k| = \sqrt{\left[ \frac{(u_{i,j}^k + u_{i+1,j}^k)}{2} \right]^2 + \left[ \frac{(v_{i,j}^k + v_{i,j+1}^k)}{2} \right]^2} \quad (74)$$

$$|\bar{U}_{i-1,j}^k| = \sqrt{\left[ \frac{(u_{i,j}^k + u_{i-1,j}^k)}{2} \right]^2 + \left[ \frac{(v_{i-1,j}^k + v_{i-1,j+1}^k)}{2} \right]^2} \quad (75)$$

$$|\bar{U}_{i,j-1}^k| = \sqrt{\left[ \frac{(u_{i,j-1}^k + u_{i+1,j-1}^k)}{2} \right]^2 + \left[ \frac{(v_{i,j}^k + v_{i,j-1}^k)}{2} \right]^2} \quad (76)$$

These formulations are calculated for Manning's  $n > 0$ . For frictionless cells, specified by  $n = 0$ ,  $D_0 = 0.0 \text{ m}^2/\text{s}$ .

In the presence of waves and wave breaking, the eddy viscosity coefficient is calculated as

$$D_{wx_{i+1/2,j}}^k = \frac{\Lambda g (H_{i,j}^2)^k T_{i,j}^k}{2\lambda_{i,j}^k \cosh\left(\frac{2\pi(h_{i,j} + \eta_{i,j}^k)}{\lambda_{i,j}^k}\right)} \quad (77)$$

$$D_{wx_{i-1/2,j}}^k = \frac{\Lambda g (H_{i-1,j}^2)^k T_{i-1,j}^k}{2\lambda_{i-1,j}^k \cosh\left(\frac{2\pi(h_{i-1,j} + \eta_{i-1,j}^k)}{\lambda_{i-1,j}^k}\right)} \quad (78)$$

$$D_{wy_{i,j+1/2}}^k = \frac{\Lambda g (H_{i,j}^2)^k T_{i,j}^k}{2\lambda_{i,j}^k \cosh\left(\frac{2\pi(h_{i,j} + \eta_{i,j}^k)}{\lambda_{i,j}^k}\right)} \quad (79)$$

$$D_{wy_{i,j-1/2}}^k = \frac{\Lambda g (H_{i,j-1}^2)^k T_{i,j-1}^k}{2\lambda_{i,j-1}^k \cosh\left(\frac{2\pi(h_{i,j-1} + \eta_{i,j-1}^k)}{\lambda_{i,j-1}^k}\right)} \quad (80)$$

Wavelength  $\lambda$  is calculated by the Eckart approximation

$$\lambda^k = \lambda_0^k \sqrt{\tanh\left(\frac{(\omega^k)^2 (h + \eta^k)}{g}\right)} \quad (81)$$

where  $\lambda_0$  is the deepwater wavelength given by

$$\lambda_0^k = \frac{g (T^k)^2}{2\pi} \quad (82)$$

and  $\omega$  is the wave frequency given by

$$\omega^k = \frac{2\pi}{T^k} \quad (83)$$

Wave parameters are calculated at locations corresponding to indices on  $D_w$ .

If waves are present but not breaking, then the mixing coefficient is calculated as a weighted function of the oceanic and wave mixing values as

$$D^k = (1 - \theta^k) (D_o)^k + \theta^k (D_w)^k \quad (84)$$

where the weighting parameter  $\theta$  is

$$\theta^k = \left( \frac{H^k}{h + \eta^k} \right)^3 \quad (85)$$

Equations 84 and 85 are calculated and applied at locations corresponding to indices on  $D_o$  and  $D_w$ .

### Wave stress scaling for shallow water

M2D accepts wave stresses calculated by a wave model and those stresses can vary spatially over the computational domain. Wave stresses must be mapped from the wave model onto the M2D domain. In water depths of 0.35 m or less, the wave stresses are reduced by

$$\tau'_s = \tau_s \frac{(h_{i,j} + \eta_{i,j}^k)}{0.35}, \quad \text{for } (h_{i,j} + \eta_{i,j}^k) \leq 0.35\text{m} \quad (86)$$

where  $\tau'_s$  is the adjusted wave stress and is applied to both  $\tau_{sx}$  and  $\tau_{sy}$  if the depth criterion is met. Equation 86 scales the wave stress toward zero as the water depth decreases.

Wave models typically perform calculations in a local right-handed coordinate system in which positive  $x$  is directed onshore and positive  $y$  is directed alongshore. Thus, the orientation of the local coordinate system may not be aligned with global geographic coordinates. M2D performs calculations on a local coordinate system that is referenced to global geographic coordinates by the deviation of the  $y$ -axis (given in degrees) from true north. If wave stresses are included in M2D calculations, mapping of those stresses from the wave model to the circulation model must take into consideration the different coordinate systems and grid orientations. Wave stresses calculated by STWAVE can be automatically mapped to M2D within the SMS (see Chapter 6).

## Continuity Equation

The continuity equation is solved explicitly for water-surface elevation  $\eta$  by a finite-volume approximation for a control volume depicted in Figure 6. Mass fluxes are approximated at each cell face. In the staggered time differencing scheme, the most recently calculated values for the  $u$  and  $v$  velocity components are entered into the spatial derivatives. The finite-volume approximation of Equation 1 is given by

$$\frac{\Delta\eta_{i,j}}{\Delta t} \Delta x_{i,j} \Delta y_{i,j} + (q_x|_{i,j}^{k+1} - q_x|_{i+1,j}^{k+1}) \Delta y_{i,j} + (q_y|_{i,j}^{k+1} - q_y|_{i,j+1}^{k+1}) \Delta x_{i,j} = 0 \dots\dots (87)$$

where  $\Delta\eta_{i,j} = \eta_{i,j}^{k+1} - \eta_{i,j}^k$  and all other variables have been previously defined.

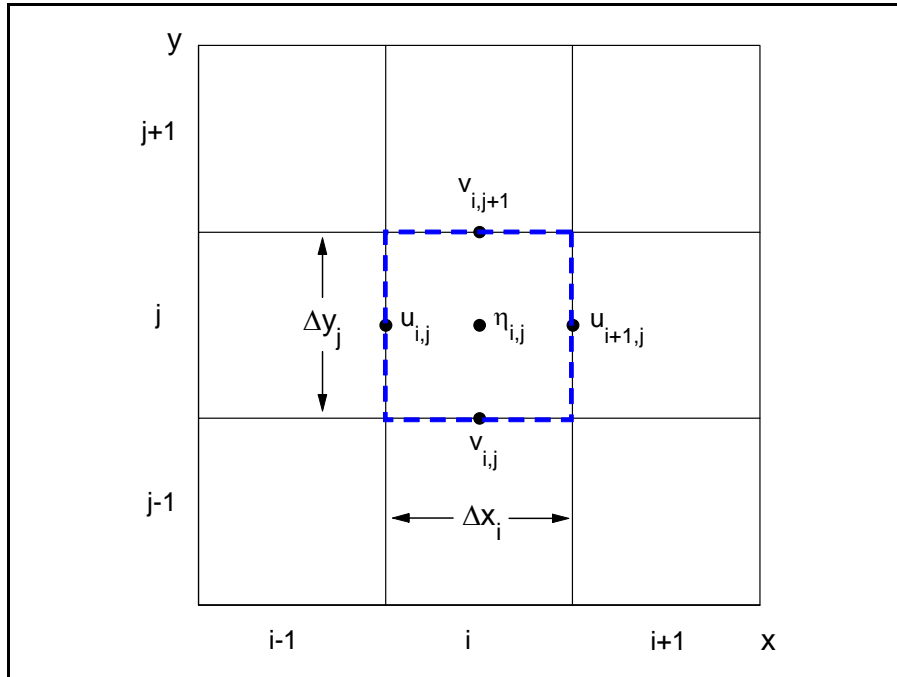


Figure 6. Control volume definition for continuity equation

## Cell Numbering

M2D stores its numerical grid in an array rather than a matrix, which saves memory for large or irregular grid domains. The numbering scheme for the computational grid is designed to be efficient such that regions that never become computationally active do not have to be stored. For model domains that have complex shorelines, this feature can save substantial computer memory. On the other hand, for simple grids, more memory may be required because pointing arrays are necessary for cell indexing.

The cell numbering system internal to M2D does not require row and column indexing, but instead assigns each cell a unique identification number. Flather and Heaps (1975) implemented a similar cell numbering system so that only cells included in hydrodynamic calculations were stored. Non-computational regions of the grid, such as the mainland and islands, do not require assigned cell numbers, so they do not occupy space in memory. Figure 7 illustrates the cell numbering system for a small domain that includes a non-computational region

indicated by hatching. Cell identification numbers of neighbors adjacent to a particular cell are stored in a pointing matrix within the model. For example, cell 9 has neighbors with cell identification numbers 12, 10, 4, and 8 moving from top, to right, bottom, and left, respectively. This clockwise order of referencing neighbor cells is taken as convention for descriptions in this document.

Locations where no cells exist, such as beyond the computational domain or in non-computational regions, such as islands within the domain, are designated with a cell number of 0. For example, cell 11 in Figure 7 lies on the boundary of the grid domain and also resides next to a non-computational area. Neighbor-cell specifications for cell 11 would be stored as 14, 0, 6, and 0. The grid does not contain any cells with cell number of zero; this value is used in neighbor specification to indicate that a computational cell does not exist at a particular location. If a cell is removed from computations, it retains its original cell number, calculations treat the interfaces of the neighbors and the inactive cell as walls.

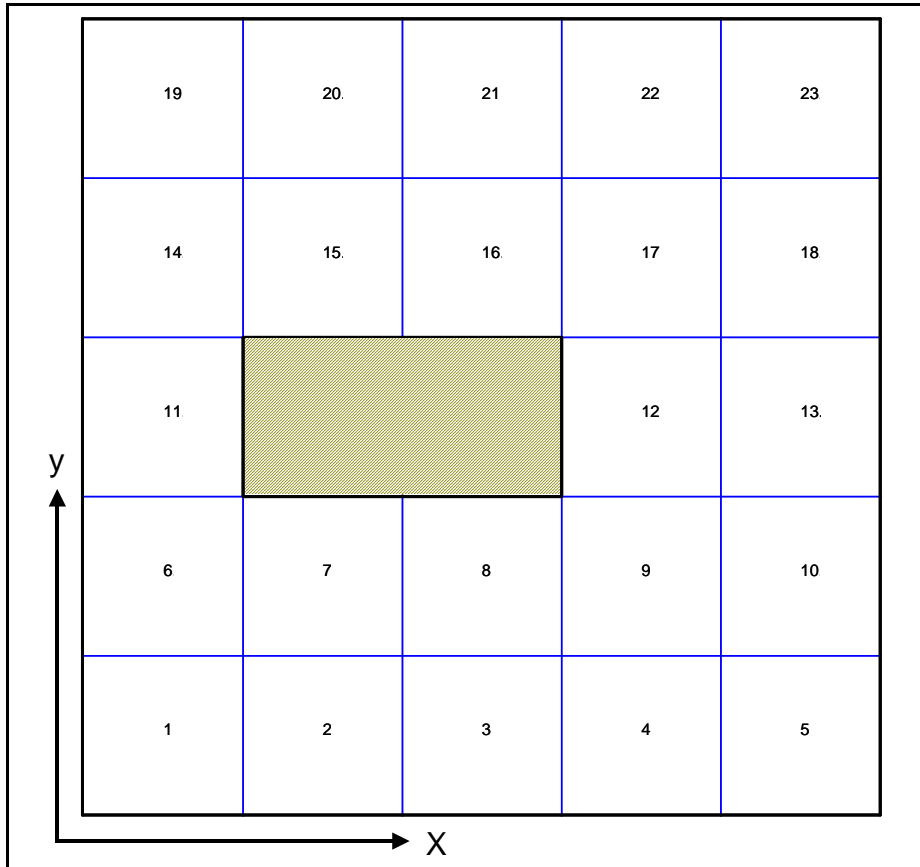


Figure 7. Cell numbering system

Removal of a cell from computations can be achieved by setting its type to inactive and changing its value to zero at locations where it is referenced as a neighbor. The inactive cell would remain in the grid and retain its original cell

number, but M2D will recognize it as a void surrounded by walls. As an example, if cell 3 were to be changed to an inactive type cell, the neighbor specifications for cell 4 would be changed from 9, 5, 0, 3 to 9, 5, 0, 0. Specifications for cell 3 would remain the same, except that the type would be changed to inactive (type 0).

## Courant Condition

For an explicit solution method, an initial estimate of the maximum time-step for a grid is calculated from the Courant number  $\xi$ , given by (Richtmyer and Morton 1967)

$$\xi \equiv u \frac{\Delta t}{\Delta s} \quad (88)$$

The theoretical maximum value of the Courant number is unity for stability of a linear, finite-difference hydrodynamic model, where for shallow-water equations  $u = \sqrt{gh}$  refers to long waves, such as the tide.

Because M2D solves the nonlinear shallow-water equations, stability will be maintained for a Courant number less than unity. Also, for a general situation, multiple forcing is possible from a superposition of sources other than or in addition to the tide. Contributions to the current can be produced by wind, surface waves, and tributary discharges. Assigning a velocity component to each of these forcings, denoted with a subscript, the Courant number is more accurately defined as

$$\xi \equiv \left( u_{tide} + u_{wind} + u_{waves} + u_{tributary} \right) \frac{\Delta t}{\Delta s} \quad (89)$$

In strong or focused-flow regions of a model domain, such as at ebb shoals and in the surf zone, the wave-driven current can be significantly stronger than the tidal current. Moreover, these are typically areas of greater spatial grid resolution. The combination of strong currents and small grid cells limit the allowable size of the time-step.

## 4 Boundary Conditions

---

Six types of boundary conditions are implemented in M2D, and these can be distinguished as specifying forcing and non-forcing boundaries. Table 1 lists the boundary-condition types and contains a short description of each. Each boundary-condition type is described next.

<b>Table 1 Boundary Condition Types</b>	
<b>Boundary Condition</b>	<b>Description</b>
Tidal-constituent water level forcing	Water level specified as sum of tidal constituents
Time series water level forcing	Water level specified from time series input file
Time series water level and velocity forcing	Water level and velocities specified from time series input files
Time series flow rate forcing	Flow rate specified from a time series input file
Closed, reflective (non-forcing)	Impermeable boundary, velocity must flow parallel to boundary
Wave-adjusted water level and velocity forcing	Boundary water level and velocity values are adjusted for presence of radiation-stress gradients. Provides compatibility of boundary forcing with wave forcing

### Water Level Forcing Boundary Conditions

Water level forcing can be specified through either tidal constituents or by time series water level read in from a file. These two boundary conditions apply the same finite-difference approach, with the difference between them being the source of the water level prescribed at the boundary.

If a cell is designated as a water surface elevation boundary cell, the continuity equation for that cell is not solved, and the water level is updated each time-step according to:

$$\eta_{i,j}^{k+1} = \eta_{i,j}^b \quad (90)$$

where  $\eta_{i,j}^b$  is a prescribed value. If tidal forcing is specified, then

$$\eta_{i,j}^b = \eta_{tide} \quad (91)$$

### Tidal-constituent forcing

Tidal-constituent forcing in M2D can accommodate up to eight components of the astronomical tide. The user can select from the following constituents:  $M_2$ ,  $S_2$ ,  $N_2$ ,  $K_2$ ,  $K_1$ ,  $O_1$ ,  $M_4$ , and  $M_6$ . Although the  $M_4$  and  $M_6$  constituents are harmonics, they can be generated in continental shelf areas and may be present as components of the tidal forcing at the grid boundary. Specification of tidal constituents requires input information for the local amplitude and phase values. Tidal forcing by M2D is simple and does not include advanced tidal calculations or relations to Greenwich tidal parameters (Schureman 1924).

Tidal elevation  $\eta_{tide}$  is given by

$$\eta_{tide} = \sum_{l=1}^8 A_l \cos\left(\frac{2\pi}{360}(s_l t - \phi_l)\right) \quad (92)$$

where  $A$  is the amplitude (m),  $s$  is the speed (deg/hr), and  $\phi$  is the phase (deg) of the tidal constituent. Constituents can be eliminated from the tidal forcing by setting their amplitudes to zero. If the tidal elevation boundary condition is invoked, water levels at tidal boundary cells are computed at every time-step. Tidal phase and amplitude is held constant across the tidal-constituent boundary. For applications requiring amplitude and phase variation over an open boundary, solutions from regional models can be applied to map water surface elevations as boundary conditions for M2D.

### Time series water level forcing

The time series water level forcing boundary condition is specified by water levels ( $\eta_{i,j}^b$ ) read into the model from an input file. Time increments of the forcing data are not required to be equal to, or in multiple increments of, the model time-step. Because the model will usually have smaller time-steps than the water level forcing data input, M2D must be instructed on treatment of the water level boundary value between times that its value is specified in the input file. One option is to keep the water level constant between input water level values. A second option is to linearly interpolate in time between input water level values. The boundary condition input file for water level contains a parameter that sets the interpolation option.

## Time Series Water Level and Velocity Forcing Boundary Condition

The time series water level and velocity forcing boundary condition applies velocities at cell boundaries in addition to water levels. Application of water levels for this boundary type is identical to that previously described for water level forcing boundary conditions. Velocities prescribed on the boundaries enter the momentum equation through the advective terms. Discretization of the momentum equations for applying velocities on the boundaries is identical to the implementation for nonboundary cells described in Chapter 3.

## Time Series Flow Rate Forcing Boundary Condition

The time series flow rate forcing boundary condition can be assigned at locations where the flow rate is known. Typical examples where this boundary condition is applied are natural tributaries (rivers, streams, and creeks), controlled-discharge canals, and anthropogenic intake or discharge locations such as for power plant cooling water or treatment plant outfalls.

A flow rate boundary condition specifies discharge at one or more cells on the grid boundary. If a cell is designated as a flow rate boundary cell, the momentum equation for the appropriate cell face is not solved, and the flow-component normal to the face is prescribed. Because M2D operates on a staggered grid, “imaginary” cells are added to the right or top of the grid at flow rate forcing boundary cells prescribed on those sides. This addition of imaginary cells is required to provide access to cell faces on the right or top of the grid.

For a flow rate forcing cell located on the right side of the grid at location  $i+1, j$ , the flux is given by

$$q_{x_{i+1},j}^{k+1} = \frac{Q_{x_{i+1},j}^b}{\Delta y_{i+1,j}} \quad (93)$$

where  $Q_{x_{i+1},j}^b$  is the input flow rate directed parallel to the x-axis and  $i+1$  denotes an imaginary cell adjacent and to the right of the  $i^{\text{th}}$  cell.

For a flow rate forcing cell located on the left side of the grid at location  $i-1, j$ , the flux is given by

$$q_{x_{i-1},j}^{k+1} = \frac{Q_{x_{i-1},j}^b}{\Delta y_{i,j}} \quad (94)$$

For a flow rate forcing cell located on the top side of the grid at location  $i,j+1$ , the flux is given by

$$q_{y_{i,j+1}}^{k+1} = \frac{Q_{y_{i,j+1}}^b}{\Delta x_{i,j+1}} \quad (95)$$

where  $Q_{y_{i,j+1}}^b$  is the input flow rate directed parallel to the y-axis.

For a flow rate forcing cell located on the bottom side of the grid at location  $i,j-1$ , the flux is given by

$$q_{y_{i,j}}^{k+1} = \frac{Q_{y_{i,j-1}}^{k+1}}{\Delta x_{i,j-1}} \quad (96)$$

## Closed, Reflective Boundary Condition

The closed, reflective boundary condition is specified at impermeable boundaries, such as the land-water interface. These boundaries behave as walls; water can flow parallel to the wall face, but not through it. The boundary conditions are similar to flow rate boundary conditions except that zero flow is prescribed.

The normal velocity at the closed boundary on the left cell face is

$$Q_{x_{i,j}}^{k+1} = 0 \quad (97)$$

and the normal velocity at the closed boundary on the bottom face is

$$Q_{y_{i,j}}^{k+1} = 0 \quad (98)$$

Closed boundaries on the right and top cell faces are prescribed at the imaginary cells  $i+1,j$  and  $i,j+1$ , respectively.

## Wave-Adjusted Water Level and Velocity Forcing

Simulations for nearshore areas may have available boundary forcing information that does not include the presence of waves. The wave-adjusted water level and velocity boundary condition modifies the prescribed forcing values to account for waves. If water level forcing or mixed water level and velocity forcing are applied together with radiation-stress forcing, then in this boundary condition, boundary values are adjusted for wave-driven current and setup or setdown. The boundary adjustment is conducted by creating a surface deflection (setup and setdown) consistent with that of the interior solution so that radiation stress-forced flow can move smoothly through the boundary. It is

believed that this boundary condition is new to coastal circulation modeling and will be reported in more detail elsewhere (Reed and Militello, in preparation).

Adjustment to the prescribed boundary conditions is conducted by solving the 1-D continuity and momentum equations normal to the boundary, in which the radiation stress gradient is included in the momentum equation. The forms of the 1-D continuity and momentum equations for the x-direction are

$$\frac{\partial(h + \eta_b + \eta')}{\partial t} + \frac{\partial Q'_x}{\partial x} = 0 \quad (99)$$

$$\frac{\partial Q'_x}{\partial t} + \frac{\partial u' Q'_x}{\partial x} + \frac{1}{2} g \frac{\partial(h + \eta_b + \eta')}{\partial x} = -\tau_{bx} + \tau_{wx} + \tau_{sx} \quad (100)$$

in which

$$\eta = \eta_b + \eta' \quad (101)$$

where  $\eta$  is the applied boundary condition,  $\eta_b$  is the prescribed boundary value (read from a file), and  $\eta'$  and  $u'$  are the solutions from Equations 99 and 100, and  $Q'_x$  is given by

$$Q'_x = u' (\bar{h}(x) + \bar{\eta}'(x)) \quad (102)$$

where  $\bar{h}(x)$  and  $\bar{\eta}'(x)$  are denote face-centered averages that place  $h$  and  $\eta'$  at the same position as  $u'$ . If the boundary is specified a mixed water surface elevation and velocity boundary, then the  $u$ -component of velocity assigned at the boundary is modified by

$$u = u_b + u' \quad (103)$$

where  $u$  is the applied velocity at the boundary and  $u_b$  is the prescribed velocity (read from a file).

The 1-D continuity and momentum equations for the y-direction are

$$\frac{\partial(h + \eta_b + \eta')}{\partial t} + \frac{\partial Q'_y}{\partial y} = 0 \quad (104)$$

$$\frac{\partial Q'_y}{\partial t} + \frac{\partial v' Q'_y}{\partial y} + \frac{1}{2} g \frac{\partial(h + \eta_b + \eta')}{\partial y} = -\tau_{by} + \tau_{wy} + \tau_{sy} \quad (105)$$

where  $\eta'$  and  $v'$  are the solutions from Equations 104 and 105, and  $Q_y'$  is given by

$$Q_y' = v' (\bar{h}(y) + \bar{\eta}'(y)) \quad (106)$$

where  $\bar{h}(y)$  and  $\bar{\eta}'(y)$  are face-centered averages that place  $h$  and  $\eta'$  at the same position as  $v'$ . If the boundary is specified as a mixed water surface elevation and velocity boundary, then the  $v$  component of velocity assigned at the boundary is modified by

$$v = v_b + v' \quad (107)$$

where  $v$  is the applied velocity at the boundary and  $v_b$  is the prescribed velocity (read from a file).

The wave-adjusted boundary condition is demonstrated for an idealized beach in Appendix G.

# 5 Model Features

---

Features have been implemented into M2D to improve the representation of calculated hydrodynamics and to provide flexibility to the user. This chapter describes these features and provides information on model options. Topics covered are: flooding and drying, hot-start options, model spin-up, coupling with larger-scale circulation models, coupling with wave models, and output options.

## Flooding and Drying

Numerical modeling of shallow-water areas with expansive tidal or wind-tidal flats is most accurately performed if realistic and robust flooding and drying algorithms are included in the computations. Representation of flooding and drying also eliminates the need to modify grid depth to avoid artificially induced instabilities. Numerical simulation of flooding and drying of cells or elements in hydrodynamic models has been performed with various techniques such as application of barrier and weir equations (Reid and Bodine 1968; Butler 1978; Wanstrath 1978) and moving boundaries (Yeh and Chou 1978). A simple and robust flooding and drying algorithm has been implemented to represent inundation and drying of shallow areas of the model domain.

Criteria were established for the flooding and drying algorithms implemented in M2D and are given in Table 2. The criteria were specified so that the algorithms would produce realistic behavior, and numerical problems, such as oscillations and flutter, would be minimized.

<b>Table 2 Criteria for Flooding and Drying Algorithms</b>	
<b>Flooding</b>	<b>Comments</b>
Water depth must exceed a predetermined minimum depth in adjacent cells	Transfer of physically meaningful water volume, avoids flutter
Water must be moving toward dry cell	Takes into account wind-induced setup, avoids instability
<b>Drying</b>	<b>Comments</b>
Total water depth is less than predetermined minimum depth	Definition of drying

Every wet cell is checked to determine whether or not it has dried after new water level and velocity values have been calculated over the model domain. The criterion for a cell to be dry is

$$H_{i,j} = h_{i,j} + \eta_{i,j} \leq H_{cr} \quad (108)$$

where  $H_{i,j}$  is the total water depth, and  $H_{cr}$  is a depth below which drying is assumed to occur. If a cell or its adjacent neighbor to the south or west has become dry, restrictions on flow between the two cells are imposed. Restrictions governing flow across the two faces are imposed for the following conditions:

a. Both cells on each side of a face are dry

$$H_{i,j} \leq H_{cr} \text{ and } H_{i-1,j} \leq H_{cr}, \quad u_{i,j}^k = u_{i,j}^{k+1} = 0 \quad (109)$$

$$H_{i,j} \leq H_{cr} \text{ and } H_{i,j-1} \leq H_{cr}, \quad v_{i,j}^k = v_{i,j}^{k+1} = 0 \quad (110)$$

This restriction sets the velocity at the face to zero so that there is no transfer of water between dry cells.

b. Neighbor to south or west is dry, and cell  $i,j$  is wet

$$H_{i,j} > H_{cr} \text{ and } H_{i-1,j} \leq H_{cr} \text{ and } u_{i,j}^k > 0, \quad u_{i,j}^k = u_{i,j}^{k+1} = 0 \quad (111)$$

$$H_{i,j} > H_{cr} \text{ and } H_{i,j-1} \leq H_{cr} \text{ and } v_{i,j}^k > 0, \quad v_{i,j}^k = v_{i,j}^{k+1} = 0 \quad (112)$$

This restriction sets the velocity at the face to zero if the velocity at the previous time-step indicates transfer of water from a neighboring dry cell to the wet cell  $i,j$ . Water is allowed to flow from the wet cell to the neighboring dry cell.

c. Neighbor to south or west is wet, and cell  $i,j$  is dry

$$H_{i,j} \leq H_{cr} \text{ and } H_{i-1,j} > H_{cr} \text{ and } u_{i,j}^k < 0, \quad u_{i,j}^k = u_{i,j}^{k+1} = 0 \quad (113)$$

$$H_{i,j} \leq H_{cr} \text{ and } H_{i,j-1} > H_{cr} \text{ and } v_{i,j}^k < 0, \quad v_{i,j}^k = v_{i,j}^{k+1} = 0 \quad (114)$$

This restriction sets the velocity at the face to zero if the velocity at the previous time-step indicates transfer of water from dry cell  $i,j$  a neighboring wet cell. Water is allowed to flow from the neighboring wet cell to the dry cell  $i,j$ .

## Hot-Start Capabilities

M2D has two hot-start capabilities and both can be invoked during a simulation. The two hot-start types are:

- a. Hot-start file written once during a simulation at a user-specified time. The file name prefix is given by the user. This file can be opened in future simulations to initialize M2D at a convenient time, such as after the model has spun up.
- b. Hot-start file written at user-specified intervals. If this option is invoked, M2D will alternate hot-start file names `HOTSTART1.M2I` and `HOTSTART2.M2I` each time a hot-start file is written. An information file called `HOTSTART.INFO` is also written that contains the name of the last hot-start file that was written and the simulation time, in hours, when the hot-start file was saved. These hot-start files are helpful in restarting simulations that terminate unexpectedly, such as by power outage.

## Model Spin-Up: Ramp Function

Model spin-up is controlled by a hyperbolic tangent function that scales the model forcing over a user-specified interval. A time-dependent scaling factor  $f_{ramp}$  is computed as

$$f_{ramp} = \tanh\left(4.5\frac{t}{T_{ramp}}\right) \quad (115)$$

where  $T_{ramp}$  is the time over which the model is spun up. All model forcing is multiplied by the scaling factor over the duration of the ramp. After the simulation time exceeds the ramp duration, the scaling factor is set to 1.0.

## Coupling with Larger-Domain Model

M2D can be operated as a detailed inset of a larger-domain model. This capability provides a means of maintaining hydrodynamic properties at the M2D boundaries, flexibility in resolution over the project area, and application of options contained within M2D that may not be available in other models. Coupling can be invoked by application of water surface elevations or the combination of water surface elevations and velocities as M2D forcing boundaries, where the values have been obtained from a larger-domain model. SMS provides an automated procedure for extracting and mapping boundary information from a larger-domain model to M2D (see Chapter 6 for details).

M2D can accept boundary information from any larger-domain model, including another M2D project. Considerations for coupling with a larger-domain model are discussed here with an example shown for M2D forced by water surface elevations and velocities calculated by ADCIRC. If a larger-domain model is to provide boundary conditions for M2D, mesh or grid resolution of the larger-domain model in the area of the M2D boundary must be sufficient to describe details of the hydrodynamic field at the scales required for the particular project. Figure 8 shows an M2D grid overlaid on a portion of an ADCIRC mesh developed for Shinnecock Inlet, NY. Distances between ADCIRC nodes are a few times larger than the M2D cell sizes, but are not greatly larger. If the ADCIRC nodes were spaced further apart, having only a few nodes in the vicinity of the M2D boundary, details of the flow field would not be adequately described to capture the inlet and ocean hydrodynamics of the area.

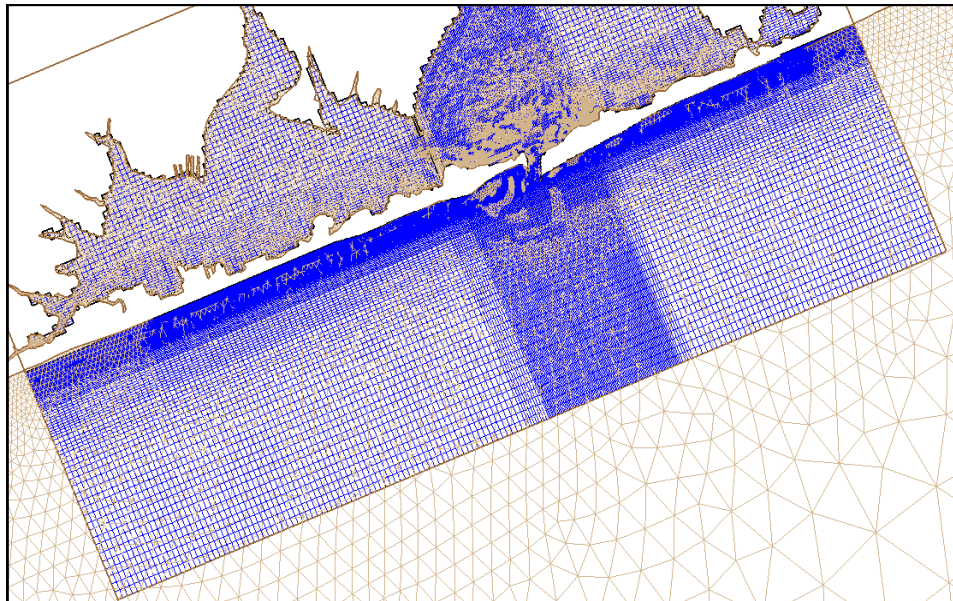


Figure 8. M2D grid and ADCIRC mesh for Shinnecock Inlet, NY

Temporal resolution of the boundary information provided to M2D from the larger-domain model must also be considered. Output frequency of larger-domain model solutions should be set to minimize error in forcing for the scales of motion calculated. As an example, water level curves calculated by the function  $\eta = \sin(2\pi t / 12.42)$ , where  $t$  is in hours, and output at increments of 1.0 and 0.25 hr are shown in Figure 9. Output at 0.25 hr produces a curve that describes the water level significantly better than the curve output at 1.0 hr. An example of the error introduced by the 1-hr interval output is shown at the second peak, in which a 3-cm difference is encountered.

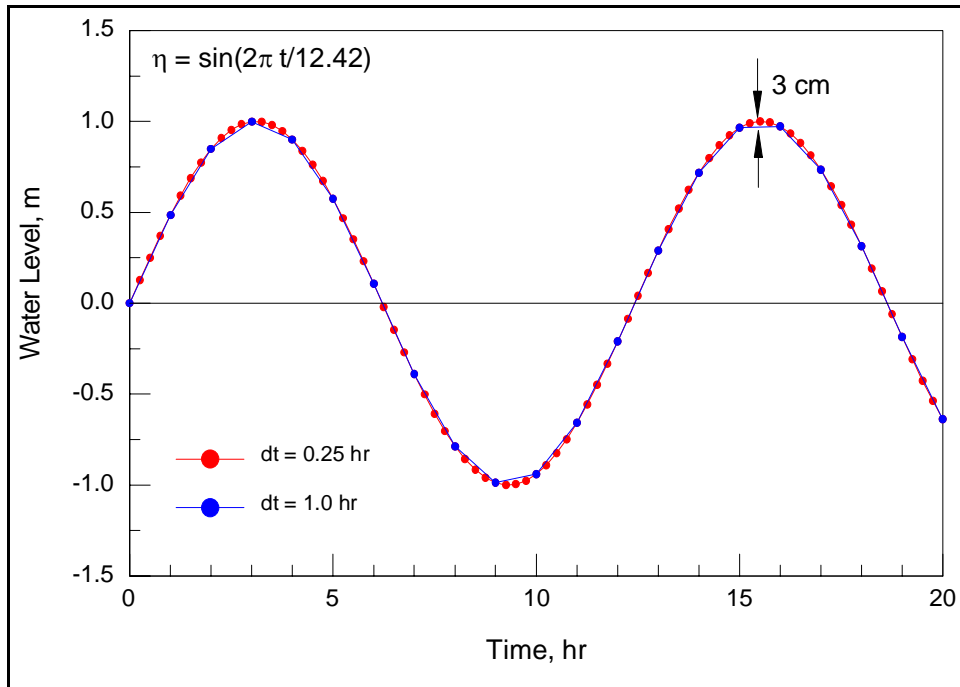


Figure 9. Time discretization of a sinusoidal water level curve

## Coupling with STWAVE

M2D and STWAVE can be coupled through the SMS Steering Module (refer to Chapter 6 for details). Coupling can be conducted by forcing M2D with radiation-stress gradients calculated by STWAVE and by applying currents and water depth ( $h + \eta$ ) calculated by M2D as input to STWAVE. The user has the option of selecting one or more of these linkages. Guidance is provided here to assist the user in setting up a correct and successful coupled simulation.

M2D and STWAVE calculate on different coordinate systems that may or may not be aligned, depending on the orientation of the shoreline relative to geographic coordinates. The coordinate system for M2D is  $\pm 45$  deg from geographic coordinates, meaning, that positive  $x$  is directed within 45 deg of east and positive  $y$  is directed with 45 deg of north. An angle provided in the M2D control file defines the deviation of the M2D grid from geographic coordinates. STWAVE operates on a grid aligned such that the  $x$ -axis is directed onshore and the  $y$ -axis is directed alongshore. Figure 10 shows three examples of M2D and STWAVE coordinates for different shoreline orientations. Each model must be independently set up so that its coordinate system is consistent with its computational approach. For coupling, the M2D and STWAVE grids overlap and information is mapped from one model to the other. SMS automatically calculates any required rotations of components when mapping fields between STWAVE and M2D.

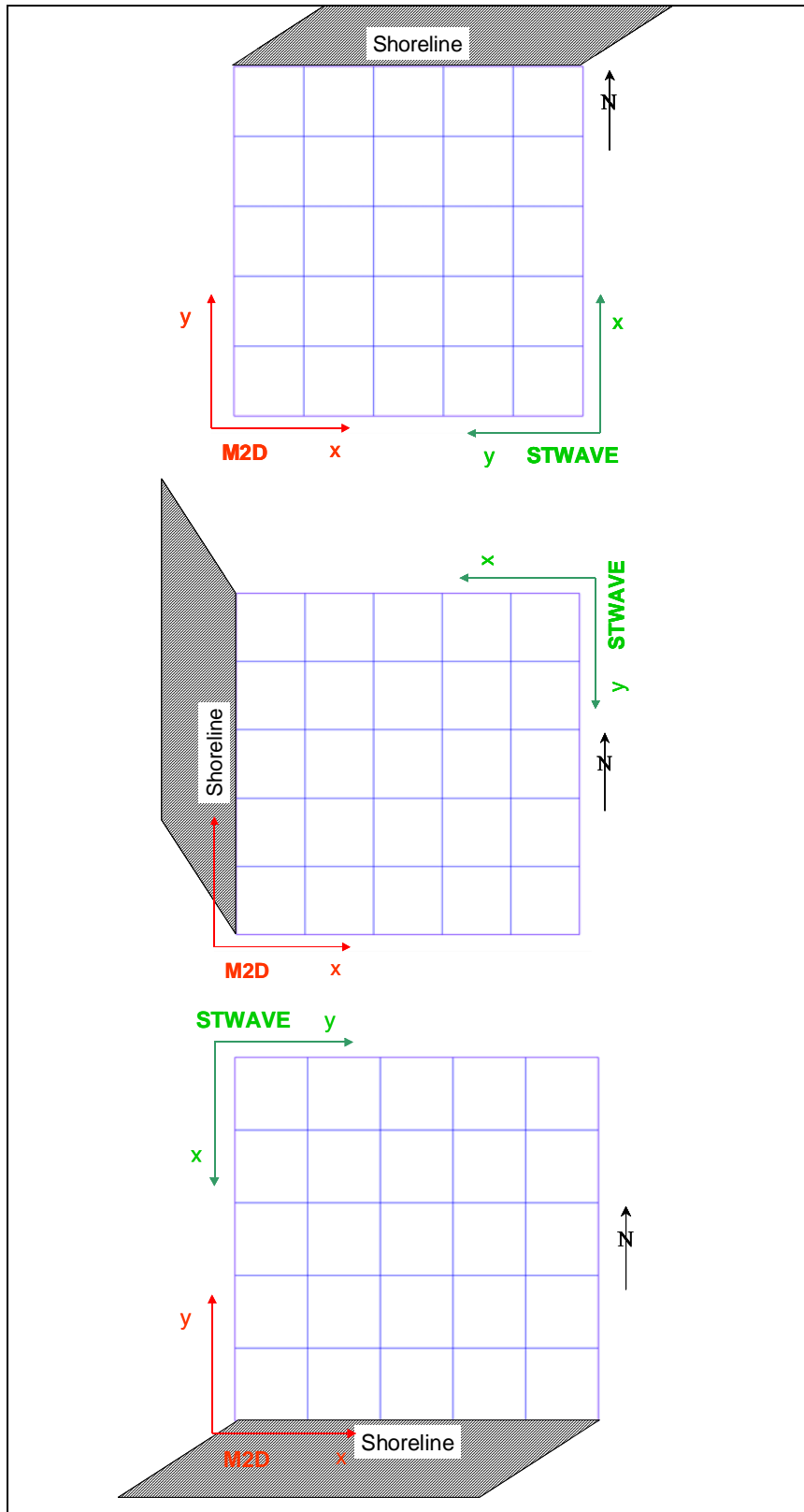


Figure 10. Example M2D and STWAVE grid orientations

In areas of the computational domain where wave breaking or strong wave-current interaction takes place, resolution for M2D and STWAVE should be similar. By specifying cells in both models to have similar spacing, coupling efficiency is maximized because high-resolution details calculated by one model are not lost when the solution field is mapped to the other model. Figure 11 shows STWAVE and M2D grid spacing in the nearshore area. Surf zone width is indicated by the line denoting 10 STWAVE cells. In this area, M2D and STWAVE have similar spacing in the cross-shore. Cell sizes in the M2D grid become larger seaward of the surf zone.



Figure 11. Example M2D and STWAVE grid spacing

Coupling M2D and STWAVE requires that the user specify the steering interval, or elapsed time between calls to STWAVE. Selection of the steering interval is dependent on the processes that are most significant to the goals of the modeling effort. A smaller steering interval tightens coupling between the models, increasing accuracy. However, smaller steering intervals require more STWAVE runs and thus increase the overall computation time. Thus, the user must balance the cost of run time versus accuracy.

Temporal scales of processes being modeled also play a role in the selection of the steering interval. For example, if a mean wave condition is being applied in a predominantly tidal situation and the wave properties do not change much over time, the steering interval can be set to a relatively large value. If a storm is being modeled and full coupling between STWAVE and M2D is required, then the steering interval should be set to a smaller value. If a situation is studied in which there is strong wave-current interaction, such as at an inlet, then a shorter steering interval may be specified to capture the modification of the waves by the tidal current and the time-varying water level. Typical steering intervals are 3 hr for fair weather conditions, and for storm waves the steering interval should be more frequent. Judgment and experience must be exercised, as for all numerical models, and sensitivity analysis is recommended for a particular application to determine the most appropriate steering interval.

## Output Options

M2D provides two types of output that can be selected by the user. Time series of calculated variables at specific cells, called observation cells, can be saved at user-specified time intervals. Global fields can be written at user-specified times.

All variables are output at their computational location in the cell. Thus, water surface elevation is at the cell center, the  $u$ -component of velocity and  $x$ -component of flow rate are at the left cell face, and the  $v$ -component of velocity and  $y$ -component of flow rate are at the bottom cell face.

### Observation cell time series

Time series of water surface elevation,  $u$ -component of velocity,  $v$ -component of velocity,  $x$ -component of flow rate, and  $y$ -component of flow rate can be saved at observation cells. The user can specify any number of cells as observation cells. Any combination of variable output may be selected ranging from one to all five previously listed. A time interval for output must be specified and the most accurate output is achieved if the output interval is specified as an integer multiple of the calculation time-step. Observation cell output will take place from the start to the end of the simulation. The SMS interface provides tools for specifying all aspects of the observation cell output. Time series of each variable selected for output is written to a separate file and

values for all observation cells are included in that file. Chapter 7 describes the format and provides an example of the time series observation cell output files.

### **Global field output**

Global output of water surface elevation and velocity components can be written at user-specified times. Water surface elevations are written to a separate file from the global velocities. M2D reads a file containing times at which global output is specified for each variable (water surface elevation or velocity). Thus, global output times for the two files are not required to be concurrent, and the increment between successive times does not have to be constant. By specifying discrete time stamps, the user has flexibility for creating global files with more dense temporal resolution during certain time intervals. The SMS interface provides tools for specifying all aspects of the global output. Chapter 7 describes the format and provides an example of the global output files.

# 6 Surface-Water Modeling System Interface for M2D

---

A graphical interface for M2D has been implemented within the SMS Versions 8.0 and higher that contains tools for grid development, parameter specification, control file setup, boundary specification including extraction of water surface elevation and/or velocities from regional models such as ADCIRC, model runs, post-processing of global field values, visualization, and coupling of M2D with STWAVE through the Steering Module. This chapter provides instruction on creating and working with M2D projects within the SMS. Dialogs shown are from SMS 8.1.

Access to the M2D interface is obtained through the 2D Cartesian Grid Module in SMS. The Cartesian Grid Module also accesses the Map Module via an M2D Coverage. The interface for M2D includes:

- a. M2D Coverage and Map tools
- b. Cartesian Grid Module (tools and display options)
- c. M2D Menu
- d. Steering Module

## Required Information

An M2D grid is a Cartesian Grid with cells that may be of varying sizes. Each cell has a location, side dimensions ( $\Delta x$  and  $\Delta y$ ), and depth. Grid definition within SMS includes:

- a. A geographic location – the position of the first cell and the orientation of the grid.
- b. Dimensions – domain extent and number of cells in each direction.
- c. Cell sizes – the width of each column and height of each row in the grid.
- d. Depths – the water depth at the center of each cell.

The SMS interface provides tools and methodology for the user to define each of these components and to develop the grid. Depths over the model domain are the most complex component of the grid because these values can represent any geometric shape. Bathymetric information is provided to the SMS by the user as either a constant depth, or as a set of data points each of which has a depth associated with it. SMS can read Digital Elevation Model (DEM) grids or scattered data point surveys and display them as a surface to show the area over which a grid will be generated. A typical scattered data set is illustrated by the red crosses in Figure 12. SMS interpolates scattered data to the grid to define the depths at each cell. For more information on scatter data sets and the Scattered Data Module refer to the SMS Help file or the SHOALS toolbox documentation (Wozencraft et al. 2002).

After depth values are defined, the user specifies the position, orientation and extent of the grid using a rectangular object called a grid frame. Simple grids with constant-sized cells can be created in the Cartesian Grid Module. More complex grids are created in the Map Module.

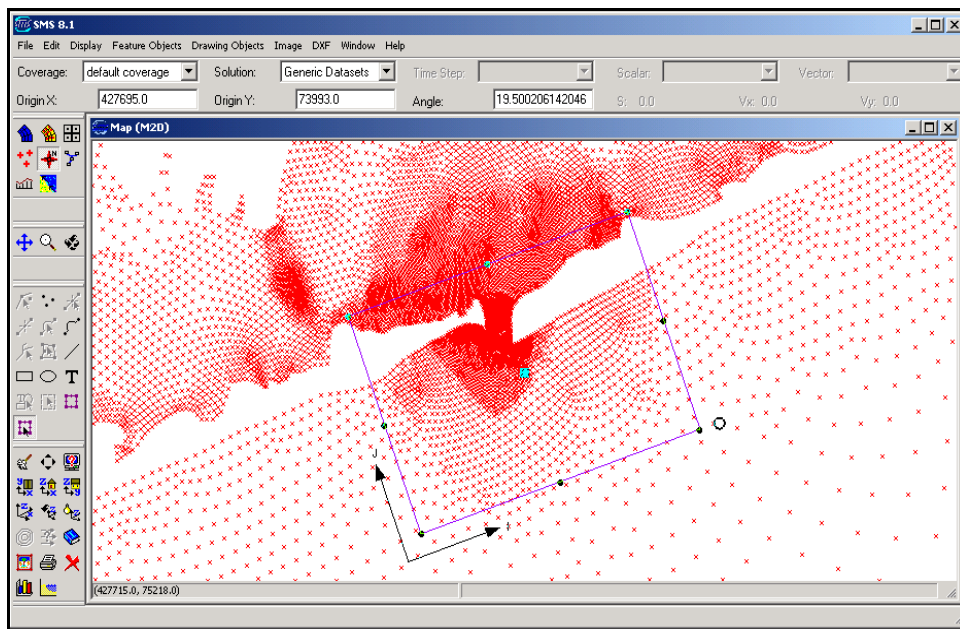


Figure 12. Grid frame around scattered data points

## Grid Generation from M2D Coverage

Most grids will be developed within the Map Module. Information in the Map Module is stored in layers or coverages. Each coverage has a specific type, which defines the properties of the information stored in that layer. SMS includes an M2D coverage type to allow the definition of an M2D simulation. There is a default coverage in SMS at all times. This coverage can be used to create an M2D coverage by changing its type or a new coverage with type M2D

can be created. Either of these options can be invoked by issuing the *Coverages* command in the *Feature Objects* menu in the Map Module. By changing the default coverage to be an M2D coverage, the modeler has instructed SMS to create M2D grids from the information being entered.

### Grid frame creation and editing

With an M2D coverage active, the grid frame is defined by selecting the *Create Grid Frame* tool . When this tool is active, clicking in the main display window of SMS defines the position and extents of a grid frame. The first click defines the origin of the grid, the second click defines the bottom edge of the grid and its size in the “I” direction, and a third click defines the size of the grid frame in the “J” direction. A new grid frame or enclosing shape for the grid is created on the screen (Figure 12). This grid frame can be moved, rotated, enlarged or reduced in size either graphically or by accessing edit windows before the grid is generated to fill the frame.

To edit a grid frame, the modeler selects the *Select Grid Frame* tool  and clicks on the grid frame to be edited. Handles appear at the corners and sides of the selected grid frame as shown in Figure 12. The user may drag any of these handles to change the size and position of the grid frame. A circular handle that extends from the “I” axis of the grid frame can be dragged to change the orientation of the grid frame. The following graphical editing operations and their functions are available when a grid frame is selected:

- a. Move Frame - Click the box located at the center of the frame interior and drag.
- b. Resize Frame - Click a highlighted corner or edge and drag to resize.
- c. Rotate Frame - Click inside the circle near the bottom right corner of the frame and drag to rotate the frame.

Grid frame parameters can also be explicitly modified using the edit window at the top of the screen. These parameters are:

- a. Grid Origin – The X and Y edit fields at the top of the screen allow the user to explicitly specify the bottom left corner location of the grid frame.
- b. Angle of rotation – The angle edit field at the top of the screen can be used to set the angle that the grid frame will be rotated counterclockwise from the +x-axis. This angle should be between -45 and 45 deg.

The grid frame size is displayed at the lower edge of the screen as it is being edited.

## Grid generation

After the grid frame is defined, an M2D grid is generated in SMS with the *Feature Objects / Map -> 2D Grid* command. This command opens the *Map->2D Grid* dialog. For a simple grid frame, this dialog allows the user to specify the number of cells in each direction (or the cell size in each direction) and the source for depth data. The resulting grid will consist of constant-sized cells.

M2D allows varying cell sizes to provide greater resolution in areas where needed. The interface provides for the development of grids with greater resolution in specific areas through the creation of refine points. A refine point is produced by creating a feature point  at the location where specific resolution is to be assigned. Double clicking on the feature point (with the Select Feature Point tool  active) invokes the *Refine Point* attributes dialog. This dialog allows for specification of cell sizes around the point, spatial change in cell sizes with distance from the refine point, and a maximum cell size. For the settings shown in Figure 13, the cell around the refine point would be a 10-m  $\times$  10-m cell, the cells would get 10 percent bigger with each row or column, and the largest cell would be 20 m  $\times$  20 m.

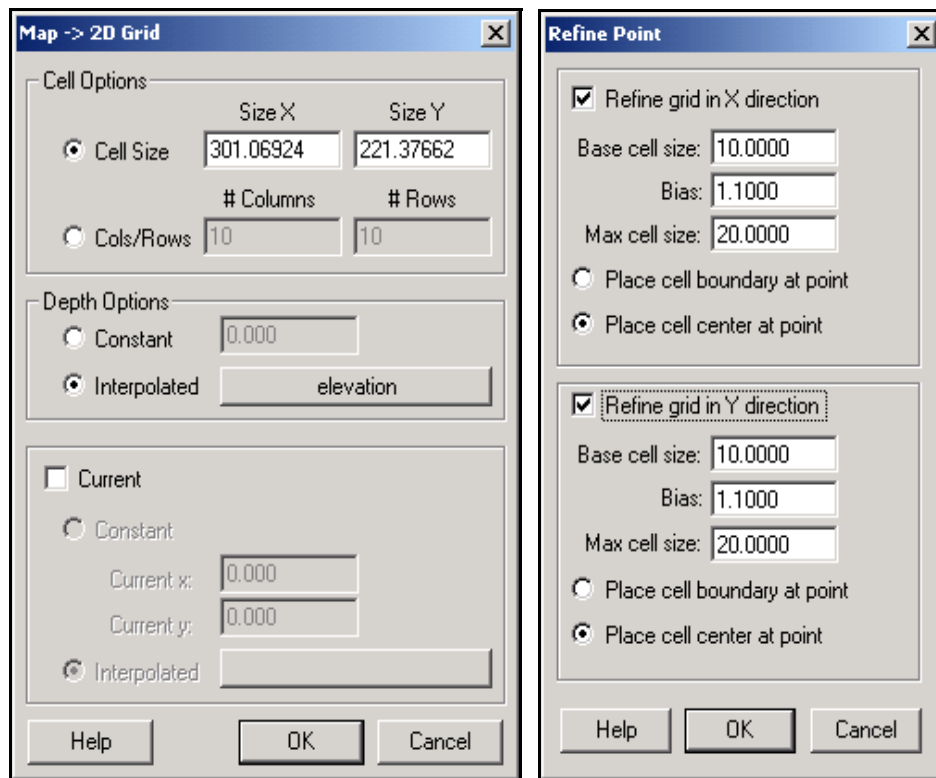


Figure 13. *Map-> 2D Grid* and *Refine Point* dialogs

When refine points are present in the M2D coverage, the top portion of the *Map->2D Grid* dialog is dimmed out. SMS will generate cells that match the

refine point specifications. If multiple refine points are present and conflict with each other, cells will be created to meet the criteria of all refine points as closely as possible. Figure 14 shows a grid developed with a refine point in the inlet and cell strings around the grid boundary.

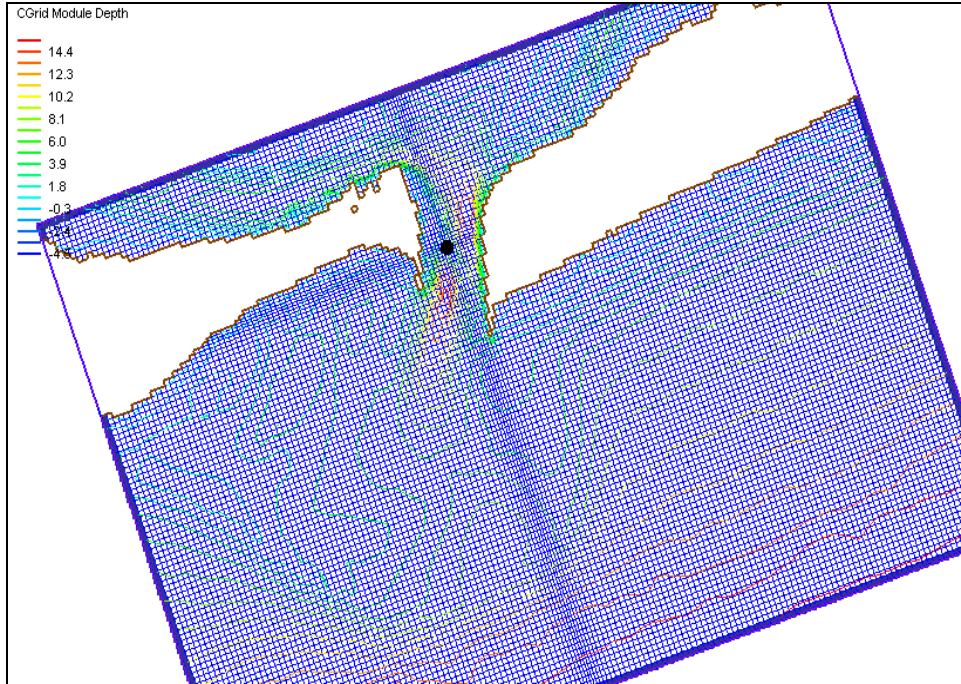


Figure 14. SMS generated grid

Each cell will be assigned a depth based on the depth option, and cells will be assigned to be land or water based on the resulting depths. However, the modeler may force islands, or other coastline features into a grid by creating arcs with the Create Feature Arc tool . These arcs will then represent the coastline in the M2D coverage. Attributes of the arc can be specified by selecting the arc with the Select Feature Arc tool  and then clicking on *Feature Objects* in the pull-down menu, then entering the *Attributes* dialog (Figure 15). Cells generated along this arc will be treated as specified by the arc type. By default, cells intersected by these coastline arcs are classified based on the percent of the cell on the “land” side (percent preference arc). If more than half the cell is land, the cell is classified as land. However, in some situations, the model may require a continuous stretch of either land or water to represent a specific shoreline feature, such as a jetty or narrow canal. In these situations, the coastline arcs may also be flagged as “land” or “water” preference. Thus, the three options for arc preferences are:

- a. Percent preference: If more than 50 percent of the cell through which the arc cuts is land, then the cell will be land. If more than 50 percent of the cell is water, then the cell will be water.

- b. Land preference: Forces cells lying on the arc to be land.
- c. Water preference: Forces cells on the arc to be water.

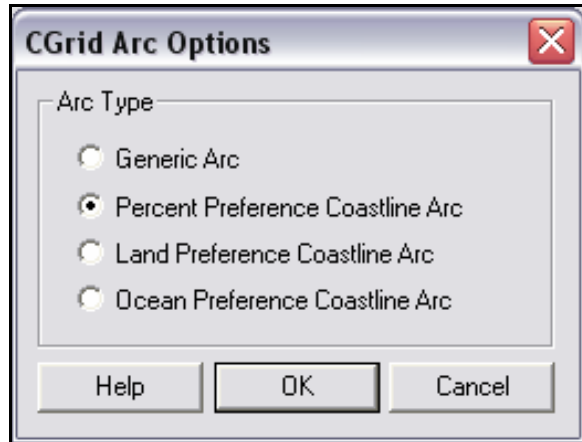


Figure 15. Arc options for generating coastlines

After an arc type is specified, selecting the arc will reveal the water and land sides of the arc, which are displayed as blue and brown arrows, respectively. If the water and land sides of the arc are opposite from what they should be, the arc direction can be reversed by clicking *Reverse Arc Direction* under the *Feature Objects* pull-down menu.

The *Map->2D Grid* command also creates cell strings across all ocean boundaries of the grid. These strings are described in the following section and are tools for assigning boundary conditions for the numerical model run.

## Cartesian Grid Module

The 2D Cartesian Grid Module  contains tools for editing 2D Cartesian finite difference grids. These grids consist of cells aligned with a rectilinear coordinate system. An existing grid can be read in from an M2D simulation file, or created through the Map Module. With a grid in memory, the following tools are available to edit the grid:

### Select Cell

The Select Cell tool is used to select a grid cell. A single cell is selected by clicking on it. A second cell can be added to the selection list by holding the SHIFT key while selecting it. Multiple cells can be selected at once by dragging a box around them. A selected cell can be de-selected by holding the SHIFT key as it is clicked.

When a single cell is selected, its Z coordinate is shown in the Edit Window. The Z coordinate can be changed by typing a new value in the edit field, which updates the depth function. If multiple cells are selected, the Z coordinate field in the Edit Window shows the average depth of all selected cells. If this value is changed, the new value will be assigned to all selected cells.

With one cell selected, the Edit Window shows the cells  $i,j$  location. With multiple cells selected, the Edit Window shows the number of selected cells.

### **Select Row/ Select Column**

The Select Row and Select Column tools are used to select cell rows and columns. Multiple rows and columns are selected in the same manner as selecting multiple individual cells: holding the SHIFT key, etc.

### **Insert Column/ Insert Row**

When the Insert Column or Row tools are active, clicking within a cell splits the row/column containing the selected cell, creating a new row or column in the grid. The Z-values of all split cells are the same as the original cells values.

### **Drag Column/ Drag Row Boundary**

The position of the edge of rows or columns in a grid can be changed with the Drag Column or Row tools. These tools make one column/row narrower while making its neighbor wider.

These tools allow for manual specification of the resolution in specific portions of the grid. Note that depth values are not adjusted so significant dragging of boundaries should be avoided, or depths should be reinterpolated after the boundaries are modified.

### **Create Cell String**

The Create Cell String tool allows the modeler to group a string of cells together for the purpose of assigning boundary conditions. Cell strings are created automatically around water boundaries when a grid is generated. The user may create others as desired or delete and replace the automatically-generated cell strings. When the Create Cell String tool is active, the modeler selects each cell to be added to the string. By holding down the SHIFT key, all

boundary cells between the previously selected cell and the selected cell are added to the cell string.

## **Select Cell String**

To specify a boundary condition, the modeler must create a cell string over the desired region, and then select the cell string while the Select Cell String tool is active. Boundary conditions applied to the selected cell string are assigned through the *Assign BC* dialog, which is accessed through the M2D pull-down menu.

## **M2D Menu**

The M2D menu includes commands for managing the simulation. The management operations are editing boundary conditions and cell attributes, checking the simulation for common errors, and running a model. Commands from the menu are explained in the following sections:

### **Delete Simulation**

The *Delete Simulation* command deletes the 2D grid and all information associated with it.

### **Assign BC**

The *Assign BC* command allows the user to assign a boundary condition to the cell string through the *M2D Boundary Conditions* dialog (Figure 16). This command is only active if a cell string is first selected.

Boundary conditions specified within this dialog include the following:

- a. **Unassigned Boundary:** When a cell string is created, the string receives this assignment. This designation is not a boundary condition, but rather indicates that the boundary has not been assigned yet and has no influence on the model.
- b. **Flow Rate-forcing:** This type of boundary condition allows the modeler to define a time series of flow rates to be prescribed at the boundary. The time series associated with this boundary contains a list of times and flow rates in  $\text{m}^3/\text{s}$  to be applied at boundary cells. Each cell contained in

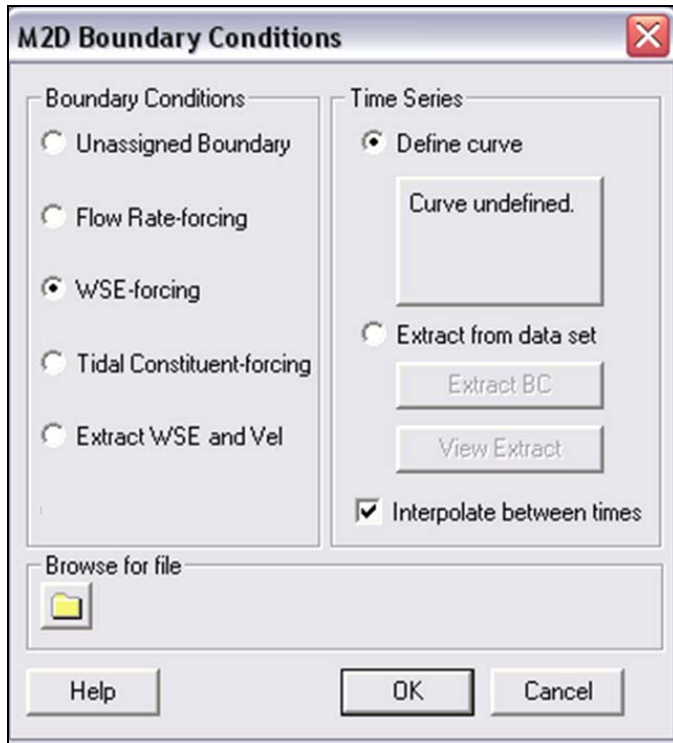


Figure 16. *M2D Boundary Conditions* dialog

the cell string will have the prescribed flow rate. Time series can be developed within SMS by entering the *Define Curve* dialog.

Alternatively, a pre-existing file can be assigned by clicking on the *Browse* for file tab. If the Interpolate box is checked, M2D linearly interpolates between flow rate values at every time-step. If the Interpolate box is not checked, boundary flow rate values are only updated at the times that they are provided in the input file.

- c. WSE-forcing: This type of boundary condition allows the modeler to define a time series of water level. The time series associated with this boundary contains a list of times and water levels in meters to be prescribed along the boundary. The Interpolate between times checkbox instructs M2D on how the time series water level information is to be treated within M2D when forcing a boundary. If the Interpolate box is checked, M2D linearly interpolates between water level values at every time-step. If the Interpolate box is not checked, water level values applied as boundary conditions are only updated at the times that they are provided in the input file. Two options for assigning a water surface elevation boundary condition are available as follows:
  - (1) Single time series across a boundary: Time series of water surface elevation can be developed with SMS by clicking on the

*Define Curve* button. Alternately, a pre-existing file can be assigned by clicking on the *Browse* file tab.

- (2) Multiple time series across a boundary: SMS detects if a regional model such as ADCIRC and its global water surface elevation solution are loaded, and activates the extract from data set capability as a possible source of the boundary condition. When the boundary condition is assigned to be an extracted boundary condition, SMS prompts the user to specify the source of the extracted information (a functional data set from the regional model) using the *Extracted Boundary Condition* dialog. Extraction of water surface elevations is available for specification of boundary conditions from any regional 2-D model that can be brought into SMS.
- d. Tidal Constituent-forcing: These boundary conditions apply up to eight tidal constituents to force water surface elevations along the selected cell strings. Tidal constituents are specified within the *M2D Tidal Constituent* dialog accessed in the *Model Control* dialog.
- e. Extract WSE and Vel forcing: For this boundary condition type, SMS detects if a regional model, such as ADCIRC, and its global water surface elevation and velocity solution files have been loaded, and activates the extract capability as a possible source of the boundary condition. When the boundary condition is assigned to be an extracted boundary condition, SMS prompts the user to specify the source of the extracted information (a functional data set from the regional model) using the *Extracted Boundary Condition* dialog. Both water surface elevation and velocity from the regional model must be present to extract values for this boundary type. Extraction of water surface elevations and velocities is available for specification of boundary conditions from any larger-domain 2-D model that can be brought into SMS.

File formats for use with M2D are described in Chapter 7 and Appendix A.

## Delete BC

The *Delete BC* command allows the user to delete the boundary condition assigned to a cell string. A cell string must be selected to activate this command.

## Assign Cell Attributes

The *Assign Cell Attributes* command (Figure 17) allows the modeler to set the status for one or more selected cells. A cell can be active (water), inactive (land), or observation. Observation cells are numerical stations and assigned to be active. Bottom roughness can also be specified through this dialog.



Figure 17. *Assign Cell Attributes* dialog

Observation cells can be assigned so that M2D will write time series of water surface elevation and velocity, and/or flow rate output files. Settings for output files written for observation cells are specified in the Output Control portion of the *Model Control* dialog discussed later in this chapter.

## Merge Cells

The *Merge Cells* command allows the modeler to merge consecutive rows or columns into one. The command is enabled only if rows or columns have been selected with the appropriate tool (select row or column).

## Model Check

The *Model Check* command performs a number of checks on the simulation to ensure a valid model. These checks are:

- a. All water boundaries have boundary conditions specified.
- b. Cell aspect ratio is no greater than 2.
- c. Maximum time-step size is suggested according to an internal calculation made within SMS.
- d. Correct model control specifications (i.e., if a tidal boundary exists, make sure that tidal constituents have been defined for forcing).

## Model Control

The *Model Control* command displays the *Model Control* dialog (Figure 18). Input and output file names are specified from within the *M2D Model Control*. In addition, the user defines the time control associated for the simulation from within the *Model Control*. A wind-forcing file can also be assigned from within the *Model Control*. Options within this dialog include the following:

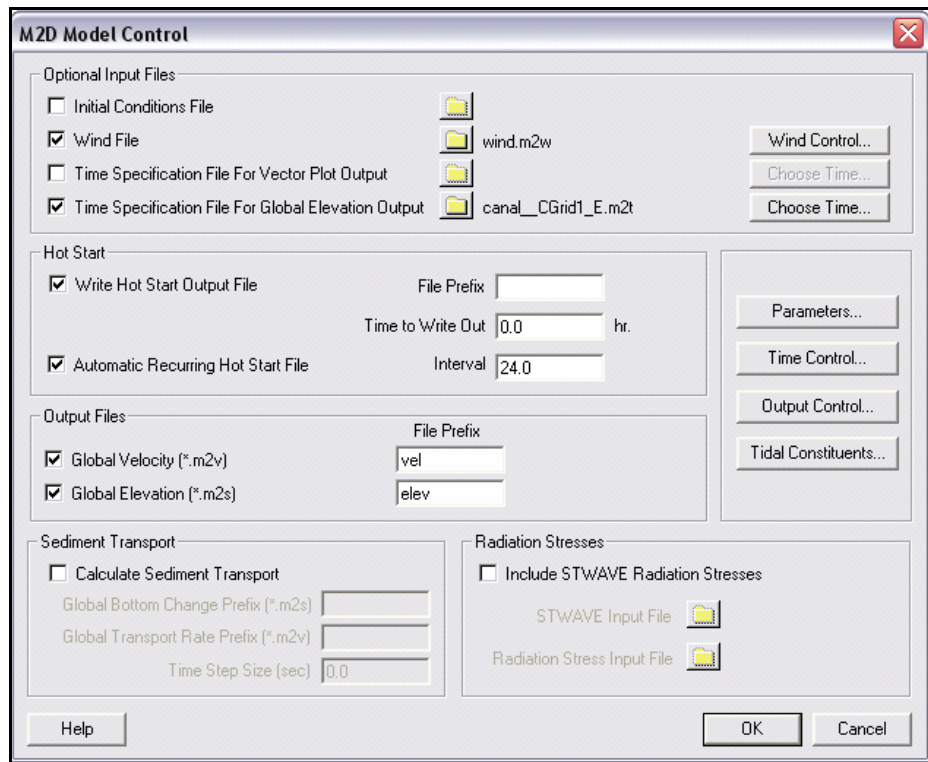


Figure 18. *M2D Model Control* dialog

**Optional input files.** Although not required, externally-generated input files can be accessed in the simulation. By turning on the toggle next to each input file type, an already-existing file can be selected by clicking on the *File Browse* button. If none exists, the user can manually create the input file by clicking on the button to the right that identifies each file type. For example, in Figure 18, a wind input file will be read by M2D and it is called “wind.m2w.” Alternatively, the user can specify the wind information by entering the *Wind Control* dialog.

**Initial conditions (\*.m2i).** The initial conditions file contains a line for every cell in the grid containing information on the state and status of each cell. This information includes cell identification number, depth, water surface elevation,  $u$ - and  $v$ -components of velocity,  $\partial\eta/\partial t$ , and  $u'$  and  $v'$  (solutions of Equations 100 and 105). Status of cell activity and boundaries are also provided. A full description of the initial conditions file is given in Chapter 7.

**Wind (\*.m2w).** The wind file contains a list of time-steps containing wind magnitude and direction. Each line contains three values: time (hours), magnitude (m/s), direction from (deg). Wind directions are referenced as from north = 0 deg, from east = 90 deg, etc. Note that this wind direction convention is different from the convention described for the governing equations (Chapter 2). M2D converts the wind velocity from the input file convention to the computation convention internally. Clicking the *Wind Control* button brings up a dialog where wind magnitude and direction time series can be specified.

**Time specification for vector plot output (\*.V.m2t).** The *Time Specification* dialog allows the user to specify time stamps for global solution output (in hours). The vector plot output time specification corresponds to the global velocity solution file (\*.m2v). Time increments between global output can vary, allowing the user to have more or less frequent output.

**Time specification for global elevation output (\*.E.m2t).** The *Time Specification* dialog allows the user to specify time stamps for global solution output (in hours). The scalar plot output time specified is associated with the times at which M2D will write out the global elevation file (\*.m2s). Time increments between global output can vary, allowing the user to have more or less frequent output.

**Hot start.** Two independent hot start options are available for M2D. Checking the Write Hot Start Output File box allows the user to specify a time at which a file of the same format as the initial conditions file will be written. The hot start file can be later used as an initial conditions file for subsequent model runs. The user specifies a prefix for the hot start file name and the elapsed time, in hours, at which the file will be written. By checking the Automatic Recurring Hot Start File box and providing a time interval (hours), hot start files will be written at the time interval specified. Hot start files are written with file names alternating with HOTSTART1.M2I and HOTSTART2.M2I. These files can be later input as initial conditions files for a subsequent simulation. The file HOTSTART.INFO is also written and contains the name (HOTSTART1.M2I or HOTSTART2.M2I) and time of the last saved hot start file.

**Global velocity output (\*.m2v).** By checking this toggle box, a global velocity solution will be written out by M2D at the times specified in the *M2D Output Time Specification* dialog for Vector Plot. The file extension “.m2v” is appended to the prefix specified. The global velocity file format contains a line with the time-step, followed by subsequent lines for each grid cell with four values:  $x$ -position in present coordinate system,  $y$ -position in present coordinate system,  $u$ -component of velocity, and  $v$ -component of velocity. Position values have units of meters and velocity values have units of m/s.

**Global elevation output (\*.m2s).** The explanation provided for the Global Velocity applies here as well, with the difference being that a global elevation solution will be written out. The global elevation file format is the same as that of the global velocity solution file, with the exception that the  $u$ - and  $v$ -component velocity values are replaced by the water level in meters at each cell.

**Global bottom change output (\*.m2s).** The file written out for the global bottom change file is associated with sediment transport. This file also contains the “.m2s” extension, so the prefix should be different from that for the global elevation solution file. The format is the same as the global elevation file, except that the water level value at each cell is replaced by the depth in meters.

**Parameters.** The *Parameters* button invokes a *Model Parameters* dialog that allows specification of anemometer height, the ratio of air to water density, the latitude of the grid, momentum equation options, and wetting/drying parameters. Standard anemometer height is 10 m, but data may be obtained from an anemometer installed at a different height, which can be specified in the *Model Parameters* dialog. The ratio of air to water density is 0.0012 and should not be modified. Momentum equation options let the user specify whether or not to include, independently, the advective and diffusion terms. Wetting and drying options are to allow wetting and drying and to set the depth at which cells are considered dry, usually in the range of 0.05 to 0.08 m.

**Time control.** The *Time* button invokes a *Time Control* dialog that allows specification of the start date and time, simulation duration, ramp duration, and the time-step. SMS can compute a theoretical maximum time-step based on celerity. Practical application of M2D requires that the time-step be less than the theoretical maximum. A general guideline is to set the time-step to half of the theoretical maximum, and then adjust the time-step according to the hydrodynamic properties of the simulation.

**Output control.** The *Output Control* button invokes an *Output Control* dialog that allows specification of output frequency, and what variables are to be output for time series and flow rates. This dialog sets the output control for Observation cells.

**Tidal constituents.** The *Tidal Constituents* button invokes a *Tidal Constituent* dialog that allows the specification of tidal constituents to be assigned, and their local amplitudes and phases. Amplitude and phase is held spatially constant along an entire cell string for each tidal constituent. Phase must be specified in the same time zone as other model inputs.

## Run M2D

The *Run M2D* command makes sure the current simulation is saved to disk, and launches M2D to run the present simulation.

## Steering Module

Coupling of M2D with STWAVE is conducted through the Steering Module. This feature controls interaction of the two models by alternating STWAVE and M2D runs for a specified time, called the Steering Interval, and provides mapped

fields of variables to each model. Seven interaction options for steering the two models are available and described as follows:

- a. 1-way steering: radiation stress gradients from STWAVE provided to M2D.
- b. 1-way steering: currents from M2D provided to STWAVE.
- c. 1-way steering: total depths from M2D provided to STWAVE.
- d. 1-way steering: total depth and currents from M2D provided to STWAVE.
- e. 2-way steering: radiation stress gradients from STWAVE provided to M2D and currents from M2D provided to STWAVE.
- f. 2-way steering: radiation stress gradients from STWAVE provided to M2D and total depth from M2D provided to STWAVE.
- g. 2-way steering: radiation stress gradients from STWAVE provided to M2D and currents and total depth from M2D provided to STWAVE.

The user controls the steering options by checking boxes in the *Steering Module* dialog for each type of interaction needed for the specific simulation (Figure 19).

To invoke the Steering Module, M2D and STWAVE files must be loaded into SMS. All inputs and options for both models must be specified before launching the steering process. Users should consult the STWAVE User's Manual (Smith et al. 1999, 2001) for information on setting up STWAVE in SMS.

The *Steering Module* dialog is opened from the Data drop-down menu (Figure 19). The steering interval is set by specifying the time requested by the "Run STWAVE every" inquiry. Interaction between the models is selected by clicking the available options in the M2D→ STWAVE (meaning M2D passes velocities and/or total depth to STWAVE) and STWAVE→M2D (meaning STWAVE passes wave information to M2D) portions of the dialog.

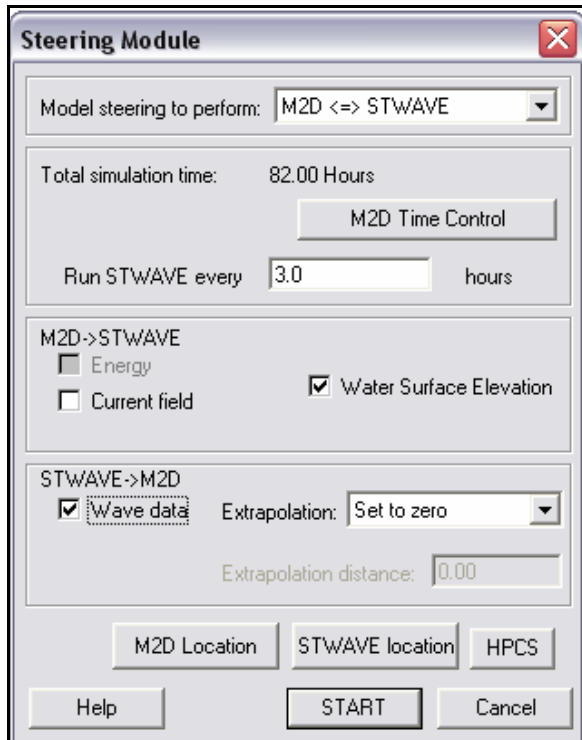


Figure 19. *Steering Module* dialog

Locations of the M2D and STWAVE models (executables) are specified through the *M2D Location* and *STWAVE Location* commands. After the Steering Module setup is complete, clicking *Start* invokes the steering process and a progress screen will be shown.

During steering, SMS creates two output files that provide information on the steering process and on the model progress. The file “steeringstatus.txt” provides information on the steering options and status of the steering process. The file “screenoutput.txt” contains text that M2D and STWAVE write to the screen.

# 7 Model Setup and File Structure

---

Setup of M2D requires development of a computational grid and preparation of one or more input files. The SMS creates all model input files in the correct format so that editing or input file generation is generally not required. The only exceptions to this are preparation of time series of wind speed and direction, water level, or flow rate files for input as forcing. These files can be created within the SMS, but often the user has data from which these files are developed. This section describes the structure of files required to run the M2D model and its output files to assist the user in understanding the file formats. All input and output files to M2D are ASCII. Unless otherwise noted, files are free format.

## Input Files

Required input files for M2D are the grid and control files. A particular simulation may require additional input files that may include any combination of: initial conditions, water level time series, flow rate time series, tidal constituents, wind speed and direction, waves stress, and output specification (for both selected cells and global values). The structure of these input files is described here. Sample files are provided in Appendix A.

### Grid file

The grid file for M2D is structured such that all information pertaining to a cell is found on the same line as the cell identification number. This format is convenient for the user so that once a cell is located in the grid file, its properties are easily viewed or modified. The grid file contains information that is not used within M2D, but is retained for user reference and post-processing.

The first line of the grid file is a header line that describes the columns of information that make up the grid. Only one line is allowed for the header. All lines after the first specify cell information. Cells are defined by their cell identification number and the cell numbers of adjacent cells, referred to by local direction (north, east, south, west). These directions are relative to the local (grid) coordinate system defined by the grid, which may or may not be aligned

with global geographic coordinates. For example, if the grid is oriented with its y-axis parallel to north-south, then the grid coordinate system is aligned with global geographic coordinates. If the grid is rotated at an angle such that its y-axis is not parallel to north-south, then the local coordinate system is not aligned with global geographic coordinates. In the latter case, directions specified in the grid file and within M2D correspond to the local coordinate system.

Each line describing a cell consists of the following information:

Cell number, NC, EC, SC, WC, NB, EB, SB, WB, IACTV, DX, DY, H, N, ROW, COL, LAT, X-DIST, Y-DIST

where descriptions of parameters are given in Table 3. Details of the cell activity parameter IACTV are given in Table 4.

<b>Table 3 Definitions of Parameters in Grid File</b>	
<b>Parameter</b>	<b>Description<sup>1</sup></b>
Cell Number	Cell identification number (referred to as ICELL within M2D)
NC	Cell number of cell adjacent to and north of ICELL
EC	Cell number of cell adjacent to and east of ICELL
SC	Cell number of cell adjacent to and south of ICELL
WC	Cell number of cell adjacent to and west of ICELL
NB	Boundary type at northern edge of ICELL
EB	Boundary type at eastern edge of ICELL
SB	Boundary type at southern edge of ICELL
WB	Boundary type at western edge of ICELL
IACTV	Cell type or active status
DX	Cell width parallel to the x-axis (m)
DY	Cell width parallel to the y-axis (m)
H	Still-water depth relative to a user-specified datum (m)
N	Manning roughness coefficient (m/s <sup>1/3</sup> )
ROW	Row position of cell <sup>2</sup>
COL	Column position of cell <sup>2</sup>
LAT	Latitude (decimal degrees)
X-DIST	X coordinate or distance from grid origin (m) <sup>3, 4</sup>
Y-DIST	Y coordinate or distance from grid origin (m) <sup>3, 4</sup>
1. Directional description (north, east, south, west) refers to the grid coordinate system 2. Parameter is not applied in M2D calculations 3. Parameter is not applied in M2D calculations, but is written in global output files 4. Coordinates are located at cell centers	

<b>Table 4 Cell Types and their Function in M2D</b>		
<b>Type Index</b>	<b>Type</b>	<b>Function</b>
0	Inactive	Cell not included as part of calculation domain
1	Active regular cell	Non-forcing, regular cell
2, 6	Water-level forcing boundary cell	Water level specified as a boundary condition at this cell. Type indices of 2 and 6 denote whether the forcing file contains an individual time series (Type Index = 2) or multiple time series (Type Index = 6).
3	Flow-rate forcing boundary cell	Flow rate specified as a boundary condition at this cell
5	Tidal-constituent forcing boundary cell	Water-level specified through tidal constituents as a boundary condition at this cell
7	Mixed water level and velocity forcing cell	Water level and velocity applied as boundary condition at this cell. Requires multiple time series file.

Cell-center coordinates ( $x$ -dist and  $y$ -dist) can be given in any Cartesian coordinate system, such as State Plane or UTM. M2D does not apply the cell-center coordinates in calculations, but does export the values in global files of water surface elevation and velocity. Because no specific coordinate system is required, the user can apply a coordinate system that is convenient for the particular application.

A grid file is required for all M2D projects. SMS saves M2D grid files with the extension “.m2g.”

### **Model control**

Model control specifications are defined in an input file called “m2d.m2c” or “projectname.m2c” where “projectname” is given to SMS by the user. SMS saves the control file as “m2d.m2c” and as “projectname.m2c.” Each line of the control file contains the parameter or character string followed by a description. The description is optional as M2D does not read it. File names for input and output are user-specified for M2D, with the exception of the alternating hot-start files, and are listed as input parameters in the control file. Names of files are limited to 50 characters in length. There must be at least one space between the parameter or character string and the description. Information contained in the control file is listed in Table 5 in the required order. The format of the control file is the same for all model and project configurations. All parameters listed in Table 5 must be included in the control file.

Two types of output files can be specified: time-series of variables at specified cells and global values of variables at specified times. To specify time-series of variables, cell numbers are identified at locations to output information and a separate file is created to save each variable. Files denoted in Table 5 as

“Cell-specification files” list cell identification numbers at which time series information is stored. Each line of a cell-specification file contains one cell identification number.

Files denoted in Table 5 as “Time-specification files” are for global velocity and elevation output, and contain a list of times to save data. Times are specified as elapsed hours since the beginning of the simulation. Each line in the file contains one value of time and times must be in sequential order. The interval between successive outputs can vary through the simulation. For example, a time specification file may have output times prescribed as 0, 1, 2, 2.5, 3, 3.5, 4, 4.25, and 5 hr.

<b>Table 5 Model Control File Specifications</b>	
<b>Parameter</b>	<b>Description</b>
Version	M2D Version number
Anemometer height (m)	Height of anemometer above water or land surface
Ratio of density of air to density of water	Set to 0.0012 for typical applications
Angle between true north and y-axis of grid (deg)	Defined by grid orientation
Grid origin x-coordinate	Location of x position of cell 1
Grid origin y-coordinate	Location of y position of cell 1
Time-step (s)	Model time-step
Automated hot-start interval (hr)	Time interval between automated hot-start file writes
Include advective terms	Flag for inclusion of advective terms in the momentum equation. Flag settings: 0 = do not include, 1 = include
Include mixing terms	Flag for inclusion of mixing terms in the momentum equation. Flag settings: 0 = do not include, 1 = include
Allow wetting and drying	Flag for allowing flooding and drying. Flag settings: 0 = do not allow, 1 = allow.
Depth (m) to begin drying cells	If wetting and drying are allowed, drying will occur if the total depth in a cell is less than or equal to the depth specified here.
Calculate sediment transport <sup>1</sup>	Flag for calculation of sediment transport. Flag settings: 0 = do not calculate, 1 = calculate
Sediment transport time-step <sup>1</sup>	Time-step for sediment transport calculations
Starting Julian Day (YYDDD OR DDD)	Date of beginning of simulation
Start time (hr)	Time of beginning of simulation
Realization time (hr)	Duration of simulation
Ramp duration (day)	Duration of ramp
<i>(Sheet 1 of 3)</i>	

<b>Table 5 (Continued)</b>	
<b>Parameter</b>	<b>Description</b>
Steering Module elapsed time	Cumulative time at beginning of present simulation; applied for multiple simulations with Steering Module
Time to write output for hot-start (hr)	Time when hot start output is to be written. Use a value of 0 if no hot-start information is to be saved,
Grid file name	Name of grid file (required)
Initial conditions file name	Name of file containing initial conditions. If starting the simulation from quiescent conditions, use "default" (without the quotes) instead of a file name.
Tidal constituents file name	Name of file containing tidal constituents <sup>2</sup> .
Wind input file name	Name of file containing wind speed and direction (required).
Include radiation stresses	Flag for inclusion of radiation stress forcing. Flag settings: 0 = no radiation stress forcing, 1 = include radiation stress forcing
Wave properties file	Name of a file containing the names of wave-properties files for height, period, direction, and breaking
Radiation stress file	Name of radiation stress file <sup>2</sup> .rad.
Hot-start output file name	Name of hot start output file <sup>2</sup> .
Time-specification file for vector plot output	Name of file containing times for vector plot (global u, v) output <sup>2</sup> .
Time-specification file for global elevation output	Name of file containing times for global elevation output <sup>2</sup> .
Time-series output cell-specification file	Name of file containing cell numbers for time-series output of $u$ , $v$ , $\eta$ .
Flow rate output time-series cell-specification file	Name of file containing cell numbers for flow rate output <sup>1</sup> .
Time between output file writes (s) for $u$ , $v$ , $\eta$ time-series file	Time should be a multiple of the simulation time-step
Time between output file writes (s) for flow-rate file	Time should be a multiple of the simulation time-step
Time-series output file for $u$	Name of file to contain $u$ time series <sup>2</sup> .
Time-series output file for $v$	Name of file to contain $v$ time series <sup>2</sup> .
Time-series output file for $\eta$	Name of file to contain $\eta$ time series <sup>2</sup> .
Flow rate output file for $Q_x$	Name of file to contain time series of $Q_x$ <sup>2</sup> .
Flow rate output file for $Q_y$	Name of file to contain time series of $Q_y$ <sup>2</sup> .
Prefix for vector output file name	M2D appends ".m2v" to the user-specified prefix when naming the vector output file.
Prefix for global elevation output file name	M2D appends ".m2s" to the user-specified prefix when naming the global elevation file.
<b>(Sheet 2 of 3)</b>	

<b>Table 5 (Concluded)</b>	
<b>Parameter</b>	<b>Description</b>
Prefix for global bottom change output file name	M2D appends “.m2s” to the user-specified prefix when naming the global bottom change file.
Prefix for transport rate output file name	M2D appends “.m2v” to the user-specified prefix when naming the global transport rate file.
HDRIVER file name	Name of file containing water surface elevation forcing information (individual time-series files).
QDRIVER file name	Name of file containing flow rate forcing information.
MHDRIVER file name	Name of file containing water surface elevation forcing information (multiple time-series files).
MVDRIVER file name	Name of file containing velocity forcing information (multiple time-series files).
<b>(Sheet 3 of 3)</b>	
<ol style="list-style-type: none"> <li>1. Sediment transport in M2D is under development and is not presently available for end user.</li> <li>2. Use “none” or “NONE” if no hot-start output for this variable is specified.</li> </ol>	

### **Initial conditions**

An initial conditions file provides the water surface elevation and velocity at the beginning of the simulation at all cells. Each line in the initial conditions file contains 13 values. The eight five values are cell number, ambient depth,  $\eta$ ,  $u$ ,  $v$ ,  $\partial\eta/\partial t$ ,  $u'$ , and  $v'$ . Depth and water level are given in m and velocity components are given in m/s. The 9th through 12th values are the cell boundary type indices (Table 3), and the 13th column is the cell activity (IACTV) parameter. M2D writes hot-start files in the correct format for reading as initial conditions. If a time-specific hot start is specified within the SMS model control, the hot-start file name will have the extension “.m2i.” If the automatic recurring hot-start capability within M2D is invoked, the hot-start files will be named “HOTSTART1.M2I” and “HOTSTART2.M2I.” Automatic hot-starts are invoked by setting the hot start time interval to a value, in hours, greater than zero.

### **Water level forcing data files**

Time-series boundary forcing for M2D can be specified as water surface elevation. Two types of files containing water surface elevation forcing information can be applied. One type contains individual time series and the other type contains multiple time series. Both the individual and multiple time series forcing can be applied in the same simulation. This capability is convenient for situations in which the time increment is not equal between different sets of time series. This capability also provides flexibility for defining multiple water level forcing cell strings within the SMS and specifying forcing

from various sources. For example, a simulation may require that one or more cell strings are forced by data from a water level gauge and use the individual forcing file, and also that one or more cell strings are forced by water levels calculated by ADCIRC and saved in a multiple time-series file.

M2D recognizes whether time series of water level are specified as forcing by identification of forcing cells in the grid file. If time series water level driving cells are found, M2D opens the HDRIVER and/or MHDRIVER files (see Table 5). The first line of the HDRIVER or MHDRIVER file contains two integer values. The first value specifies the number of files containing water surface elevation forcing time series. The second number is the total number of cells forced by water surface elevation values for HDRIVER files, and is the maximum number of cells forced by water surface elevation for MHDRIVER.DAT files. More than one multiple time series file can be applied in a simulation. The maximum number of cells forced by water surface elevation is the greatest number of cells forced for all files listed in the MHDRIVER.DAT file.

The second line contains the name of a data file that contains the forcing data. The third line of the HDRIVER or MHDRIVER.DAT file contains the number of cells that are driven by the data contained in the file listed in the second line, and an interpolation parameter. The interpolation parameter specifies whether or not the forcing data are interpolated between model time-steps. For example, water level forcing data may be available every hour, but the model time-step might be 30 s. If the interpolation parameter is set to 1, values of water level at the forcing boundaries are interpolated at each model time-step. If the interpolation parameter is set to 0, no interpolation takes place. Following the first and second lines a list of cell numbers that are forced by the time series data given in the forcing data file. For the individual time series forcing files, all cells in the list are forced by the same single time series. Cells forced by water levels contained in the multiple time series file must be listed in the MHDRIVER.DAT file in the order that their corresponding time series appear in the forcing data file.

If more than one forcing data file is applied for water level or discharge, information is specified exactly as previously described for all sets of forcing data and placed in the HDRIVER or MHDRIVER file below the information for the first file.

If individual time series of water surface elevation is specified in an M2D project, the SMS saves the HDRIVER file name as “hdriver\_projectname.dat.” If multiple time-series of water surface elevation is specified in an M2D project, the SMS saves the MHDRIVER file name as “mhdriver\_projectname.dat.”

Files containing individual time series water level forcing data (listed in HDRIVER.DAT) are specified to have two values on each line. The first value is the time stamp. The time is specified in hours since the beginning of the simulation. So, at  $t = 0$ , the time stamp would be 0.0 and at  $t = 1$  day, the time stamp would be 24.0. The second value is water surface elevation (m) relative to the same datum as the grid for water level forcing data, or flow rate ( $\text{m}^3/\text{s}$ ) for

discharge data. Time stamps must start at 0.0 and end at or after the ending time of the simulation.

Files containing multiple time-series water level forcing data (listed in MHDRIIVER.DAT) must have on each line a time stamp followed by a water level value for each of the cells listed that correspond to the particular forcing file. Thus, if  $J$  cells are to be forced with a particular multiple time series file, then  $J+1$  columns must be present in the forcing file. Columns of water-level values must be listed in the same order as the cell numbers are listed in the MHDRIIVER.DAT file. The time is specified in hours since the beginning of the simulation. So, at  $t = 0$ , the time stamp would be 0.0 and at  $t = 1$  day, the time stamp would be 24.0. Water surface elevation (m) is provided relative to the same datum as the grid for water level forcing data. Time stamps must start at 0.0 and end at or after the ending time of the simulation.

The SMS contains dialogs in which time series of water surface elevation and flow rate can be prescribed for M2D. If these dialogs are accessed to create the time series files, they will be saved with the extension “.wl.”

### Velocity forcing data files

Forcing by velocity information can be applied in conjunction with the multiple time series water level forcing. The velocity format is also a multiple time series. Velocity time series cannot be specified without water level forcing at the same cells.

M2D recognizes whether time series of combined water level and velocity values are applied as forcing by identification of forcing cells in the grid file. If time series combined water level and velocity driving cells are found, M2D opens the MHDRIIVER and MVDRIVER files (see Table 5). The file format for the MVDRIVER file is identical to that of the MHDRIIVER file described in the previous section of this chapter. SMS saves the MVDRIVER file as “mvdriver\_projectname.dat.”

Files containing multiple time series velocity forcing data (listed in MVDRIVER.DAT) must have on each line a time stamp followed by four velocity values for each of the cells listed that correspond to the particular forcing file. Velocities written for each cell are those on the cell faces and are written in the following order:  $u_{left}$ ,  $u_{right}$ ,  $v_{bottom}$ ,  $v_{top}$  where the subscripts *left*, *right*, *bottom*, and *top* denote the cell faces in the grid coordinate system. Thus, if  $J$  cells are to be forced with a particular multiple time series file, then  $4*J+1$  columns must be present in the forcing file. Columns of sets of velocity values must be listed in the same order as the cell numbers are listed in the MVDRIVER.DAT file. The time is specified in hours since the beginning of the simulation. So, at  $t = 0$ , the time stamp would be 0.0 and at  $t = 1$  day, the time stamp would be 24.0. Time stamps must start at 0.0 and end at or after the ending time of the simulation.

The SMS contains a dialog in which time series of combined water-surface elevation and velocity can be prescribed for M2D in which the boundary values are obtained from the solution of a larger-domain model. SMS automatically maps the solution to the M2D cells.

### **Flow rate forcing data files**

Flow rate is forced by files containing individual time series information. M2D recognizes whether time series flow rate values are applied as forcing by identification of forcing cells in the grid file. If time series flow rate driving cells are found, M2D opens the QDRIVER file (see Table 5). The first line of the QDRIVER file contains two integer values. The first value specifies the number of files containing flow rate forcing time series. The second number is the total number of cells forced by flow rate.

The second line contains the name of a data file that contains the forcing data. The third line of the QDRIVER file contains the number of cells that are driven by the data contained in the file listed in the second line, and an interpolation parameter. The interpolation parameter specifies whether or not the forcing data are interpolated between model time-steps. For example, flow rate forcing data may be available every hour, but the model time-step might be 30 s. If the interpolation parameter is set to 1, values of flow rate at the forcing boundaries are interpolated at each model time-step. If the interpolation parameter is set to 0, no interpolation takes place. Following the first and second lines of the QDRIVER file is a list of cell numbers that are forced by the time series data given in the forcing data file.

If more than one forcing data file is applied for flow rate, information is specified exactly as previously described for all sets of forcing data and placed in the QDRIVER file below the information for the first file.

If time series of water surface elevation is specified in an M2D project, the SMS saves the QDRIVER file name as “qdriver\_projectname.dat.”

Files containing flow rate forcing data are specified to have two values on each line. The first value is the time stamp. The time is specified in hours since the beginning of the simulation. So, at  $t = 0$ , the time stamp would be 0.0 and at  $t = 1$  day, the time stamp would be 24.0. Time stamps must start at 0.0 and end at or after the ending time of the simulation. The second value is flow rate given in  $\text{m}^3/\text{s}$ . This flow rate is specified at every cell designated as forced by the input series in the QDRIVER file. Thus, if three cells were specified as flow rate forcing cells and the value of the flow rate was  $9 \text{ m}^3/\text{s}$ , then each of the three cells would have  $9 \text{ m}^3/\text{s}$  flowing through it. The flow rate is not distributed among the three cells.

The SMS contains a dialog in which time series of flow rate can be prescribed for M2D. If this dialog is accessed to create the time series files, they will be saved with the extension “.q.”

## Wind speed and direction

Wind speed and direction are given in the user-specified wind file listed in m2d.m2c. The wind-forcing file contains three values on each line. The first value is the time stamp in hours since the beginning of the simulation. The second value is the wind speed in m/s and the third value is direction in deg. The convention for the input wind direction is 0 deg indicates wind blowing from the north, and 90 deg indicates wind blowing from the east. Wind speed must be positive. Conversion to the wind-direction convention given for Equations 2 and 3 is conducted internally within M2D.

The SMS contains a dialog in which time series of wind speed and direction can be prescribed for M2D. If this dialog is accessed to create the time series file, it will be saved with the extension “.m2w.”

## Tidal constituents

The tidal-constituent forcing file contains nine lines. The first line is a header that can identify the source of the tidal-constituent information. The header line is ignored by M2D. Each of the remaining lines contain the local amplitude (m) and phase (deg) of the water level for a specific tidal constituent. The constituents specified on lines 2 through 9 are (in order of appearance):  $M_2$ ,  $N_2$ ,  $S_2$ ,  $K_2$ ,  $K_1$ ,  $O_1$ ,  $M_4$ , and  $M_6$ . If specific constituents are not to be specified as forcing, then their amplitude values must be set to zero.

## Wave stresses

Wave stresses are given in the user-specified radiation-stress file listed in m2d.m2c. The radiation-stress file consists of sets of wave stresses prescribed at specific times. The first line in the file contains the text “TIME:” and is followed by the time in hours since the beginning of the simulation. Lines 2 through NCELLS + 1 contain three values. The first value is the cell identification number, the second and third values are the  $x$  and  $y$ -components of the wave stress, respectively. Wave stresses must be given in order of ascending cell identification numbers. Sets of information that include the time-step and wave stresses for each cell are included in the file for each time-step that wave stresses are available. Because M2D will conduct its calculations at a different time interval than the wave stress time interval, the stresses are linearly interpolated within M2D over time. If the last time stamp in the wave stress file specifies a time before the end of the M2D simulation, M2D will apply values of zero for the radiation stresses after the time of the last available wave information (no interpolation to zero is conducted).

If the Steering Module is invoked to couple M2D with STWAVE, SMS will write files containing wave stresses that have been mapped from those calculated by the wave model. SMS gives the extension “.rad” to the wave stress file. The same file extension is also given to radiation stress files for STWAVE. M2D

files can be distinguished from the STWAVE files by the prefix. M2D wave stress files contain the text “m2steer” and the STWAVE files contain “s2steer.”

### **Selected cell output specification file**

User-specified observation cells can be selected for time series output of variables or terms in the governing equations. A listing of these cells is provided in a cell output specification file. The file consists of a list of cell identification numbers with one number per line. If observation cells are selected within the SMS and saved as part of an M2D project, SMS gives the cell listing file the extension of “.ts.”

### **Global output time specification files**

Global water surface elevation and velocity are written to files at times specified in the global output time-specification files. These files consist of a list of times, in hours since the beginning of the simulation, at which global output is to be written. Each line in these files consists of one time value. Separate global output time-specification files are required for water surface elevation and velocity, providing the option to save only one global file.

Times listed in the global output time-specification files can be at constant or varying time intervals. Requirements for the times listed in the file are that they are sequential, start at values of zero or greater, and values are not repeated.

If global output times are specified within the SMS, a series of equal-increment output times can be generated. In addition, individual times can also be specified. If both water surface elevation and velocity global files are to be written, the output times from one of these variables can be written to the other so that the global output will take place at the same times. SMS writes the global output time-specification files with an extension of “.m2t.”

## **Output Files**

Two types of output files can be specified for M2D. These file types are time series of a variable at station locations and global variable files. Descriptions of these file types are given here. For both types of output files, each variable is reported from its computational location in the model. Thus, water surface elevation is reported from the cell center, the  $x$ -component of velocity is reported from the left cell face center, and the  $y$ -component of velocity is reported from the bottom cell face center.

## Time series at station locations

Time series output files for specific station locations contain a header line followed by the calculated time series values. The header specifies the cell numbers (where output is taken) above columns of output. Cell numbers in the header are written as “C#” where # denotes the cell number. The “C” is placed in the header to distinguish the cell number from data in plotting packages (software will read the information in as a character string). Lines following the header contain a time stamp (fractional days) and values of the variable.

Water surface elevation and the two components of velocity are each written to separate files for a total of three possible station output files. The user can specify any combination of time series station output files to be written.

## Global output time specification files

Global files can be created for water surface elevation, velocity, and depth change. File formats consist of sets of global variable values output at times specified by the user. Each set of information in the file contains a line with the time stamp, followed by lines containing the  $x,y$  position of each cell followed by the value of the variable, such as  $\eta$ . For velocity, these lines contain  $u$  and  $v$ . Global information is saved for each cell in the grid and written in ascending order of cell identification number. File extensions of  $.m2s$  are assigned to scalar fields and  $.m2v$  to vector fields.

Units for time series and global files are standard metric. Water surface elevation is given in m and velocity is given in m/s. Time stamps are given in hours since the beginning of the simulation.

# References

---

- Bretschneider, C. L. (1966). "Engineering aspects of hurricane surge," *Estuary and coastline hydrodynamics*. Ippen, A. T., ed., McGraw-Hill, New York, 231-256.
- Brown, C. A., Kraus, N. C., and Militello A. (1995a). "Hydrodynamic modeling for assessing engineering alternatives for elevating the Kennedy Causeway, Corpus Christi, Texas," *Proceedings of the 4<sup>th</sup> International Estuarine and Coastal Modeling Conference*, American Society of Civil Engineers, ASCE Press, New York, 681-694.
- Brown, C. A., Militello, A., and Kraus, N. C. (1995b). "Hydrodynamic assessment for elevation of the JFK Causeway, Corpus Christi, Texas," *Proceedings Texas Water '95*, Texas Section of the American Society of Civil Engineers, ASCE Press, New York, 31-41.
- Brown, C. A., Militello, A., and Kraus, N. C. (1995c). "Hydrodynamic assessment for elevation of the JFK Causeway, Corpus Christi, Texas," TAMU-CC-CBI-95-07, Conrad Blucher Institute for Surveying and Science, Texas A&M University-Corpus Christi, Corpus Christi, TX.
- Butler, H. L. (1978). "Coastal flood simulation in stretched coordinates," *Proceedings of the Sixteenth Coastal Engineering Conference*, American Society of Civil Engineers, ASCE Press, New York, 1,030-1,048.
- Charnock, H. (1955). "Wind stress on a water surface," *Quarterly Journal of the Royal Meteorological Society*, 81, 639-640.
- Cialone, M. A. (1989). "Curvilinear long wave hydrodynamic (CLHYD) model for tidal circulation and storm surge propagation," *Proceedings of the Conference on Estuarine and Coastal Modeling*, American Society of Civil Engineers, ASCE Press, New York, 16-26.
- Dally, W. R., and Brown, C. A. (1995). "A modeling investigation of the breaking wave roller with application to cross-shore currents," *Journal of Geophysical Research*, 100(C12), 24,873-24,883.
- Dally, W. R., Dean, R. G., and Dalrymple, R. A. (1985). "Wave height variation across beaches of arbitrary profile," *Journal of Geophysical Research* 90(C6), 11,917-11,927.
- Dally, W. R., and Osiecki, D. A. (1994). "The role of rollers in surf zone currents," *Proceedings 24<sup>th</sup> Coastal Engineering Conference*, ASCE, 1,895-1,905.

- Falconer, R. A. (1980). "Modelling of planform influence on circulation in harbors," *Proceedings of the Seventeenth Coastal Engineering Conference*, American Society of Civil Engineers, ASCE Press, New York, 2,726-2,744.
- Flather, R. A., and Heaps, N. S. (1975). "Tidal computations for Morecambe Bay," *Geophysical Journal of the Royal Astronomical Society London*, A210, 423-436.
- Hsu, S. A. (1988). *Coastal meteorology*. Academic Press, San Diego.
- Kraus, N. C., and Larson, M. (1991). "NMLONG: Numerical model for simulating the longshore current; Report 1: Model development and tests," Technical Report DRP-91-1, U.S. Army Engineer Waterways Experiment Station, Vicksburg, MS.
- Kraus, N. C., and Militello, A. (1996). "Hydraulic feasibility of the proposed Southwest Cut, East Matagorda Bay, Texas," TAMU-CC-CBI-96-03, Conrad Blucher Institute for Surveying and Science, Texas A&M University-Corpus Christi, Corpus Christi, TX.
- Kraus, N. C., and Militello, A. (1999) "Hydraulic study of multiple inlet system: East Matagorda Bay, Texas," *Journal of Hydraulic Engineering*, 125, 3, 224-232.
- Larson, M., and Kraus, N. C. (2002). "NMLONG: Numerical Model for Simulating Longshore Current: Report 2; Wave-current interaction, roller modeling, and validation of model enhancements," Technical Report ERDC/CHL TR-02-22, U.S. Army Engineer Research and Development Center, Vicksburg, MS.
- Luettich, R. A., Westerink, J. J., and Scheffner, N. W. (1992). "ADCIRC: An advanced three-dimensional circulation model for shelves, coasts, and estuaries; Report 1: Theory and methodology of ADCIRC-2DDI and ADCIRC-3DL," Technical Report DRP-92-6, U.S. Army Engineer Waterways Experiment Station, Vicksburg, MS.
- Militello, A. (1998). *Hydrodynamics of wind-dominated, shallow embayments*. Ph.D. diss., Division of Marine and Environmental Systems, Florida Institute of Technology, Melbourne, FL.
- Militello, A. (2000). "Hydrodynamic modeling of a sea-breeze dominated shallow embayment, Baffin Bay, Texas," *Sixth International Estuarine and Coastal Modeling Conference*, American Society of Civil Engineers, ASCE Press, New York, 795-810.
- Militello, A. (2002). "Willapa entrance and Bay Center modeling," in "Study of navigation channel feasibility, Willapa Bay, Report 2," Kraus, N. C., Arden, H. T., and Simpson, D. P., eds. Technical Report ERDC-CHL-TR-00-6, U.S. Army Engineer Research and Development Center, Vicksburg, MS.
- Militello, A., and Kraus, N. C. (1998). "Numerical simulation of hydrodynamics for proposed inlet, East Matagorda Bay, Texas," *Proceedings of the 5<sup>th</sup> International Estuarine and Coastal Modeling Conference*, American Society of Civil Engineers, ASCE Press, New York, 805-818.

- Militello, A., and Kraus, N. C. (2001). "Generation of harmonics by sea breeze in nontidal water bodies," *Journal of Physical Oceanography*, 31(6), 1639-1647.
- Militello, A., and Kraus, N. C. (2003). "Numerical simulation of sediment pathways at an idealized inlet and ebb shoal," *Coastal Sediments 2003*, CD ROM: Numerical simulation of sediment pathways at an id.pdf.
- Militello, A., Parry, R. M., and Arden, H. T. (2003). "Numerical simulation of navigation channel infilling, Bay Center, Washington," *Proceedings Dredging 2002 Conference*, ASCE, CD-ROM 40680-034, ISBN 0-7844-0680-4.
- Militello, A., and Zundel, A. K. (2002a). "Automated coupling of regional and local circulation models through boundary condition specification," *Proceedings of the Fifth International Conference on Hydroinformatics*, International Association of Hydraulic Research IWA Publishing, London, 156-161.
- Militello, A., and Zundel, A. K. (2002b). "Coupling of regional and local circulation models ADCIRC and M2D," Coastal and Hydraulics Engineering Technical Note CHETN-IV-42, U.S. Army Engineer Research and Development Center, Vicksburg, MS.
- Militello, A., and Zundel, A. K. (2003). "SMS Steering Module for coupling waves and currents, 2. M2D and STWAVE," Coastal and Hydraulics Engineering Technical Note ERDC/CHL CHETN-IV-60, U. S. Army Engineer Research and Development Center, Vicksburg, MS.
- Nishimura, H. (1988). "Computation of nearshore current," Nearshore dynamics and coastal processes. K. Horikawa, ed., University of Tokyo Press, Tokyo, Japan, 271-291.
- Putrevu, U., and Svendsen, I. A. (1992). "A mixing mechanism in the nearshore region," *Proceedings 23rd International Coastal Engineering Conference*, American Society of Civil Engineers, 2,578-2,771.
- Reed, C. W., and Militello, A. (in preparation). "Accommodating wave-induced alongshore transport in finite-volume boundary formulations," *International Journal for Numerical Methods in Engineering*, Wiley Interscience.
- Reid, R. O., and Bodine, B. R. (1968). "Numerical model for storm surges in Galveston Bay," *Journal of the Waterways and Harbors Division*, American Society of Civil Engineers, 94 (WW1), 33-57.
- Richtmyer, R. D., and Morton, K. W. (1967). *Difference methods for initial-value problems*. Interscience Publishers, New York, 405 pp.
- Roache, P. J. (1976). *Computational fluid dynamics*. Hermosa Publishers, Albuquerque, NM, 446 pp.
- Saville, T., Jr. (1953). "Wind setup and waves in shallow water," Beach Erosion Board Technical Memorandum No. 27, U.S. Army Engineer Waterways Experiment Station, Vicksburg, MS.

- Schureman, P. (1924). "A manual of the harmonic analysis and prediction of tides," U.S. Coast and Geodetic Survey, Special Publication 98, 426 pp.
- Shore Protection Manual* (1984). 4th ed., 2 Vols., U.S. Army Engineer Waterways Experiment Station, Coastal Engineering Research Center, U.S. Government Printing Office, Washington, DC.
- Smith, J. M., Larson, M., and Kraus, N. C. (1993). "Longshore current on a barred beach: Field measurements and calculation," *Journal of Geophysical Research*, 98(C12), 22,717-22,731.
- Smith, J. M., Resio, D. T., and Zundel, A. K. (1999). "STWAVE: STeady-state spectral WAVE model, Report 1: User's manual for STWAVE Version 2.0," Instructional Report CHL-99-1, U.S. Army Engineer Waterways Experiment Station, Vicksburg, MS.
- Smith, J. M., Sherlock, A. R., and Resio, D. T. (2001). "STWAVE: STeady-state spectral WAVE model: User's manual for STWAVE Version 3.0," Supplemental Report ERDC/CHL SR-01-1, U.S. Army Engineer Research and Development Center, Vicksburg, MS.
- Spaulding, M. L. (1984). "A vertically averaged circulation model using boundary fitted coordinates," *Journal of Physical Oceanography*, 14, 973-982.
- Visser, P. J. (1982). "Uniform longshore current measurements and calculations," *Proceedings 19<sup>th</sup> Coastal Engineering Conference*, ASCE, 2,192-2,207.
- Wanstrath, J. J. (1978). "An open-coast mathematical storm surge model with coastal flooding for Louisiana; Report 1: Theory and application," Miscellaneous Paper H-78-5, U.S. Army Engineer Waterways Experiment Station, Vicksburg, MS.
- Wozencraft, J. M., Lillycrop, W. J., and Kraus, N. C. (2002). "SHOALS Toolbox: Software to support visualization and analysis of large, high-density data sets," ERDC/CHL CHETN-IV-43, U.S. Army Engineer Research and Development Center, Vicksburg, MS.
- Yeh, G.-T., and Chou, F.-K. (1978). "Moving boundary numerical surge model," *Journal of the Waterway Port Coastal and Ocean Division*, American Society of Civil Engineers, 105 (WW3), 247-263.
- Zundel, A. K. (2000). "Surface-water Modeling System reference manual," Brigham Young University, Environmental Modeling Research Laboratory, Provo, UT.

# Appendix A

## Example Input and Output Files

This appendix provides example input and output files for M2D. Sample files were selected from various applications to illustrate file formats. Input files are shown first, followed by output files.

An example grid file is shown in Figure A1 for a 19-km-long frictionless channel. The channel is 19 cells long, 1 cell wide, and 1 m deep. Cells have dimensions of 1,000 m on each side. Cell-center coordinates, *x*-dist and *y*-dist, are given in meters from the grid origin.

Cell no.	NC	EC	SC	WC	NB	EB	SB	WB	IACTV	DX	DY	H	N	ROW	COL	LAT	X-DIST	Y-DIST
1	0	2	0	0	4	0	4	4	1	1000.	1000.	1.000	.00	1	1	.00	500.	500.
2	0	3	0	1	4	0	4	0	1	1000.	1000.	1.000	.00	1	2	.00	1500.	500.
3	0	4	0	2	4	0	4	0	1	1000.	1000.	1.000	.00	1	3	.00	2500.	500.
4	0	5	0	3	4	0	4	0	1	1000.	1000.	1.000	.00	1	4	.00	3500.	500.
5	0	6	0	4	4	0	4	0	1	1000.	1000.	1.000	.00	1	5	.00	4500.	500.
6	0	7	0	5	4	0	4	0	1	1000.	1000.	1.000	.00	1	6	.00	5500.	500.
7	0	8	0	6	4	0	4	0	1	1000.	1000.	1.000	.00	1	7	.00	6500.	500.
8	0	9	0	7	4	0	4	0	1	1000.	1000.	1.000	.00	1	8	.00	7500.	500.
9	0	10	0	8	4	0	4	0	1	1000.	1000.	1.000	.00	1	9	.00	8500.	500.
10	0	11	0	9	4	0	4	0	1	1000.	1000.	1.000	.00	1	10	.00	9500.	500.
11	0	12	0	10	4	0	4	0	1	1000.	1000.	1.000	.00	1	11	.00	10500.	500.
12	0	13	0	11	4	0	4	0	1	1000.	1000.	1.000	.00	1	12	.00	11500.	500.
13	0	14	0	12	4	0	4	0	1	1000.	1000.	1.000	.00	1	13	.00	12500.	500.
14	0	15	0	13	4	0	4	0	1	1000.	1000.	1.000	.00	1	14	.00	13500.	500.
15	0	16	0	14	4	0	4	0	1	1000.	1000.	1.000	.00	1	15	.00	14500.	500.
16	0	17	0	15	4	0	4	0	1	1000.	1000.	1.000	.00	1	16	.00	15500.	500.
17	0	18	0	16	4	0	4	0	1	1000.	1000.	1.000	.00	1	17	.00	16500.	500.
18	0	19	0	17	4	0	4	0	1	1000.	1000.	1.000	.00	1	18	.00	17500.	500.
19	0	0	0	18	4	4	4	0	1	1000.	1000.	1.000	.00	1	19	.00	18500.	500.

Figure A1. Example grid file for channel

An example m2d.m2c file is shown in Figure A2. In this example, a 100-hr simulation is specified with a 0.5-s time-step. The automatic recurring hot-start capability is invoked with hot-start files written every 24 hr. Advective terms in the momentum equations are included in the computations. Wetting and drying is allowed to occur and cells will dry at a water depth of 0.08 m. Wind speed and direction is specified in the file “periodic.wnd.” Global velocity and water surface elevation are to be written at times specified in the “ideal4\_v.m2t” and

“ideal4\_e.m2t” files, respectively. Time series output is to be saved every 600 s for cells listed in the file “ideal4.ts” and the variables to be saved are  $u$ ,  $v$ , and  $\eta$ .

An example time-specification file for either global vector or scalar (elevation) output is shown in Figure A3. A list of specific times, in hours, with one time value per line, are provided at which M2D will write out the global output file.

```

Version 2.00
10.0      ANEMOMETER HEIGHT (M)
0.0012   RHO_ATM/RHO_WATER
10.27    ANGLE BETWEEN TRUE NORTH AND Y-AXIS OF GRID
567607.0602  GRID ORIGIN (M), (X-COORDINATE)
77050.4225  GRID ORIGIN (M), (Y-COORDINATE)
1.0000    DELTA T (SEC)
0.000    AUTOMATIC RECURRING HOT START INTERVAL (HR)
1        INCLUDE ADVECTIVE TERMS: 0 = NO, 1 = YES
0        INCLUDE MIXING TERMS: 0 = NO, 1 = YES
1        ALLOW WETTING AND DRYING: 0 = NO, 1 = YES
0.05     DEPTH (M) TO BEGIN DRYING CELLS
0        CALCULATE SEDIMENT TRANSPORT: 0 = NO, 1 = YES
0.00     DELTA T FOR SEDIMENT TRANSPORT (SEC)
02230    STARTING JULIAN DAY (YYDDD OR DDD)
19       START TIME (HOUR)
72.000   REALIZATION TIME (HOUR)
0.500    RAMP DURATION (DAY)
0.000    STEERING MODULE (MULTIPLE SIMULATION) ELAPSED TIME (HOUR)
75.000   TIME TO WRITE OUTPUT FOR HOT START (HR)
OceanCity.m2g  GRID INPUT FILE NAME
default    INITIAL CONDITIONS FILE NAME
none      TIDAL CONSTITUENT INPUT FILE
none      WIND INPUT FILE
1         INCLUDE RADIATION STRESSES: 0 = NO, 1 = YES
OceanCity.mwv  WAVE DATA FILE
1m2steer.rad  RADIATION STRESS INPUT FILE (WRITTEN BY STWAVE)
1m2steer.m2i  HOT START OUTPUT FILE
OC_V.m2t     TIME SPECIFICATION FILE FOR VECTOR PLOT OUTPUT
OC_E.m2t     TIME SPECIFICATION FILE FOR GLOBAL ELEVATION OUTPUT
none        TIME-SERIES INPUT FILE
none        FLOW RATE TIME-SERIES INPUT FILE
0           TIME BETWEEN OUTPUT FILE WRITES (SEC) FOR TIME-SERIES FILE
0           TIME BETWEEN OUTPUT FILE WRITES (SEC) FOR FLOW RATE FILE
none        TIME-SERIES OUTPUT FILE FOR U
none        TIME-SERIES OUTPUT FILE FOR V
none        TIME-SERIES OUTPUT FILE FOR ETA
none        FLOW RATE OUTPUT FILE FOR X-DIRECTION
none        FLOW RATE OUTPUT FILE FOR Y-DIRECTION
TideWave    PREFIX FOR VECTOR OUTPUT FILE NAME
TideWave    PREFIX FOR GLOBAL ELEVATION OUTPUT FILE NAME
none        PREFIX FOR GLOBAL BOTTOM CHANGE FILE NAME
none        PREFIX FOR GLOBAL SEDIMENT TRANSPORT RATE FILE NAME
none        HDRIVER.DAT FILE
none        QDRIVER.DAT FILE
mhdriver_OC.dat  MHDRIVER.DAT FILE
mvdriver_OC.dat  MVDRIVER.DAT FILE

```

Figure A2. Example m2d.m2c file

```
0.00
1.00
2.00
3.00
4.00
5.00
6.00
7.00
8.00
9.00
10.00
11.00
```

Figure A3. Example time-specification file for global output

An example hdriver.dat file is shown in Figure A4. Two water level forcing files will be read and the total number of water surface elevation forcing cells is 10. Files “Gauge1.wl” and “Gauge2.wl” contain water level forcing data. Data from Gauge1.wl is prescribed at four cells (cell numbers 1, 2, 3, 4) and the water level is to be interpolated between model time-steps. Data from Gauge2.wl is applied at six cells (cell numbers 64, 65, 66, 67, 68, and 69) with interpolation between model time-steps. Qdriver.dat files have identical format, so a separate example is not given.

```
2 10
Gauge1.wl
4 1
1
2
3
4
Gauge2.wl
6 1
64
65
66
67
68
69
```

Figure A4. Example hdriver.dat file

An example of a time series water level forcing file is shown in Figure A5. Files “Gauge1.wl” and “Gauge2.wl” shown in Figure A4 are in this format. The first column contains time stamps (hours) and the second column provides water level (m). Flow rate forcing files have the same format as shown in Figure A5.

0	-0.0455
0.9912	0.0319
1.992	0.1373
2.9928	0.2738
3.9912	0.3948
4.992	0.4652
5.9928	0.4515
6.9912	0.3759
7.992	0.2864
8.9928	0.1967
9.9912	0.1102
10.992	0.0302
11.9928	-0.0423
12.9912	-0.1053
13.992	-0.1573
14.9928	-0.1991
15.9912	-0.2295
16.992	-0.2483
17.9928	-0.2584
18.9912	-0.2647
19.992	-0.2727
20.9928	-0.2858
21.9912	-0.3036
22.992	-0.3236
23.9928	-0.3428
24.9912	-0.2356

Figure A5. Example individual time series water level forcing file

An example wind forcing file is shown in Figure A6. The duration of the wind forcing is 22 hr and oscillates between 90 (blowing from the east) and 270 deg (blowing from the west). Wind speed ranges from 0 to 8.6 m/s.

0.0	0.0	90.0
1.0	1.0	90.0
2.0	2.0	90.0
3.0	2.5	90.0
4.0	3.0	90.0
5.0	3.5	270.0
6.0	4.0	270.0
7.0	4.5	270.0
8.0	5.0	270.0
9.0	5.5	270.0
10.0	5.8	270.0
11.0	6.0	270.0
12.0	6.5	270.0
13.0	6.8	270.0
14.0	7.0	270.0
15.0	7.0	270.0
16.0	5.0	270.0
17.0	2.5	270.0
18.0	0.0	90.0
19.0	2.5	90.0
20.0	5.0	90.0
21.0	7.0	90.0
22.0	8.6	90.0

Figure A6. Example time series wind forcing file

An example tidal-constituents forcing file is shown in Figure A7. The constituent identifiers (e.g. “: M2”) are not required in the file, but remind the user of the order of the constituents.

```

US Naval Academy, Annapolis, MD Tidal Constituents
0.1344 147.20 : M2
0.0226 175.00 : S2
0.0262 126.00 : N2
0.0061 174.5 : K2
0.0579 283.30 : K1
0.0500 294.10 : O1
0.0037 130.60 : M4
0.0 0.0 : M6

```

Figure A7. Example tidal-constituents forcing file

An example portion of an initial conditions file is shown in Figure A8. In this example, water levels are set to non-zero values, the  $u$ - and  $v$ -components of velocity are zero, values of  $\partial\eta/\partial t$  are non-zero,  $u'$  has zero and non-zero values, and  $v'$  values are zero. Cell boundary types and activity codes are also written.

```

1 0.67100000 0.24883273 0.000000 0.000000 0.08816975 0.000000 0.000000 0 7 7 4 6
2 1.36300004 0.21381602 0.000000 0.000000 0.05334590 0.007975 0.000000 0 7 7 7 6
3 2.05500007 0.17855626 0.000000 0.000000 0.01846295 0.007990 0.000000 0 7 7 7 6
4 2.73600006 0.15381116 0.000000 0.000000 -0.00601869 0.004049 0.000000 0 7 7 7 6
5 3.40400004 0.14469834 0.000000 0.000000 -0.01528861 -0.000789 0.000000 0 7 7 7 6
6 4.03200006 0.14424038 0.000000 0.000000 -0.01594494 -0.003016 0.000000 0 7 7 7 6
7 4.65199995 0.14831893 0.000000 0.000000 -0.01212788 -0.004057 0.000000 0 7 7 7 6
8 5.22100019 0.15106325 0.000000 0.000000 -0.00958566 -0.003458 0.000000 0 7 7 7 6
9 5.77400017 0.15291372 0.000000 0.000000 -0.00784420 -0.002194 0.000000 0 7 7 7 6
10 6.15199995 0.15405130 0.000000 0.000000 -0.00672851 -0.000903 0.000000 0 7 7 7 6
11 6.32700014 0.15448837 0.000000 0.000000 -0.00623937 0.000471 0.000000 0 7 7 7 6
12 6.49300003 0.15473600 0.000000 0.000000 -0.00594525 0.001190 0.000000 0 7 7 7 6
13 6.67199993 0.15503238 0.000000 0.000000 -0.00564533 0.001777 0.000000 0 7 7 7 6
14 6.85799980 0.15532908 0.000000 0.000000 -0.00537130 0.002218 0.000000 0 7 7 7 6
15 7.03599977 0.15554351 0.000000 0.000000 -0.00514706 0.002687 0.000000 0 7 7 7 6
16 7.20100021 0.15569794 0.000000 0.000000 -0.00493140 0.002957 0.000000 0 7 7 7 6
17 7.37400007 0.15586072 0.000000 0.000000 -0.00466013 0.002974 0.000000 0 7 7 7 6
18 7.55999994 0.15609157 0.000000 0.000000 -0.00429774 0.002568 0.000000 0 7 7 7 6
19 7.84700012 0.15658177 0.000000 0.000000 -0.00365273 0.001598 0.000000 0 7 7 7 6
20 8.19799995 0.15755470 0.000000 0.000000 -0.00278718 -0.001382 0.000000 0 7 7 7 6

```

Figure A8. Example portion of an initial conditions file

An example portion of a radiation-stress input file is shown in Figure A9. The format of this file requires that the radiation-stress gradients have been previously mapped to the M2D grid (SMS conducts this mapping automatically in the Steering Module). The  $x$  and  $y$  components are oriented relative to the M2D axes. The first line in the file provides the time stamp. Second and further lines up to NCELLS + 1 provide the cell number,  $x$  component of the radiation-stress gradient, and  $y$  component of the radiation-stress gradient. Sets of radiation-stress gradients for successive times are included in the same input file.

TIME:		0.000000	
	1	8.473935E-005	-1.347822E-004
	2	8.474045E-005	-1.349220E-004
	3	8.474155E-005	-1.350617E-004
	4	8.474265E-005	-1.352014E-004
	5	8.474375E-005	-1.353411E-004
	6	8.474485E-005	-1.354808E-004
	7	8.474595E-005	-1.356205E-004
	8	8.474705E-005	-1.357603E-004
	9	8.474815E-005	-1.359000E-004
	10	8.474925E-005	-1.360397E-004
	11	8.475035E-005	-1.361794E-004
	12	8.475145E-005	-1.363191E-004
	13	8.475255E-005	-1.364588E-004
	14	8.475365E-005	-1.365986E-004
	15	8.475475E-005	-1.367383E-004
	16	8.475585E-005	-1.368780E-004
	17	8.475695E-005	-1.370177E-004
	18	8.475804E-005	-1.371574E-004
	19	8.475915E-005	-1.372971E-004
	20	8.476025E-005	-1.374368E-004
	21	8.476135E-005	-1.375766E-004
	22	8.476245E-005	-1.377163E-004
	23	8.476355E-005	-1.378560E-004
	24	8.476465E-005	-1.379957E-004
	25	8.476575E-005	-1.381354E-004
	26	8.476685E-005	-1.382751E-004
	27	8.476795E-005	-1.384148E-004
	28	8.476905E-005	-1.385546E-004

Figure A9. Example portion of radiation stress input file

An example portion of a time series numerical station output file is shown in Figure A10, in which five cells were selected for output. The cell numbers for the five cells are 1, 2, 3, 4, and 5. Time is elapsed time in days since the beginning of the simulation.

Example portions of global elevation and velocity files are shown in Figures A11 and A12, respectively. In these examples, the time of the output is 5.6 hr after the beginning of the simulation. Coordinates of cell positions are given in the first two columns in order of ascending cell number. Cell coordinates are those specified in the grid file in the *x*-dist and *y*-dist columns (grid not shown for these global output examples). Water level is given in meters (third column), following cell coordinates; *x*- and *y*-components of velocity are given in meters per second (third and fourth columns, respectively). If multiple times of global values are written, they are successively appended at the end of the file with no lines between snapshots.

TIME	c1	c2	c3	c4	c5
0.0000	-0.1900	-0.1700	-0.1500	-0.1300	-0.1100
0.0000	-0.1873	-0.1700	-0.1500	-0.1300	-0.1100
0.0003	-0.1821	-0.1696	-0.1500	-0.1300	-0.1100
0.0007	-0.1753	-0.1683	-0.1499	-0.1300	-0.1100
0.0010	-0.1675	-0.1654	-0.1497	-0.1300	-0.1100
0.0014	-0.1594	-0.1606	-0.1488	-0.1299	-0.1100
0.0017	-0.1515	-0.1541	-0.1470	-0.1298	-0.1100
0.0021	-0.1439	-0.1462	-0.1438	-0.1292	-0.1100
0.0024	-0.1366	-0.1377	-0.1389	-0.1280	-0.1098
0.0028	-0.1295	-0.1292	-0.1324	-0.1259	-0.1095
0.0031	-0.1224	-0.1212	-0.1245	-0.1223	-0.1087
0.0035	-0.1150	-0.1138	-0.1158	-0.1172	-0.1072
0.0038	-0.1076	-0.1069	-0.1071	-0.1105	-0.1047
0.0042	-0.1000	-0.1001	-0.0988	-0.1026	-0.1008
0.0045	-0.0924	-0.0931	-0.0912	-0.0939	-0.0954
0.0049	-0.0849	-0.0857	-0.0842	-0.0850	-0.0886
0.0052	-0.0776	-0.0781	-0.0775	-0.0765	-0.0806
0.0056	-0.0703	-0.0703	-0.0708	-0.0688	-0.0718
0.0059	-0.0630	-0.0626	-0.0637	-0.0617	-0.0628
0.0063	-0.0556	-0.0550	-0.0562	-0.0550	-0.0543
0.0066	-0.0482	-0.0478	-0.0483	-0.0484	-0.0464

Figure A10. Example time series numerical station output file

TIME:	5.60000		
3771.25000	2786.41040	0.1500	
3833.75000	2786.41040	0.1500	
3896.25000	2786.41040	0.1500	
3958.75000	2786.41040	0.1500	
4021.25000	2786.41040	0.1500	
4083.75000	2786.41040	0.1500	
4146.25000	2786.41040	0.1500	
4208.75000	2786.41040	0.1500	
4271.25000	2786.41040	0.1500	
4333.75000	2786.41040	0.1500	
4396.25000	2786.41040	0.1500	
4458.75000	2786.41040	0.1500	
4521.25000	2786.41040	0.1500	
4583.75000	2786.41040	0.1500	
4646.25000	2786.41040	0.1500	
4708.75000	2786.41040	0.1500	
4771.25000	2786.41040	0.1500	
4833.75000	2786.41040	0.1500	
4896.25000	2786.41040	0.1500	
4958.75000	2786.41040	0.1500	
5021.25000	2786.41040	0.1500	
5083.75000	2786.41040	0.1500	
5146.25000	2786.41040	0.1500	
5208.75000	2786.41040	0.1500	
5271.25000	2786.41040	0.1500	
5333.75000	2786.41040	0.1500	
5396.25000	2786.41040	0.1500	
5458.75000	2786.41040	0.1500	
5521.25000	2786.41040	0.1500	
5583.75000	2786.41040	0.1500	
5646.25000	2786.41040	0.1500	
5708.75000	2786.41040	0.1500	
5764.35010	2786.41040	0.1500	

Figure A11. Example global elevation output file

TIME:	5.60000			
3771.25000	2786.41040	0.0000	-0.0104	
3833.75000	2786.41040	0.0000	-0.0104	
3896.25000	2786.41040	0.0000	-0.0095	
3958.75000	2786.41040	0.0000	-0.0118	
4021.25000	2786.41040	0.0000	-0.0130	
4083.75000	2786.41040	0.0000	-0.0140	
4146.25000	2786.41040	0.0000	-0.0145	
4208.75000	2786.41040	0.0000	-0.0151	
4271.25000	2786.41040	0.0000	-0.0155	
4333.75000	2786.41040	0.0000	-0.0159	
4396.25000	2786.41040	0.0000	-0.0164	
4458.75000	2786.41040	0.0000	-0.0168	
4521.25000	2786.41040	0.0000	-0.0172	
4583.75000	2786.41040	0.0000	-0.0176	
4646.25000	2786.41040	0.0000	-0.0181	
4708.75000	2786.41040	0.0000	-0.0186	
4771.25000	2786.41040	0.0000	-0.0191	
4833.75000	2786.41040	0.0000	-0.0196	
4896.25000	2786.41040	0.0000	-0.0201	
4958.75000	2786.41040	0.0000	-0.0208	
5021.25000	2786.41040	0.0000	-0.0214	
5083.75000	2786.41040	0.0000	-0.0222	
5146.25000	2786.41040	0.0000	-0.0231	
5208.75000	2786.41040	0.0000	-0.0241	
5271.25000	2786.41040	0.0000	-0.0252	
5333.75000	2786.41040	0.0000	-0.0266	
5396.25000	2786.41040	0.0000	-0.0282	
5458.75000	2786.41040	0.0000	-0.0302	
5521.25000	2786.41040	0.0000	-0.0326	
5583.75000	2786.41040	0.0000	-0.0356	
5646.25000	2786.41040	0.0000	-0.0394	
5708.75000	2786.41040	0.0000	-0.0441	
5764.35010	2786.41040	0.0000	-0.0493	

Figure A12. Example global velocity output file

# Appendix B

## M2D Citations

---

This appendix provides a listing of publications known to the authors to date that document M2D and its applications. Citations are listed in reverse chronological order.

- Bounaiuto, F., and Militello, A. (2004). "Coupled circulation, wave, and sediment transport modeling for calculation of morphology change, Shinnecock Inlet, New York," *Eighth International Estuarine and Coastal Modeling Conference*, American Society of Civil Engineers. (in press).
- Lin, L., Kraus, N. C, and Barcak, R. G. (2004). "Modeling sediment transport at the Mouth of the Colorado River, Texas," *Eighth International Estuarine and Coastal Modeling Conference*, American Society of Civil Engineers. (in press).
- Militello, A., and Zundel, A. K. (2003) "SMS Steering Module for coupling waves and currents, 2. M2D and STWAVE," Coastal and Hydraulic Engineering Technical Note ERDC/CHL CHETN-IV-60, U. S. Army Engineer Research and Development Center, Vicksburg, MS.
- Militello, A., Reed, C. W., Zundel, A. K., and Kraus, N. C. (2004). "Two-dimensional depth-averaged circulation model M2D: Version 2.0, Report 1; Documentation and user's guide," ERDC/CHL TR-04-2, U.S. Army Engineer Research and Development Center, Vicksburg, MS (this volume).
- Militello, A., and Kraus, N. C. (2003). "Numerical simulation of sediment pathways at an idealized inlet and ebb shoal," *Coastal Sediments 2003*, CD ROM: Numerical simulation of sediment pathways at an id.pdf
- Militello, A., Parry, R. M., and Arden, H. T. (2003). "Numerical simulation of navigation channel infilling, Bay Center, Washington," *Proceedings Dredging 2002 Conference*, ASCE, ASCE, CD ROM 40680-034-003, ISBN 0-7844-0680-4.
- Militello, A., and Zundel, A. K. (2002). "Coupling of regional and local circulation models ADCIRC and M2D," Coastal and Hydraulics Engineering Technical Note ERDC/CHL CHETN-IV-42, U. S. Army Engineer Research and Development Center, Vicksburg, MS.

- Militello, A., and Zundel, A. K. (2002). "Automated coupling of regional and local circulation models through boundary condition specification," *Proceedings of the Fifth International Conference on Hydroinformatics*, International Association of Hydraulic Research, IWA Publishing, London, 156-161.
- Militello, A. (2002). "Willapa entrance and Bay Center modeling," in "Study of navigation channel feasibility, Willapa Bay, report 2," Kraus, N. C., Arden, H. T., and Simpson, D. P., eds. Technical Report ERDC-CHL-TR-00-6, U.S. Army Engineer Research and Development Center, Vicksburg, MS.
- Militello, A., and Kraus, N. C. (2001). "Generation of harmonics by sea breeze in nontidal water bodies," *Journal of Physical Oceanography*, 31(6), 1639-1647.
- Militello, A. (2000). "Hydrodynamic modeling of a sea-breeze dominated shallow embayment, Baffin Bay, Texas," *Sixth International Estuarine and Coastal Modeling Conference*, American Society of Civil Engineers, ASCE Press, New York, 795-810.
- Kraus, N. C., and Militello, A. (1999). "Hydraulic study of multiple inlet system: East Matagorda Bay, Texas," *Journal of Hydraulic Engineering*, 125(3), 224-232.
- Militello, A., and Kraus, N. C. (1998). "Numerical simulation of hydrodynamics for proposed inlet, East Matagorda Bay, Texas," *Proceedings of the 5<sup>th</sup> International Estuarine and Coastal Modeling Conference*, American Society of Civil Engineers, ASCE Press, New York, 805-818.
- Militello, A. (1998). *Hydrodynamics of wind-dominated, shallow embayments*. Ph.D. diss. Division of Marine and Environmental Systems, Florida Institute of Technology, Melbourne, FL.
- Brown, C. A., and Militello, A. (1997). "Packery Channel feasibility study: Circulation and water level; Report 2 of a two-part series," TAMU-CC-CBI-96-07, Conrad Blucher Institute for Surveying and Science, Texas A&M University-Corpus Christi, Corpus Christi, TX.
- Kraus, N. C., and Militello, A. (1996). "Hydraulic feasibility of the proposed Southwest Cut, East Matagorda Bay, Texas," TAMU-CC-CBI-96-03, Conrad Blucher Institute for Surveying and Science, Texas A&M University-Corpus Christi, Corpus Christi, TX.
- Militello, A., and Kraus, N. C. (1995). "Investigation of the current and sediment movement in the Lower Laguna Madre, Texas, and implications for dredging in the Gulf Intracoastal Waterway," *Proceedings of the Western Dredging Association 16<sup>th</sup> Technical Conference*, Center for Dredging Studies, Texas A&M University, College Station, TX, 143-162.
- Brown, C. A., Kraus, N. C., and Militello A. (1995). "Hydrodynamic modeling for assessing engineering alternatives for elevating the Kennedy Causeway, Corpus Christi, Texas," *Proceedings of the 4<sup>th</sup> International Estuarine and Coastal Modeling Conference*, American Society of Civil Engineers, ASCE Press, New York, 681-694.

- Brown, C. A., Militello, A., and Kraus, N. C. (1995). "Hydrodynamic assessment for elevation of the JFK Causeway, Corpus Christi, Texas," *Proceedings Texas Water '95*, Texas Section of the American Society of Civil Engineers, ASCE Press, New York, 31-41.
- Brown, C. A., Militello, A., and Kraus, N. C. (1995). "Hydrodynamic assessment for elevation of the JFK Causeway, Corpus Christi, Texas," TAMU-CC-CBI-95-07, Conrad Blucher Institute for Surveying and Science, Texas A&M Univeristy-Corpus Christi, Corpus Christi, TX.
- Militello, A., and Kraus, N. C. (1995). "Numerical simulation of the circulation in the Lower Laguna Madre, Texas, and implications for dredging of the Gulf Intracoastal Waterway," *Estuarine Research Federation 13<sup>th</sup> Biennial International Conference, Abstracts*, 88.
- Militello, A., and Kraus, N. C. (1994). "Reconnaissance investigation of the current and sediment movement in the Lower Laguna Madre between Port Isabel and Port Mansfield, Texas," TAMU-CC-CBI-94-04, Conrad Blucher Institute for Surveying and Science, Texas A&M University-Corpus Christi, Corpus Christi, TX.

# Appendix C

## Slosh Tests

---

This appendix describes the performance of M2D for slosh tests. This set of numerical integrity tests evaluates mass conservation and numerical damping properties of the model. Finite-difference approximations to the full equations of motion truncate terms to some order in a manner that depends on the numerical solution method. Truncation of terms is known to introduce numerical viscosity (Roache 1976),<sup>1</sup> which is manifested as damping of a signal. The slosh test provides a means of examining the damping of a particular numerical computation method. In a slosh test, the initial condition of a tilted water surface is imposed, and the basin is allowed to freely propagate the resulting wave through reflection at both ends. External forcing and bottom frictional stress are set to zero so that there is no masking of the free-surface oscillations. Time-series of water elevation over the duration of the simulation provides information on model damping properties. Tests described here were patterned after those by Cialone (1989).

The slosh test was performed to examine damping properties and mass conservation for two grid configurations. Both grid configurations were rectangular, with the grid being longer parallel to the x-axis than parallel to the y-axis. A test consisted of applying a tilted water surface as the initial condition, where the direction of tilt was parallel to the x-axis. The initial deviation from still-water depth was symmetric about the channel center and increased or decreased sinusoidally along the main channel axis (Figure C1).

No variation in water level was specified across the width (parallel to the y-axis) of the channel. Initial current velocity was set to zero, and no boundary forcing, bottom friction, or wind stress were applied. The Coriolis term and lateral mixing were set to zero. Simulation duration was set to 30 days (720 hr) and the time-step was set to 5 s. General grid configurations and inclusion of advective terms are given in Table C1. Conducting identical tests with and without inclusion of the advective terms allows isolation of their contribution to damping and mass conservation.

---

<sup>1</sup> All references cited in this appendix are included in the References section at the end of the main text.

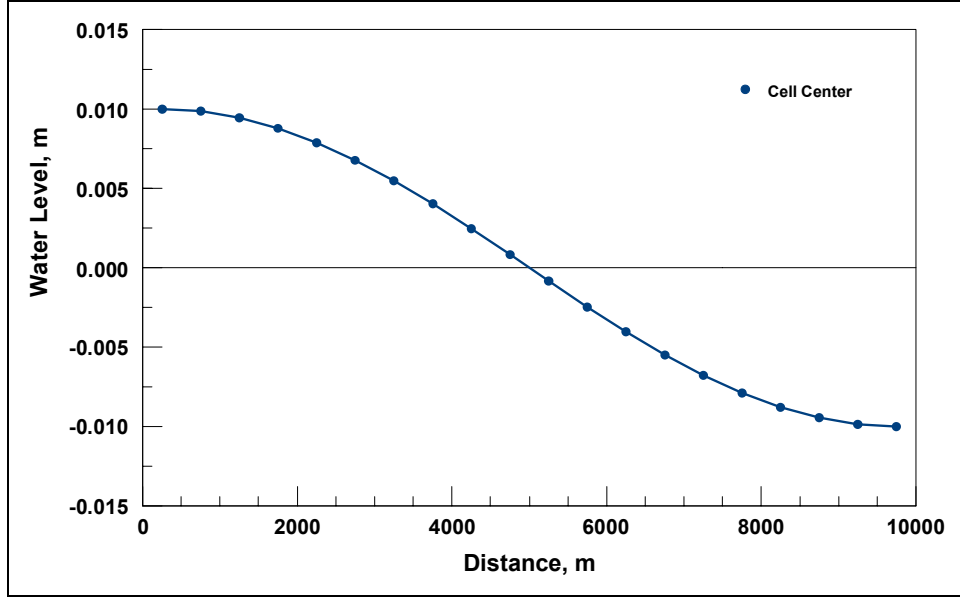


Figure C1. SLOSH test initial condition

Table C1 SLOSH Test Configurations		
Test	Bottom	Advection
1	Flat	No
2	Flat	Yes
3	Sloped	No
4	Sloped	Yes

Mass conservation was calculated as percent change in water volume over the numerical grid between time  $t = 0$  and the end of the simulation period. Percent change in water volume  $\Delta V$  was calculated as

$$\% \Delta V = 100 \left( \frac{\sum_{i=1}^n V_{f_i} - \sum_{i=1}^n V_{ic_i}}{\sum_{i=1}^n V_{ic_i}} \right) \quad (C1)$$

where  $V_f$  is the final volume,  $V_{ic}$  is the initial volume, the subscript  $i$  indicates cell number, and  $n$  is the total number of cells in the grid.

Tests 1 and 2 were conducted to evaluate damping and mass conservation of the model for a flat-bottomed, constant-spaced grid, with and without the advective terms included in the calculations, respectively. Grid configurations and numerical parameters for Tests 1 and 2 are given in Table C2 and the grid is

shown in Figure C2. Tests 1 and 2 resulted in  $5 \times 10^{-6}$  and  $1 \times 10^{-5}$  percent changes in volume, respectively.

<b>Table C2 Slosh Test Grid Configurations and Numerical Parameters for Tests 1 and 2</b>	
<b>Numerical Parameter</b>	<b>Value</b>
$\Delta s$ , m	500
$\Delta t$ , s	5
$h$ , m	10
<b>Length, m</b>	10,000
<b>Width, m</b>	2,500

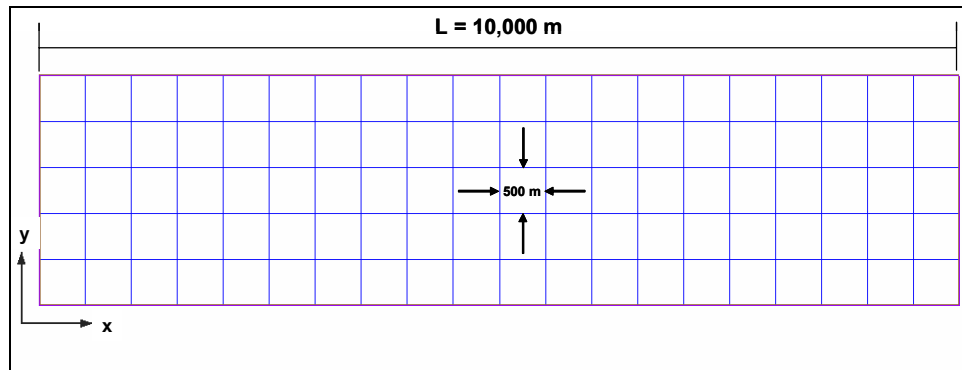


Figure C2. Computational grid for Tests 1 and 2

Damping properties for Tests 1 and 2 are shown by time series of water level in Figures C3 and C4, respectively. Water levels shown for each plot were taken  $0.5\Delta x$  from the boundary and centered with respect to channel width. Time series shown for all other tests are also taken at the same cell. Axis breaks (x-axis) were inserted into the plots so that time series at the beginning and ending portions of the simulations could be easily viewed. Test 1 does not exhibit damping over the duration of the simulation. Weak nonlinear motion owes to the nonlinear form of the continuity equation. Test 2 exhibits weak damping over the 1-month simulation. Development of nonlinearities is slightly stronger than for Test 1 owing to the contribution by the advective terms. Tests 1 and 2 were repeated with an initial surface deviation 10 times smaller than described here (results not shown). Motion induced by this smaller water surface deviation was not sufficient to develop nonlinearities and the resulting slosh motion for both cases (with and without advection) showed no variation in peak water level and no damping was exhibited.

The fundamental seiche period for a rectangular basin is given by

$$T = \frac{2l}{\sqrt{gh}} \quad (C2)$$

where  $l$  is the length of the basin. For a wave traveling parallel to the x-axis of the slosh-test grid,  $T = 0.02337$  day, corresponding to a frequency of 42.8 cycles/day (cpd). Spectrums of water levels shown in Figures C3 and C4 for Tests 1 and 2 are displayed in Figures C5 and C6, respectively. Peak amplitudes occur at 42.8 cpd. Small peaks (slightly visible in Figures C5 and C6) are contained in the spectra at 85.6 cpd, indicating the presence of a weak harmonic of the primary seiche frequency. These tests indicate that the discretized equations applied for calculation of water level in Tests 1 and 2 do not introduce erroneous frequencies into the solution.

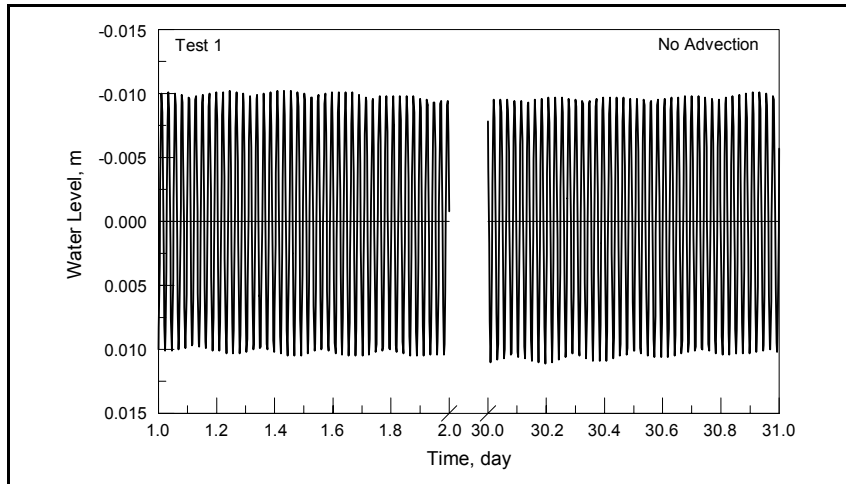


Figure C3. Time series of water level for Test 1

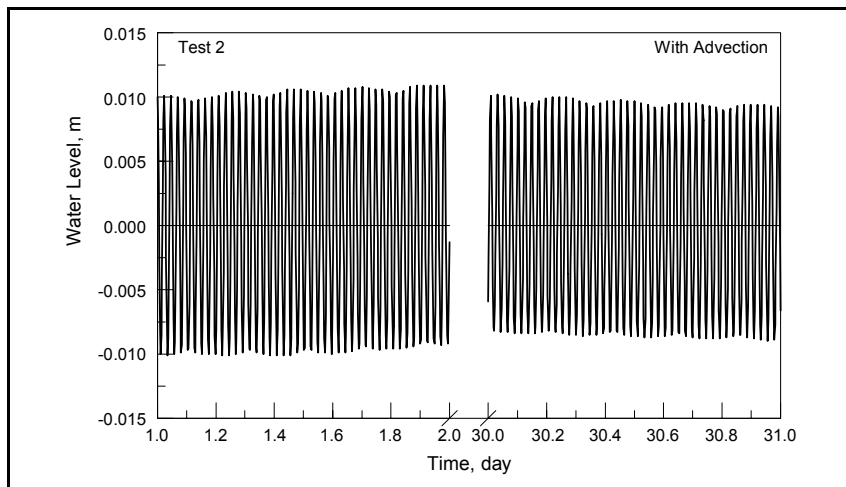


Figure C4. Time series of water level for Test 2

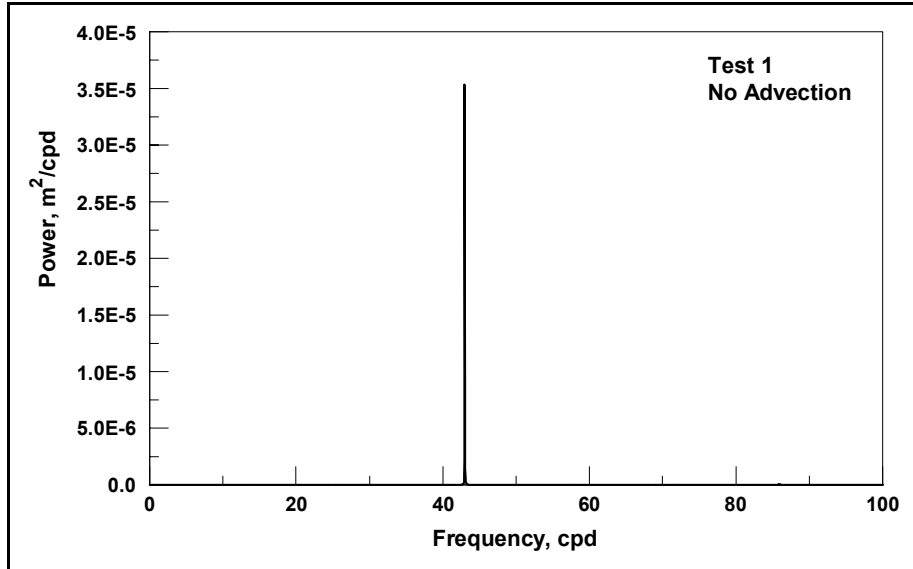


Figure C5. Spectrum of water level for Test 1

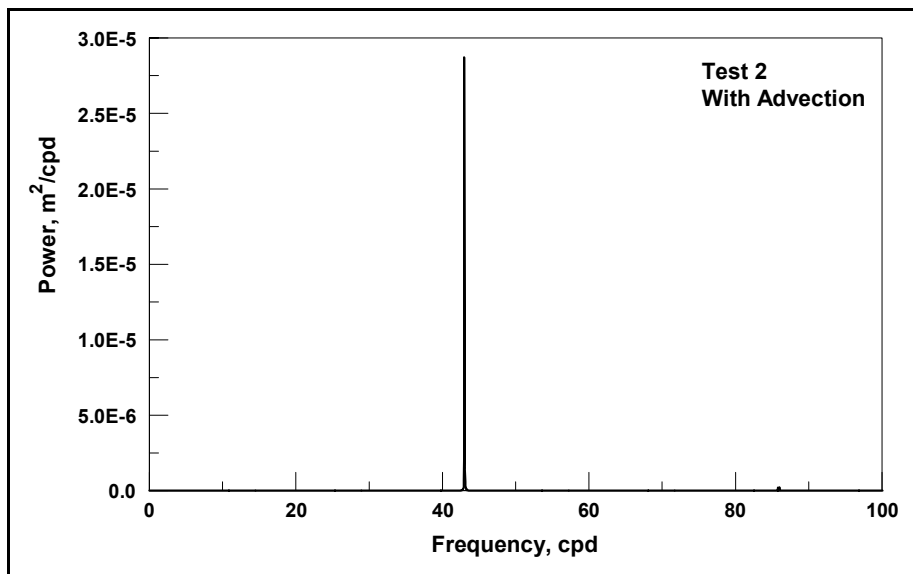


Figure C6. Spectrum of water level for Test 2

Tests 3 and 4 were designed to determine how damping and mass conservation properties respond to a grid with sloped bottom and constant cell sizes. Grid configurations and numerical parameters for Tests 3 and 4 are given in Table C3 and the grid is shown in Figure C7. Changes in volume of  $5 \times 10^{-6}$  and  $1 \times 10^{-5}$  percent were calculated for Tests 3 and 4, respectively.

<b>Table C3 Slosh Test Grid Configurations and Numerical Parameters for Tests 3 and 4</b>	
<b>Numerical Parameter</b>	<b>Value</b>
$\Delta s$ , m	500
$\Delta t$ , s	5
$h$ , m	Min = 9 m, Max = 11 m, $\Delta h / \Delta x = 0.0002$
<b>Length, m</b>	10,000
<b>Width, m</b>	2,500

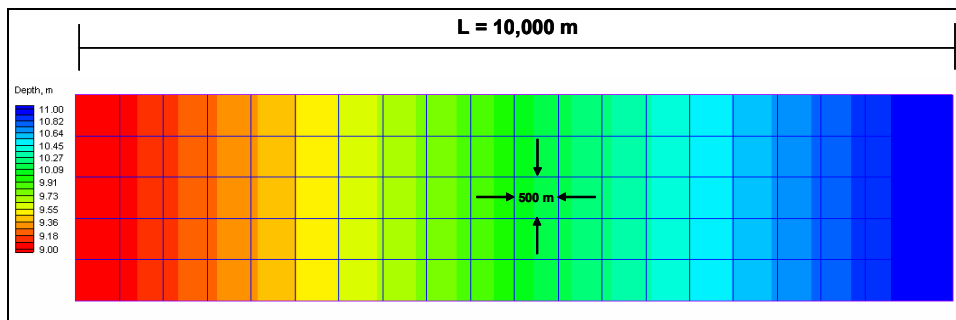


Figure C7. Computational grid for Tests 3 and 4

Damping properties for Tests 3 and 4 are shown by time series of water level in Figures C8 and C9, respectively. Starting maximum water level for both Tests was 0.01 m at  $0.5\Delta x$  from the end of the grid. Test 3 does not exhibit damping over the duration of the simulation. Water levels from Test 4 are slightly damped by properties of the numerical algorithm for the advective terms. In both tests, water levels are weakly nonlinear, as described for Tests 1 and 2.

Spectrums of water levels for Tests 3 and 4 are displayed in Figures C10 and C11, respectively. Peak amplitudes occur at 42.4 cpd. Small peaks (slightly visible in Figures C5 and C6) are contained in the spectra at 84.8 cpd, indicating the presence of a weak harmonic of the primary seiche frequency. These spectra demonstrate that the discretized equations applied for calculation of water level in Tests 3 and 4 do not introduce erroneous frequencies into the solution.

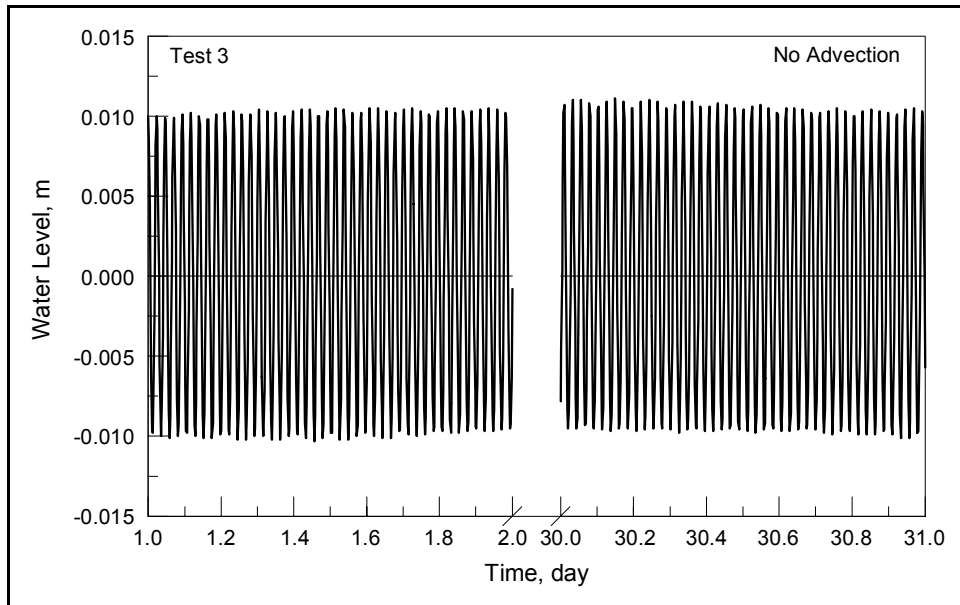


Figure C8. Time series of water level for Test 3

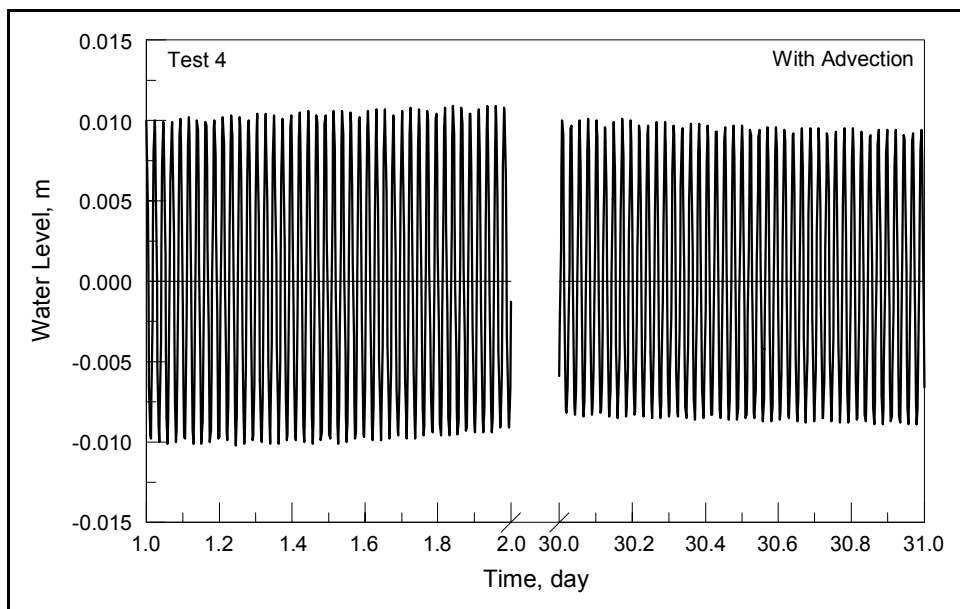


Figure C9. Time series of water level for Test 4

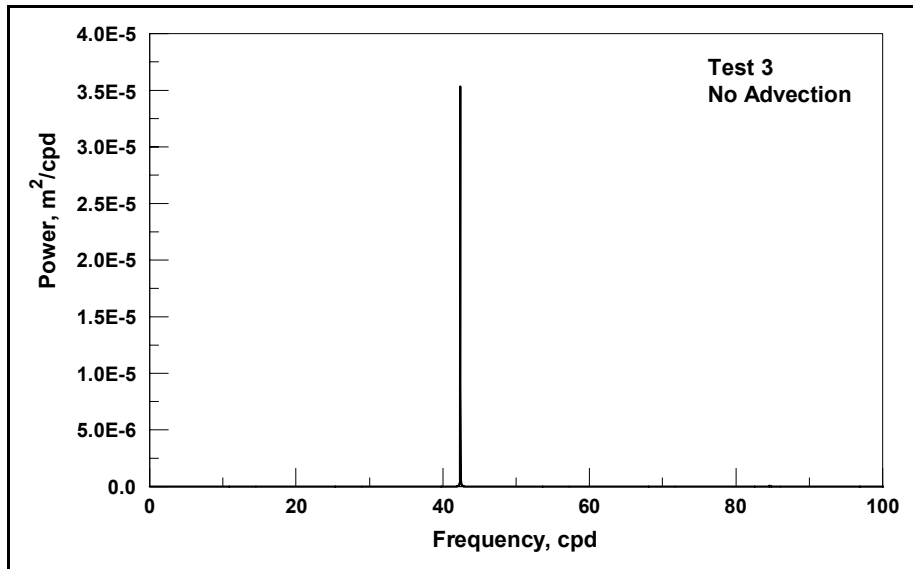


Figure C10. Spectrum of water level for Test 3

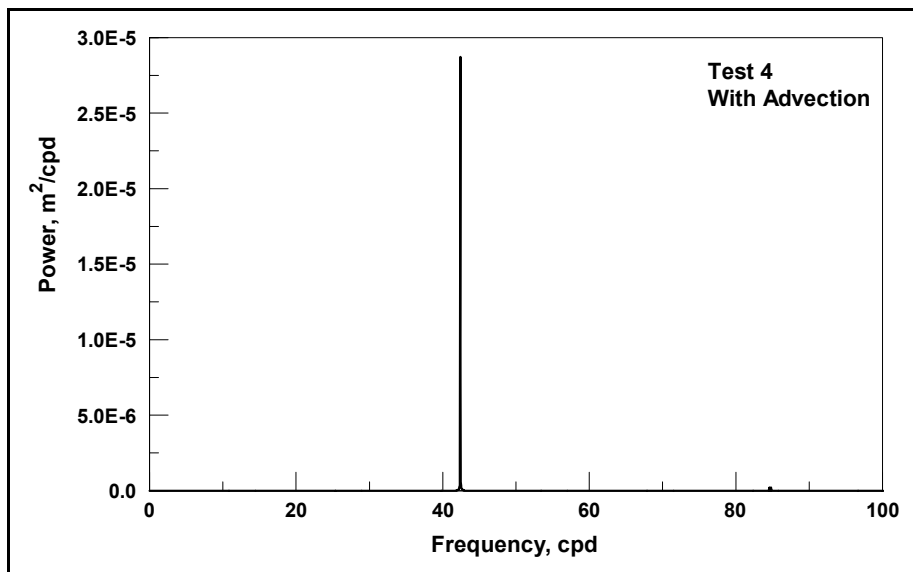


Figure C11. Spectrum of water level for Test 4

# Appendix D

## Wind Setup Tests

---

This appendix describes tests designed to evaluate model performance under wind forcing. Two tests were performed to examine model response. The first test compares the results of numerical calculations to those of an analytical solution for a rectangular channel. The second test evaluates model response to wind forcing in a basin of arbitrary shape.

Wind setup in a rectangular channel for steady-state conditions is maintained by a balance of the pressure gradient, wind forcing, and bottom friction. For 1-D flow, the momentum equation (Equation 2) can be reduced to (Bretschneider 1966)<sup>1</sup>

$$\frac{d\eta}{dx} = \frac{(\tau_w + \tau_b)}{\rho_w g(h + \eta)} \quad (D1)$$

where  $\tau_w$  is the wind stress, and  $\tau_b$  is the bottom stress. In the absence of bottom friction, Equation D1 of Bretschneider can be rewritten as

$$\frac{d\eta}{dx} = \frac{\kappa W^2}{g(h + \eta)} \quad (D2)$$

where  $\kappa = 3.3 \times 10^{-6}$ . The coefficient  $\kappa$  was derived from wind and bottom-stress coefficients determined in a study of Lake Okeechobee, FL (Saville 1953). Application of Equation D2 to the present study required modification of  $\kappa$  to be equal to the wind-stress coefficient applied in M2D, which varies with wind speed, so that analytical and numerical solutions could be compared. Integration of Equation D2 gives

$$\eta = \sqrt{2 \frac{\kappa W^2}{g} (x + C) + h^2} - h \quad (D3)$$

---

<sup>1</sup> All references cited in this appendix are included in the References section at the end of the main text.

where  $C$  is a constant of integration which is determined by the position of the channel origin if no bottom is exposed, and by the position of the water-land interface if drying has occurred. The parabolic form of Equation D3 indicates a locally wind-forced water surface in a rectangular channel does not have a linear distribution along the channel axis. Instead, the water surface will be curved, with the curvature being dependent on the channel length and depth, and the wind speed.

For comparison of the analytical and numerical solutions of Equation D2, a 1-D grid was developed that had a total length of 9,500 m and was 95 cells long. Each square cell had side dimensions of 100 m. The still-water depth was set to 2 m and the time-step was 10 s. The wind speed set to 10 m/s and held constant. A 10-m/s wind speed corresponds to  $\kappa = 1.9375 \times 10^{-6}$ . Figure D1 compares water level computed analytically from Equation D2 and numerically by M2D, under steady-state conditions. The numerical solution well reproduces the steady-state, wind-induced setup and setdown of the analytical solution for simulations applied to shallow water.

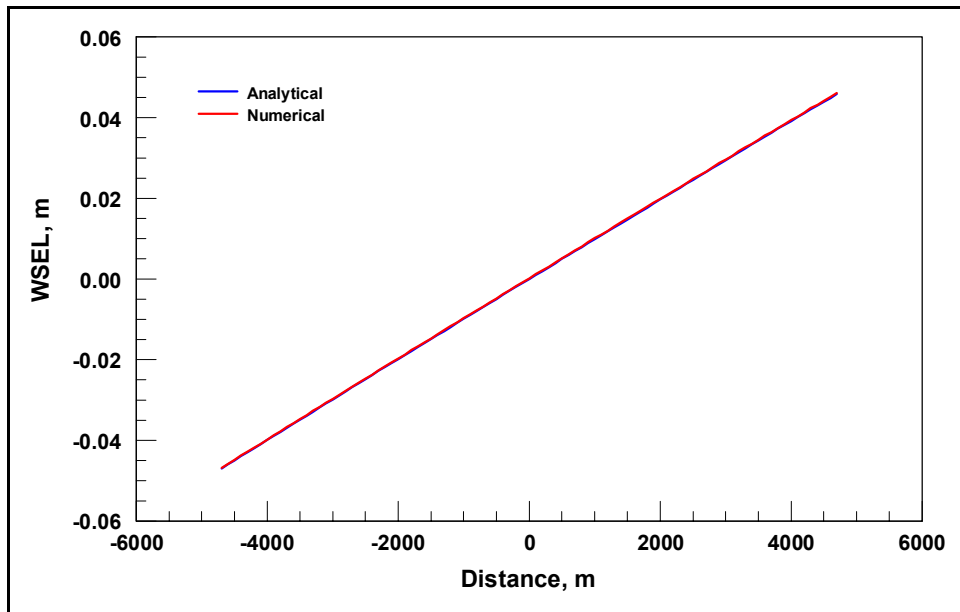


Figure D1. Comparison of analytical and numerical solutions of steady-state, wind-induced setup, no exposed channel bottom

To test the response of the model to wind forcing in a basin of arbitrary geometry, a modified version of the hourglass test developed for a curvilinear grid (Spaulding 1984) was examined. An hourglass-shaped grid was developed with constant cell-side lengths set to 500 m and an ambient depth of 5 m. The time-step was set to 30 s. Two tests were performed, one for wind blowing from the west (from the negative x-axis) and the other for wind blowing from the north (from the positive y-axis). For each test, the wind was ramped up over a 24-hr interval and held constant at 10 m/s for the remainder of the 100-hr simulation.

Water surface elevation for the west wind test is shown in Figure D2. The setup and setdown are symmetric between the upper and lower portions of the grid. The water surface elevation contours for the north wind test are shown in Figure D3. The water surface elevation for the north wind test is equally distributed between the left and right portions of the grid. Symmetry in both tests demonstrates that there is no inconsistency in calculations at wall boundaries. The results of this test demonstrate that the model responds to wind forcing with qualitatively correct patterns of water surface deviation. Wind setup calculated by M2D is qualitatively similar to results displayed graphically by Spaulding (1984) and by Cialone (1989).

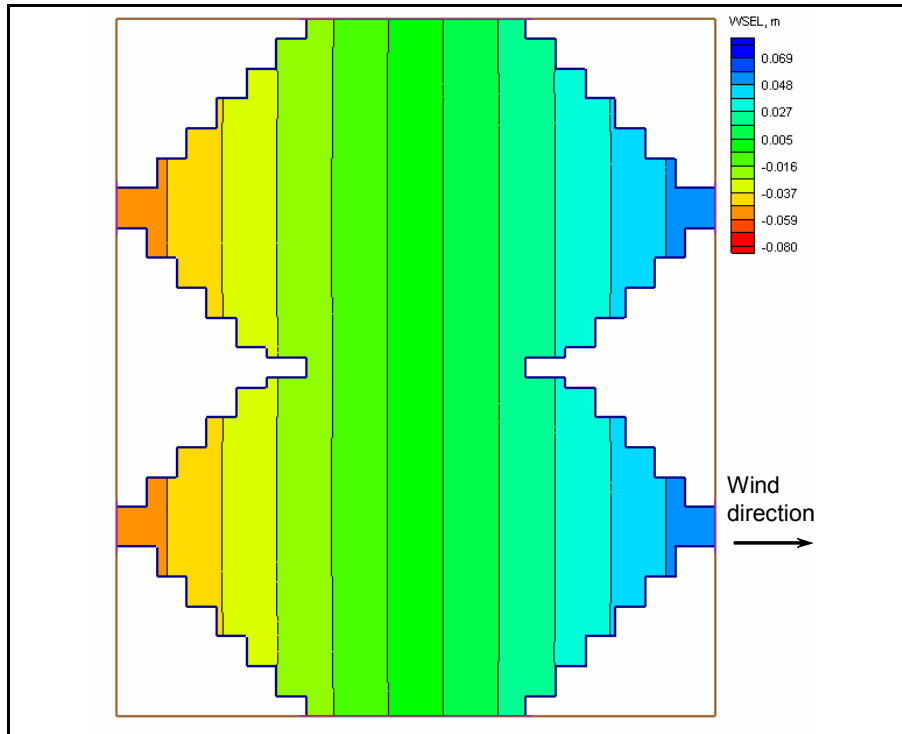


Figure D2. Water surface elevation contours for west wind

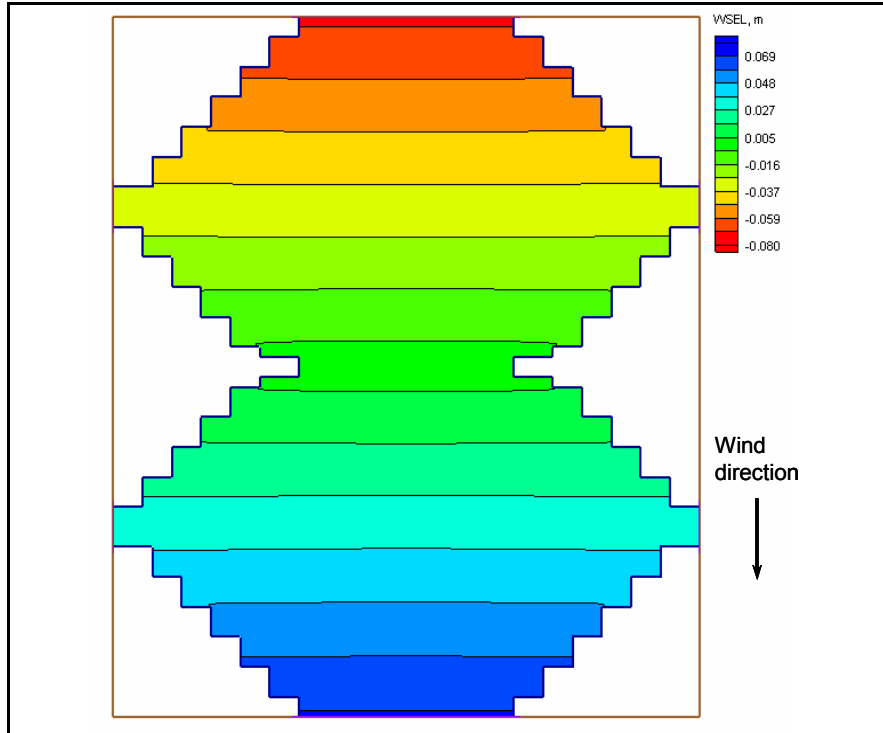


Figure D3. Water surface elevation contours for north wind

# Appendix E

## Advection Test

---

Advective terms were examined by developing a grid with an idealized jettied inlet and displaying the current field during ebb flow. Inclusion of the advective terms in the momentum equations allows the model to properly simulate eddies and an ebb jet as the ebb flow exits the inlet. No eddies or jet will develop without advective terms included in the calculations.

The idealized inlet grid was specified to have a flat bottom with a still-water depth of 5 m. Inlet dimensions were 300 m wide and 800 m long. Cell-side lengths were 25 m on all sides in the inlet and nearshore areas. Cell size increased to 50 m offshore. The time-step was set to 1 s. Water level was forced with a sine wave having amplitude of 0.5 m and period of 12.42 hr.

Two simulations were conducted, one without advective terms included in the computations and one with them. Figure E1 shows the current field from the test without the advective terms during the ebb tidal cycle. No eddies are present and flow exiting the inlet spreads laterally, but does not form a jet. However, with the advective terms included in the computations (Figure E2), a well-developed ebb jet is formed and eddies are present on each side of the jet. The ebb jet and eddies are symmetrical about the axis of the inlet, demonstrating that there is no directional bias in the advection algorithm.

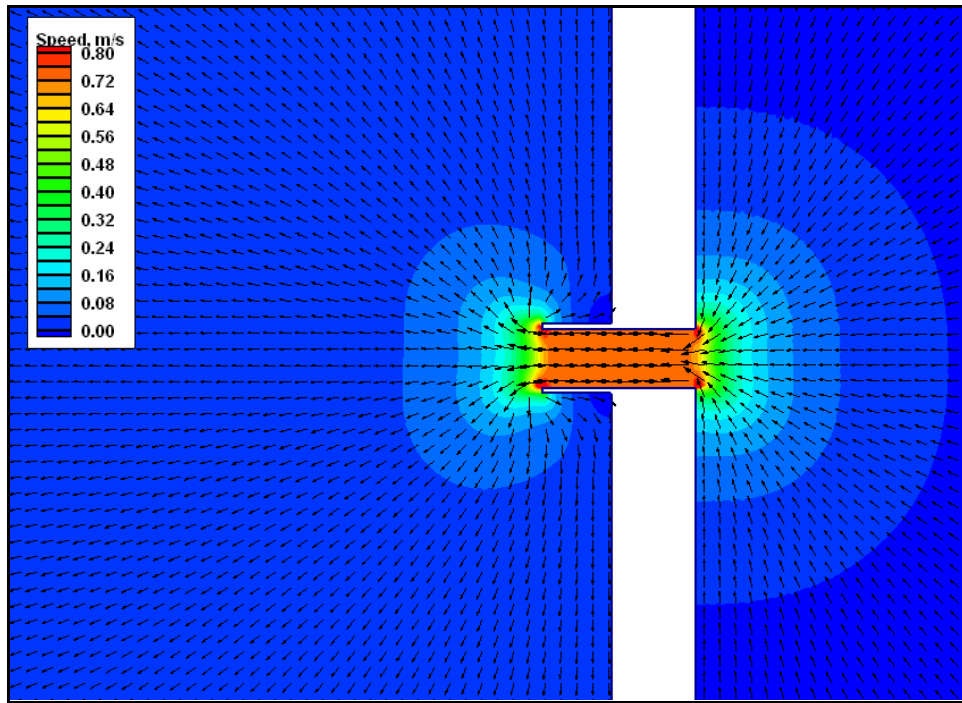


Figure E1. Ebb current field for advection test: no advective terms

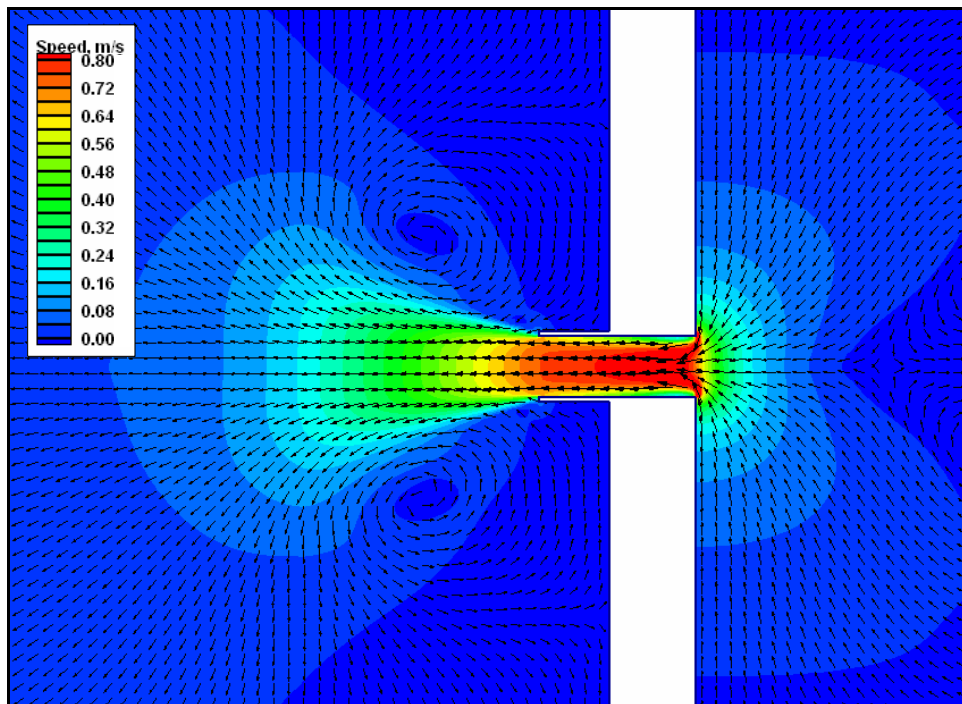


Figure E2. Ebb current field for advection test: with advective terms

# Appendix F

## Wetting and Drying Tests

---

Tests were performed on a sloped-bottom grid to determine the stability properties of the wetting and drying algorithms. One- and two-dimensional tests were conducted to demonstrate the behavior of the flooding and drying algorithms under different sources of hydrodynamic forcing and basin geometries. A list and brief description of the tests are given in Table F1. Detailed descriptions and model results are provided in specific test sections of this appendix.

<b>Table F1 List and Description of Flooding and Drying tests</b>		
<b>Test Number</b>	<b>Title</b>	<b>Description</b>
1	Channel with sloping bottom	Test wetting and drying of a 1-D canal forced by time-varying wind.
2	Depression in a square grid	Test stability for wetting dry cells surrounding a ponded area. 2-D grid.

### Test 1: Channel with Sloping Bottom

A one-dimensional (1D) test was conducted to examine the flooding and drying algorithms for a channel with simple geometry. The test consisted of a channel with a sloping bottom that was forced by a time-varying wind. The channel length was 150,000 m with 101 cells along the main channel axis (parallel to the x-axis) and 1 grid-cell wide. Cells were square with side lengths of 1,500 m. The time-step was 100 s. The bottom slope of the channel was  $1.67 \times 10^{-5}$  with a maximum still-water depth of 3 m and a minimum still-water depth of 0.5 m. Forcing for the test consisted of a wind that blew along the channel from the shallow end toward the deep end. The wind was ramped up over 10 hr to a maximum speed of 10 m/s and held constant from hour 10 to hour 100. The wind was turned off at 101 hr and remained off for the remainder of the 200-hr simulation.

Time series of water elevation for the sloping-bottom test are shown in Figure F1 in 10-hr intervals. Twenty-six cells on the shallow end of the grid are

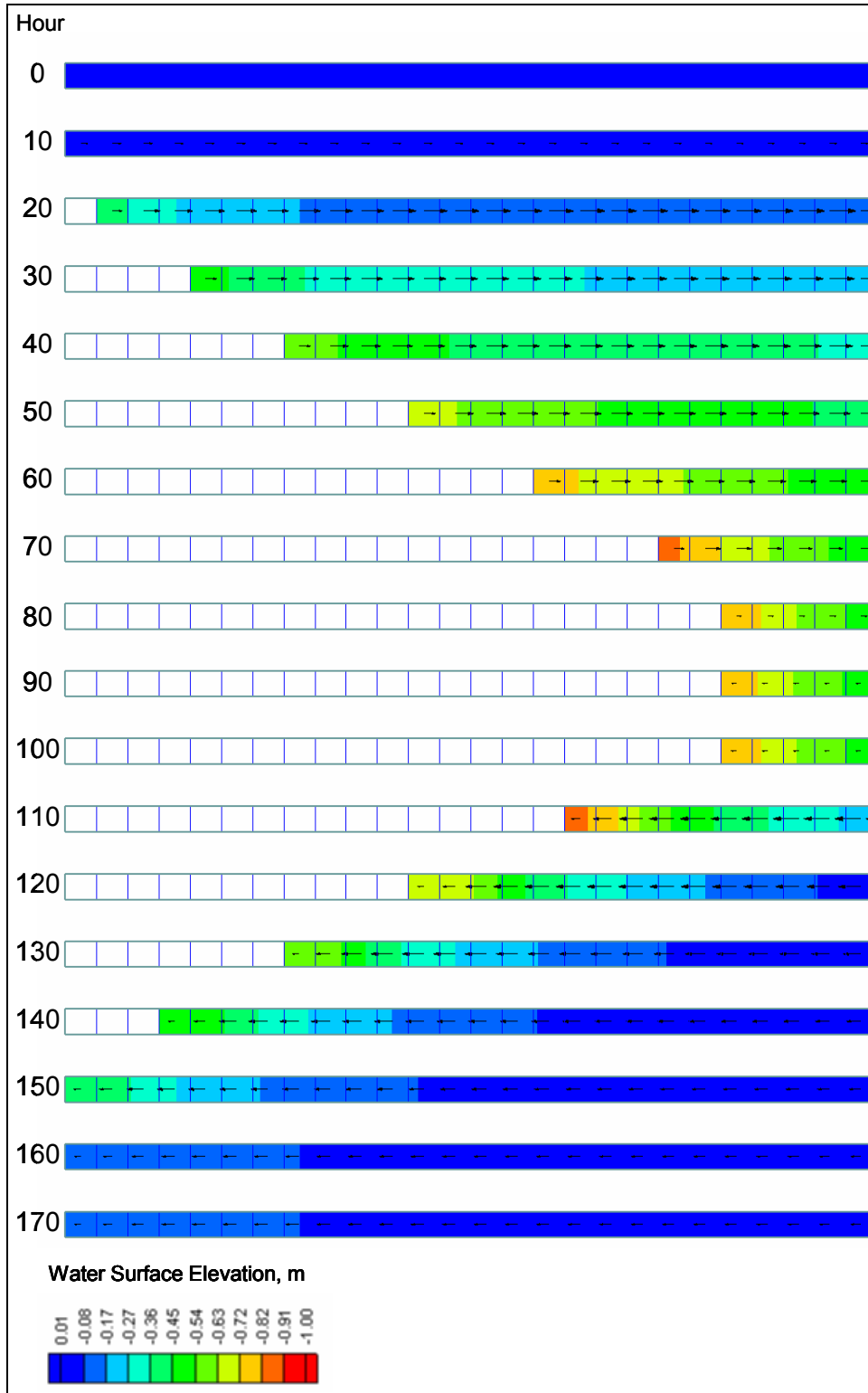


Figure F1. Demonstration of flooding and drying of sloped channel

shown out of the 101 cells in the grid. Ambient water depths in the channel increase from left to right. Dry cells are shown as white. Over the duration the wind stress applied to the channel (0 to 100 hr), water is forced out of the shallow area so that successive drying of cells occurs from left to right. A maximum of 21 cells dried during the simulation. After the wind was turned off (hour 101), water flows from right to left, successively inundating the dry cells.

## Test 2: Depression in Square Grid

A source of instability in some flooding and drying algorithms is rewetting of dry cells that surround an area that has formed a pond. A robust flooding algorithm will remain stable with any pattern of wet and dry cells. This test was designed to determine the behavior of the wetting and drying algorithms where ponding takes place.

A square grid consisting of 400  $50 \times 50$ -m cells was developed in which the central area contained a square ring of shallow cells surrounding deeper cells (Figure F2). Outside the shallow ring, the depth was set to 2 m everywhere. Cells in the shallow ring were specified with depths of 0.3 m, with adjacent interior cells having depths of 0.5 m, and adjacent outer cells having depths of 1.0 m. Four cells in the center of the depression were 1-m deep.

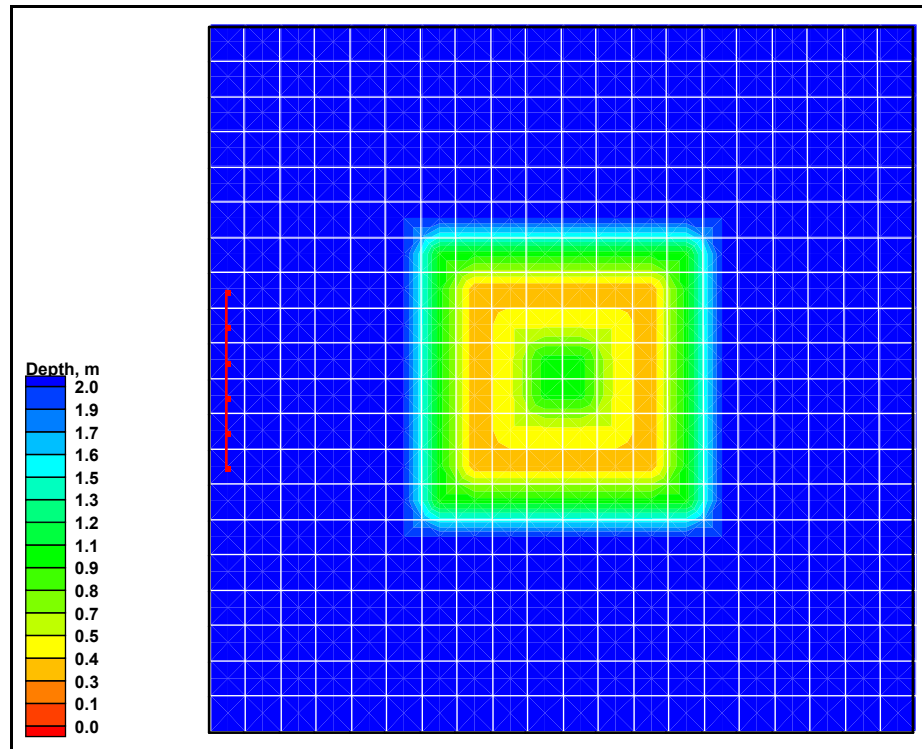


Figure F2. Grid with central depression surrounded by shallow area

The grid was forced with water surface elevation at six cells located on the left side of the grid, denoted by the red line in Figure F2. A sinusoidal forcing was applied having amplitude of 1 m and period of 12 hr. The depth at which cells are deemed dry was specified as 0.05 m. The model was run for duration of 50 hr, with a ramp of 1 day and time-step of 5 s. Plots of water level and circulation are shown in Figures F3 through F10 at hourly intervals starting at hour 42. During hours 43 to 47, the water level was lowered to expose the ring of shallow cells. The dry cells are denoted by white with no current vectors. A pond was formed within the interior of the ring of dry cells.

Water level rises from hours 45 through 49. At hour 46 (Figure F7), cells on the outer portion of the shallow ring (with ambient depths of 1 m) have rewetted. By hour 48 (Figure F9), all previously dry cells have rewetted. During the process of flooding and drying, no instabilities were encountered. Thus, the wetting and drying algorithms in M2D function properly for the situation of flooding around a ponded area.

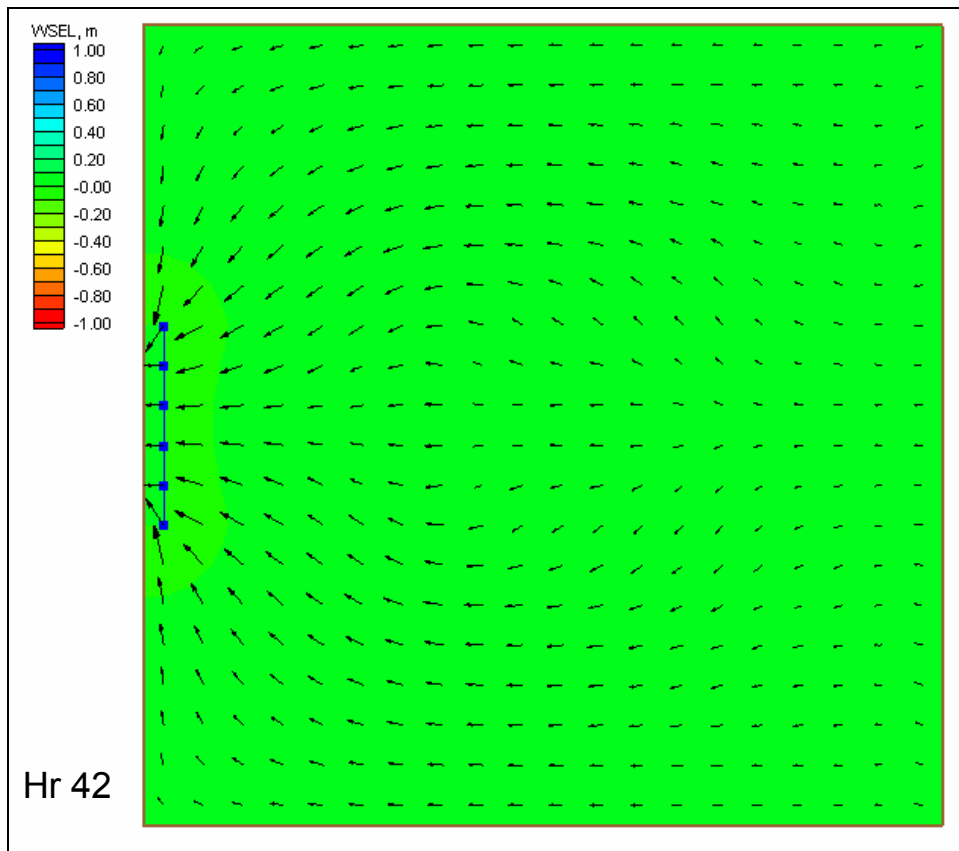


Figure F3. Water level and circulation pattern at hour 42

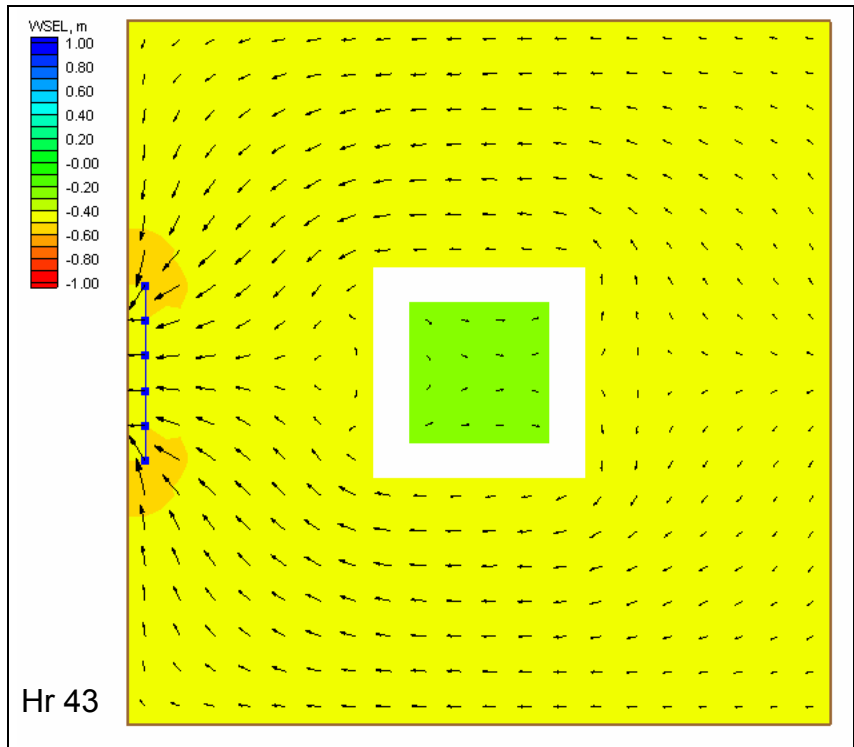


Figure F4. Water level and circulation pattern at hour 43

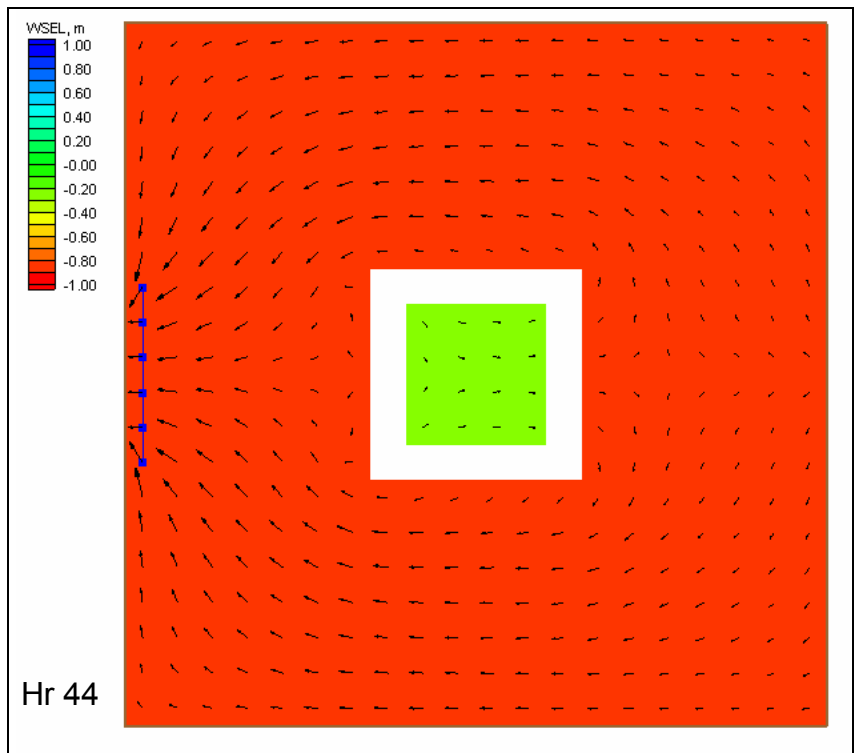


Figure F5. Water level and circulation pattern at hour 44

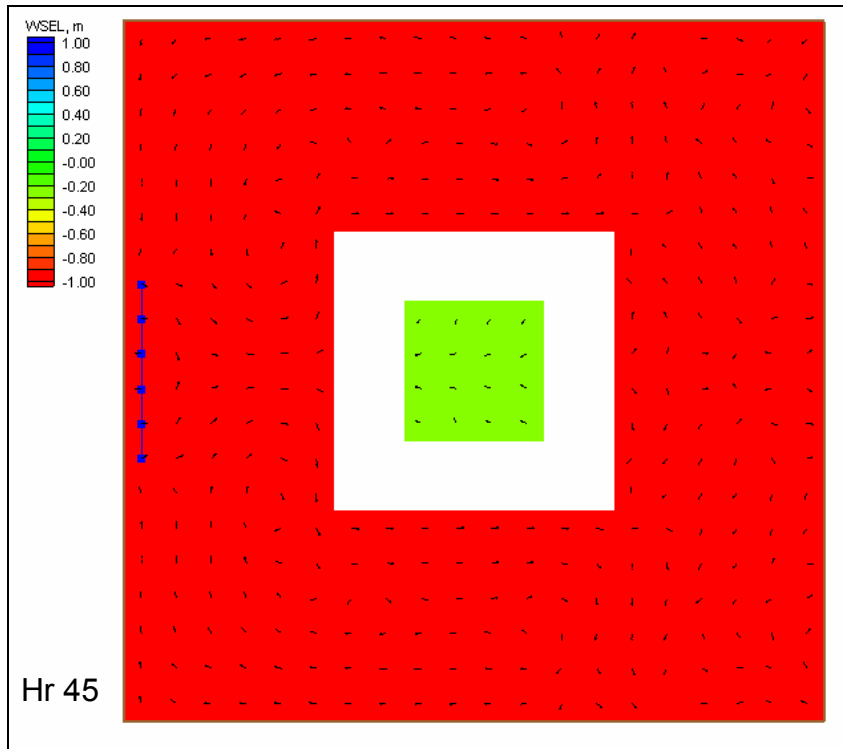


Figure F6. Water level and circulation pattern at hour 45

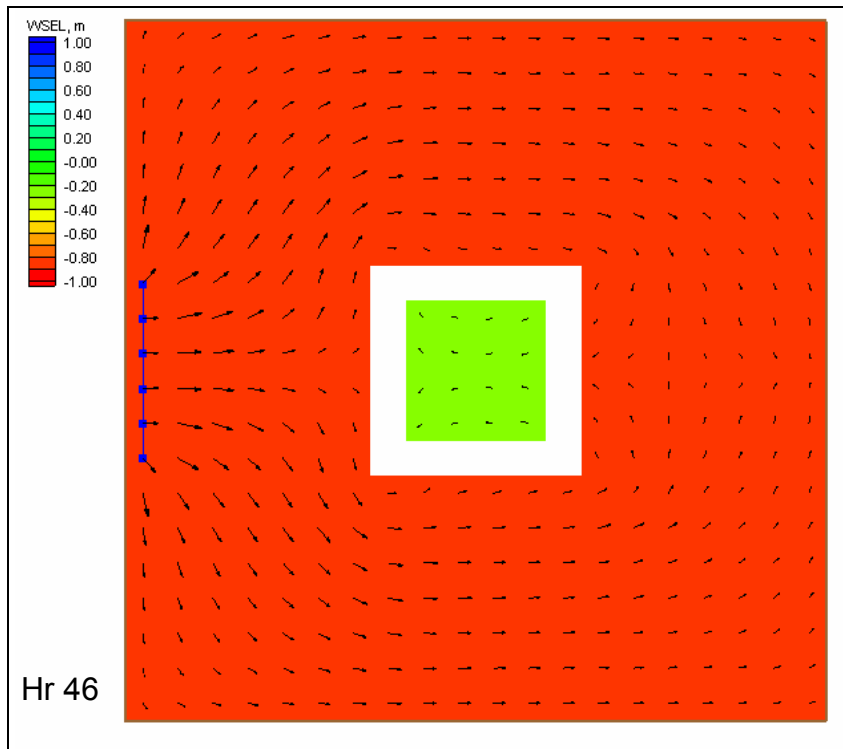


Figure F7. Water level and circulation pattern at hour 46

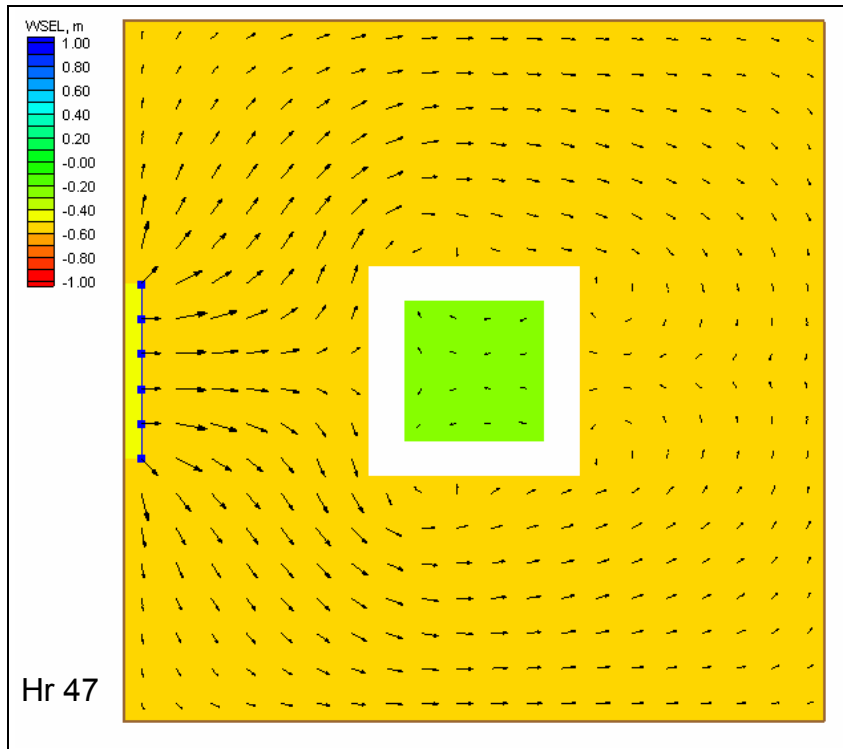


Figure F8. Water level and circulation pattern at hour 47

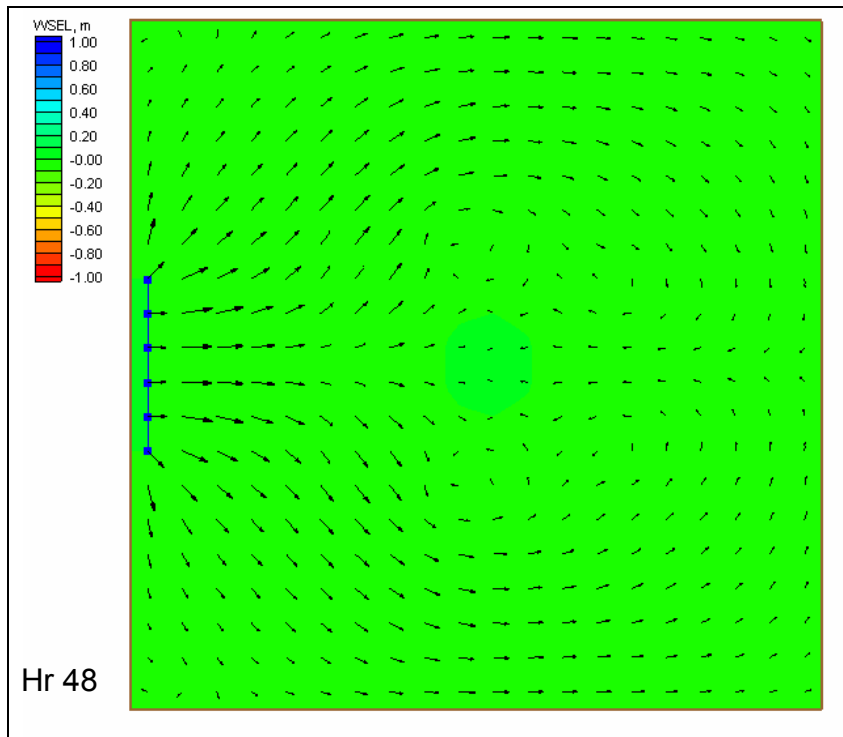


Figure F9. Water level and circulation pattern at hour 48

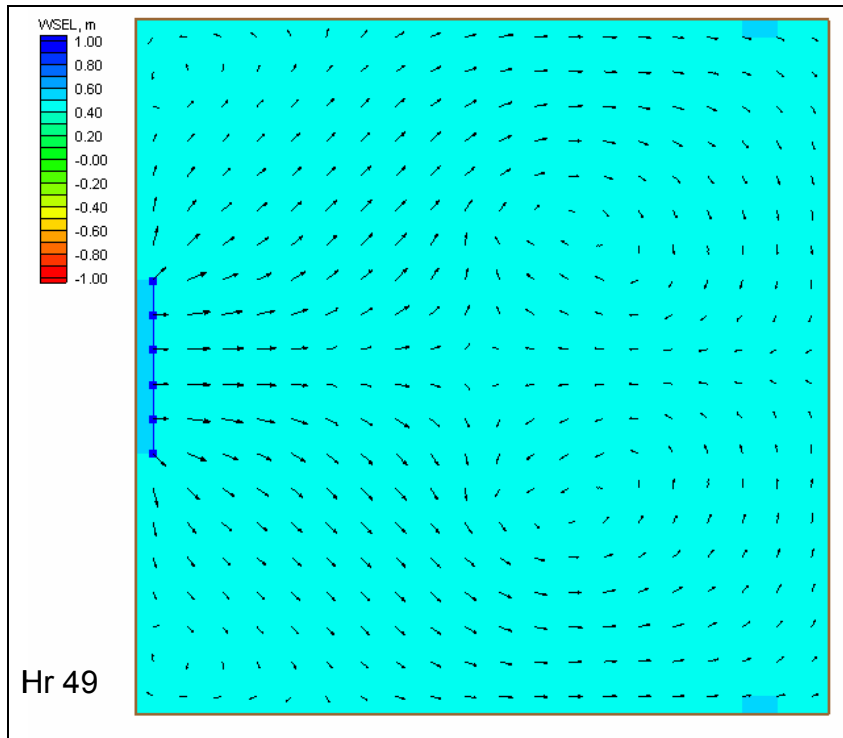


Figure F10. Water level and circulation pattern at hour 49

# Appendix G

## Wave-Adjusted Boundary Condition Test

---

This appendix demonstrates the wave-adjusted boundary condition for an idealized beach. In the example, wave forcing is applied to calculate an alongshore current. The wave-adjusted boundary condition modifies the water level and velocity on boundaries forced by water surface elevation to account for the presence of wave forcing. Thus, the prescribed boundary forcing is applied after being adjusted for the presence of waves. This adjustment promotes realistic circulation patterns and wave setup and setdown at the boundaries, making values at the lateral boundaries compatible with values calculated within the calculation domain near the boundaries. A simulation without the wave-adjusted boundary condition is also shown, which illustrates the necessity of the modification of water level and velocity at the boundary.

An idealized beach computational grid was developed (Figure G1) having grid spacing of 50 m in each horizontal direction, and depths ranging from 1.13 m at the shoreline to 18.4 m at the seaward boundary. M2D and STWAVE domains were identical for the idealized beach simulations.

Forcing for the models was specified as:

- a. STWAVE: Wave height of 2.0 m, period of 10.0 s, and wave angle of 25.0 deg. Spectral spreading parameters were  $\gamma = 3.3$  and  $nn = 4$ .
- b. M2D: Water surface elevation set to 0.0 m along lateral and seaward boundaries.

M2D was run for 12.5 hr with a 2-s time-step and ramp duration of 0.02 day. Results from the simulation without the wave-adjusted boundary condition are described first, followed by those with the wave-adjusted boundary condition.

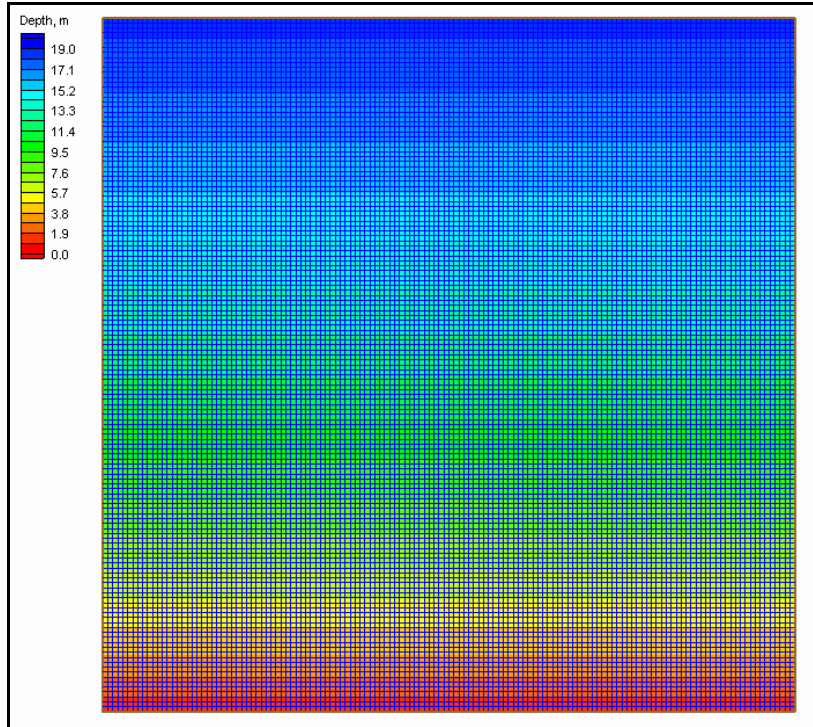


Figure G1. Computational grid for idealized beach

Water surface elevation and velocity as computed by the standard water surface elevation forcing boundary condition (boundaries not adjusted for presence of wave forcing) are shown in Figures G2 and G3, respectively. Setup is calculated at the shoreline, but decreases to zero at the lateral boundaries. An alongshore current is develops in the nearshore area, but velocities at the lateral boundaries are weaker than inside the calculation domain and display unrealistic patterns. The unrealistic velocity patterns and water surface elevations at the lateral boundaries owe to the absence of the wave stresses there.

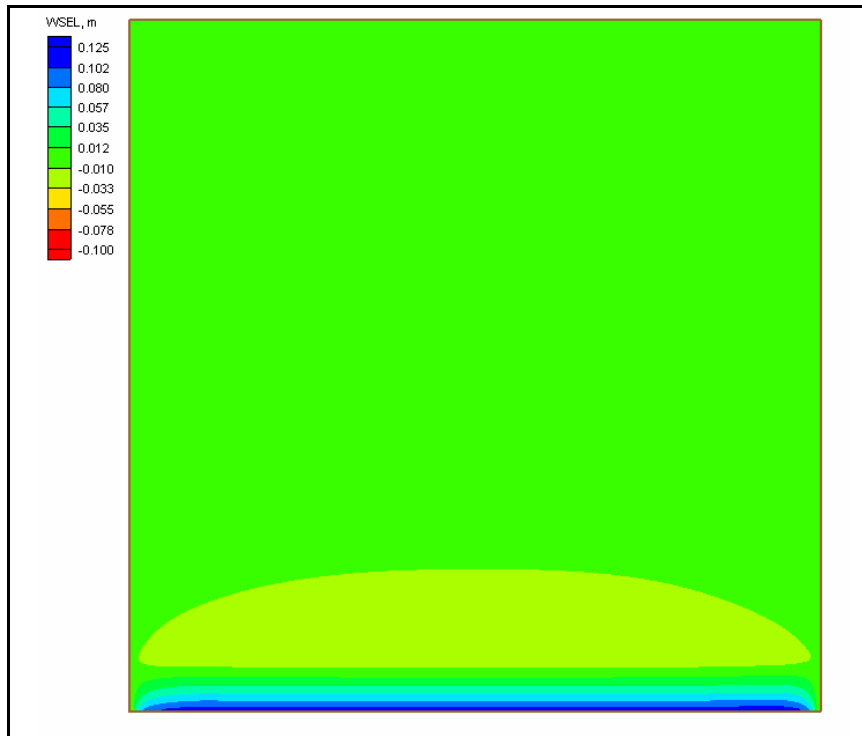


Figure G2. Water surface elevation calculated with standard water surface elevation boundary condition

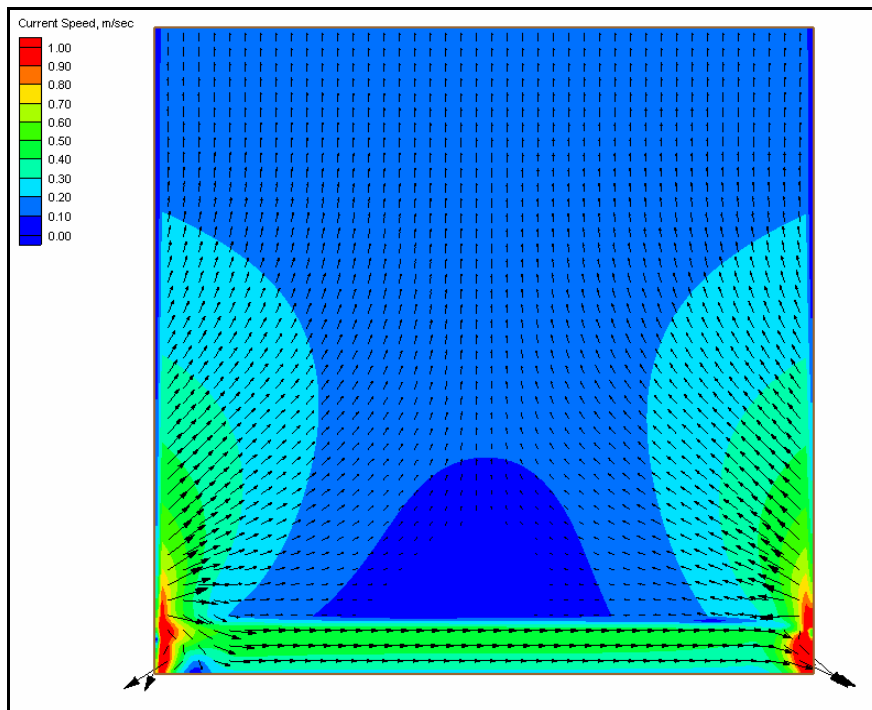


Figure G3. Velocity calculated with standard water surface elevation boundary condition

Water surface elevation and velocity as computed by the wave-adjusted boundary condition are shown in Figures G4 and G5, respectively. Setup is calculated at the shoreline and extends nearly uniformly across the entire grid. An alongshore current is well developed in the nearshore area, both near the lateral boundaries and away from them. Because the boundary conditions were adjusted for the presence of wave forcing, the circulation patterns are realistic. Water can flow onto and off of the grid along the lateral boundaries without incompatibility between the boundary condition and interior hydrodynamic processes.

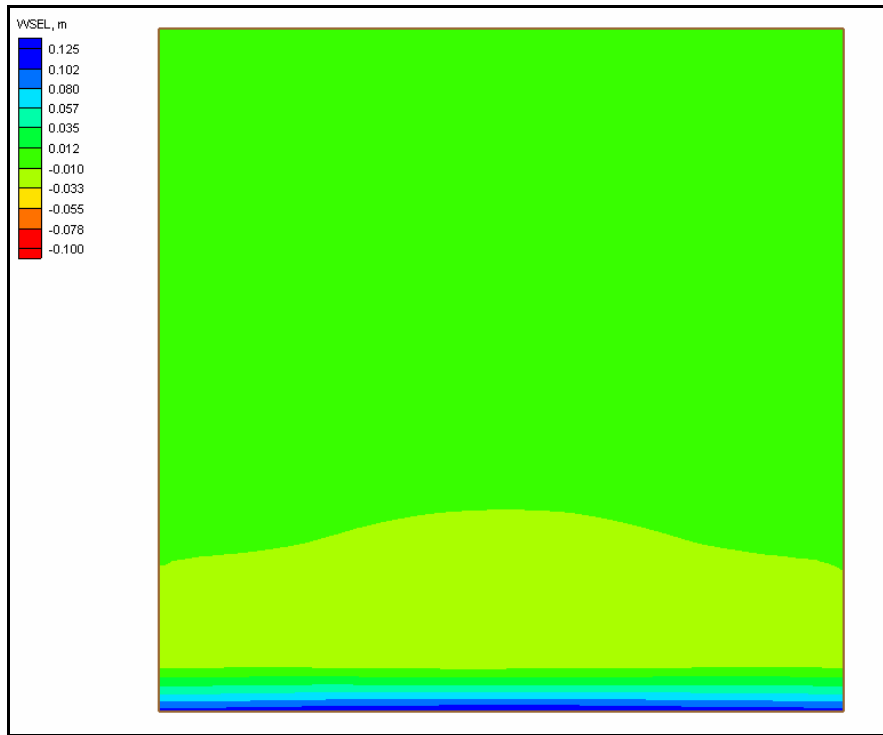


Figure G4. Water surface elevation calculated with wave-adjusted boundary condition

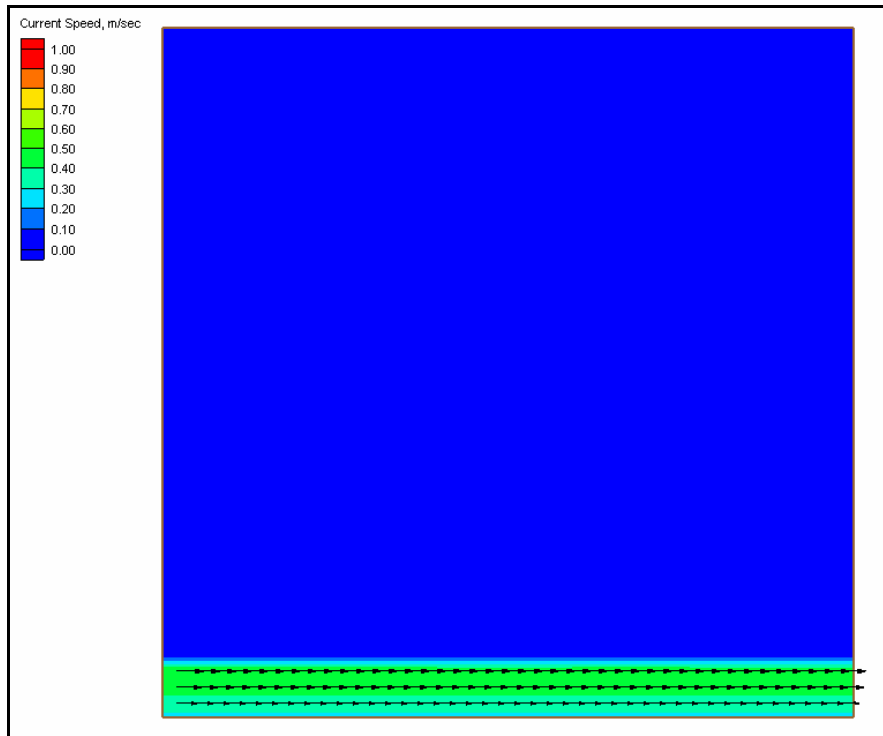


Figure G5. Velocity calculated with wave-adjusted boundary condition

# Appendix H

## Surf Zone Verification Tests

---

To verify M2D's response to wave forcing, calculations were compared to laboratory data collected by Visser (1982).<sup>1</sup> Because the laboratory experiments were conducted with monochromatic waves and the bathymetry was uniform alongshore, M2D was modified to include a 1-D monochromatic wave-transformation model. This model applies linear wave theory to compute wave transformation and computes wave height of depth-limited breaking and broken waves by the wave stability relationship of Dally et al.(1985). It also includes representation of the wave roller as described by Dally and Brown (1995) and Dally and Osiecki (1994). Water levels calculated by M2D are passed to the wave transformation model to allow waves to respond to the setup and setdown.

Larson and Kraus (2002) provide succinct descriptions of the wave stability relationship and roller model together with comparisons of calculated and measured longshore current, including comparisons to the Visser (1982) data, with and without the roller model. Their results demonstrate that inclusion of the roller momentum for calculation of the longshore current and wave setup increases accuracy. Without the roller momentum, peak longshore current was calculated to be seaward of the measured peak, whereas including the roller shifted the peak toward the beach and generally aligned it with the measured peak. This adjustment of the cross-shore distribution of the longshore current modified the setup with an increased setup with the roller as compared to without it.

Calculation of longshore current and setup are conducted for two of the Visser (1982) data sets, Cases 4 and 7. Wave properties for each case are listed in Table H1, and cross-shore profiles and roughness information are listed in Table H2. The major difference between these two cases is the bottom roughness. Case 4 was run on a smooth concrete bottom, whereas bottom roughness elements were introduced for Case 7, with the wave conditions held to be the same as much as possible. By choosing these two tests, performance of M2D in the surf zone over a great difference in bottom roughness can be demonstrated.

---

<sup>1</sup> All references cited in this appendix are included in the References section at the end of the main text.

<b>Table H1 Wave Properties at Offshore End of Basin and Breaker to Depth Ratio for Selected Visser (1982) Laboratory Experiments</b>				
<b>Case</b>	<b>Wave Height, m</b>	<b>Wave Period, s</b>	<b>Wave Angle, deg</b>	<b>Breaker to Depth Ratio</b>
4	0.076	1.02	19.9	0.83
7	0.078	1.02	18.4	0.74

<b>Table H2 Cross-Shore Profiles and Roughness Information for Selected Visser (1982) Laboratory Experiments</b>				
<b>Case</b>	<b>Distance Across Shore, m</b>	<b>Depth, m</b>	<b>Beach Slope<sup>1</sup></b>	<b>Bottom Roughness</b>
4	-0.472	-0.040	0.050	smooth
	7.328	0.350		
	8.253	0.350		
7	-0.472	-0.040	0.050	rough
	7.328	0.350		
	9.503	0.350		

<sup>1</sup> Beach slope calculated for sloping portion of basin.

Computational grids were developed for each bathymetric profile, and depths were uniform alongshore. For each grid, the cell spacing parallel with the alongshore direction ( $\Delta y$ ) was 0.10 m. Cell spacing parallel with the cross-shore direction ( $\Delta x$ ) was 0.01 m from the offshore boundary to approximately 1 m from the shoreline. Resolution was increased nearer to the shore to capture details of the setup calculation. As an example, resolution change for the Case 7 computational grid is shown in Figure H1.

Simulations were conducted with identical parameter settings and time-step, with the exception of the Manning roughness coefficient and the breaker-to-depth ratio for which settings were case dependent. The depth at which cells were specified as dry was 0.001 m and the time-step was 0.025 s. Breaker-to-depth ratios for each case are provided in Table H1. The Manning roughness coefficient, serving as an adjustment parameter, was set to 0.0125 for Case 4 and to 0.022 for Case 7, after numerical experimentation. Wave calculations proceeded shoreward until a minimum wave height of 0.001 m was reached.

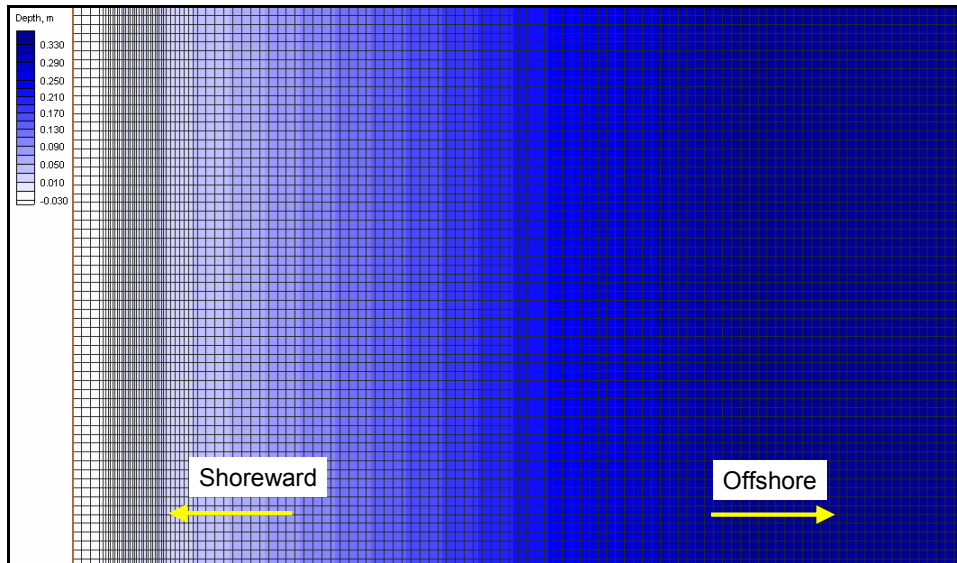


Figure H1. Detail of computational grid for Case 7 showing cross-shore variation in cell spacing

Comparison of measurements and calculations for wave height, longshore current speed, and setup for Case 4 are shown in Figures H2, H3, and H4, respectively. Calculated wave height compared well with measurements, except for the maximum wave height, which was underestimated by the wave-transformation model. The calculated breakpoint took place directly shoreward and nearly at the measured location.

Calculated longshore current speed well reproduced the distribution determined by the measurements (Figure H3). Peak current speeds compare well, with the calculated peak located directly seaward of the measured peak. Seaward of the breakpoint, calculated weakening of the longshore current closely follows the measured reduction in current.

Setup calculations also compare favorably to the measurements (Figure H4). The slope of the setup is slightly reduced in the calculations as compared to measurements, but the overall result indicates that the model is reproducing the wave-induced setup.

Comparison of calculated and measured wave height and longshore current speed for Case 7 (artificial roughness) are shown in Figures H5 and H6, respectively, and calculated setup is shown in Figure H7 (setup measurements are not available for Case 7). Calculated peak wave height underpredicts the measured peak wave height. However, because measured wave heights before breaking are not available, there is no indication of whether strong nonlinear shoaling took place. Calculated longshore current speed closely matches measurements over the peak and offshore reduction in speed.

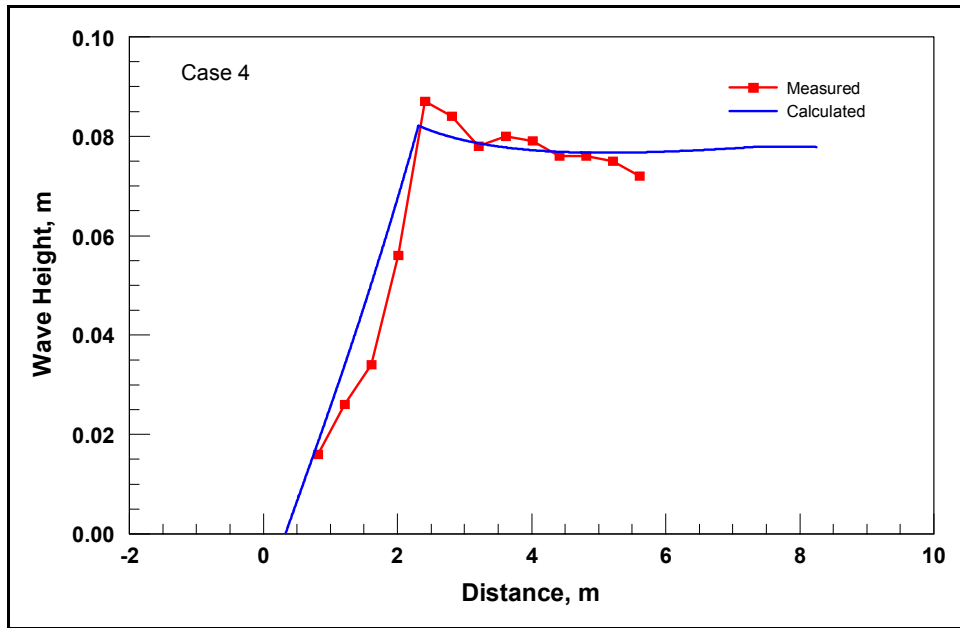


Figure H2. Wave height comparison for Case 4

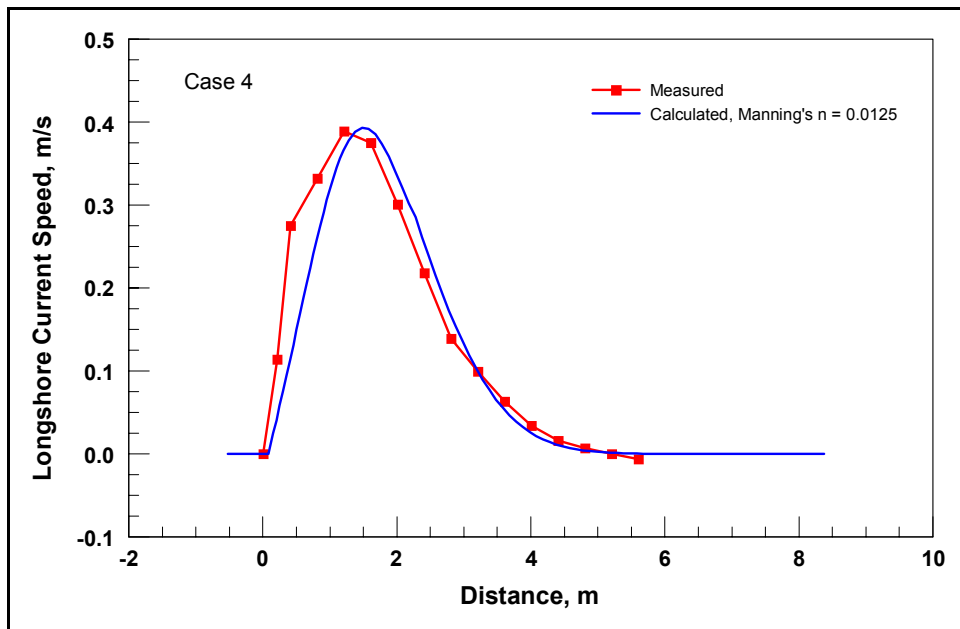


Figure H3. Longshore current comparison for Case 4

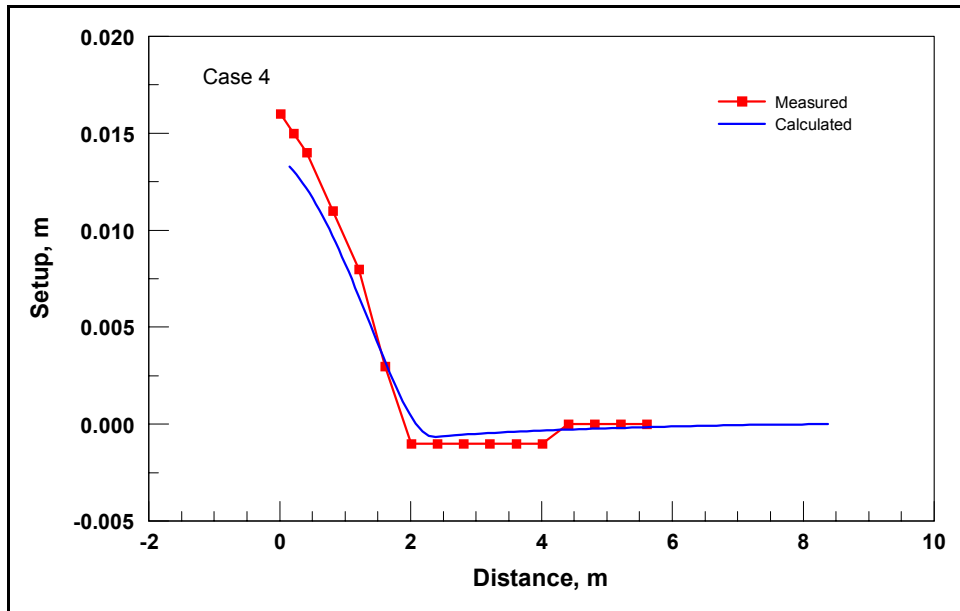


Figure H4. Wave-induced setup comparison for Case 4

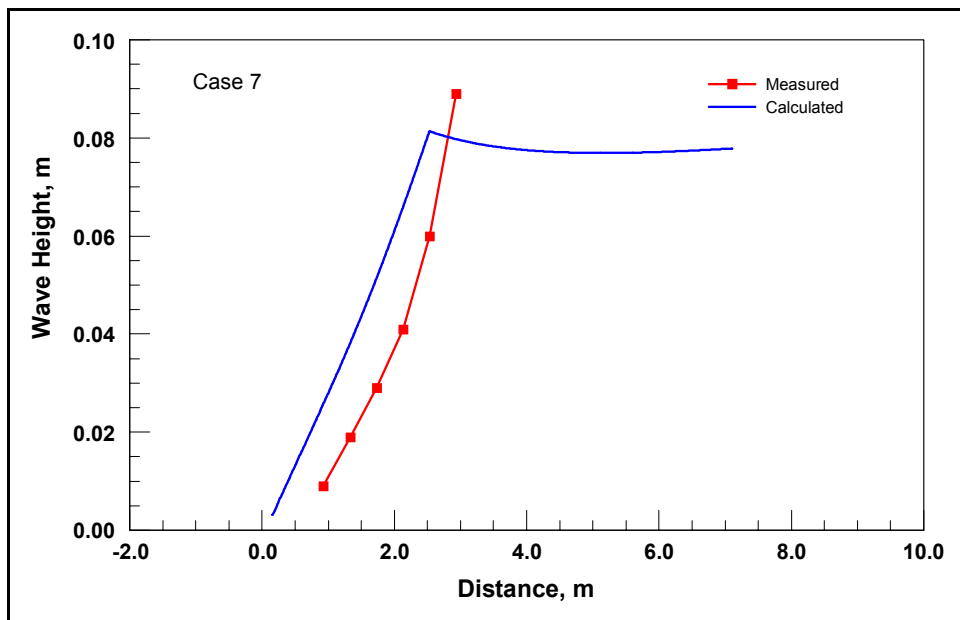


Figure H5. Wave height calculated by roller model for Case 7

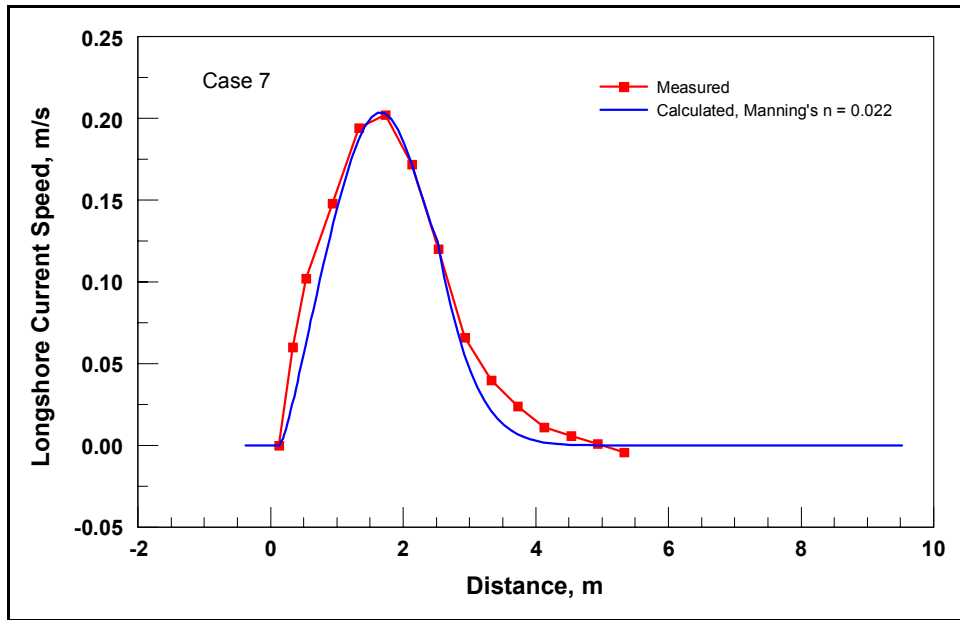


Figure H6. Longshore current calculated by M2D for Case 7

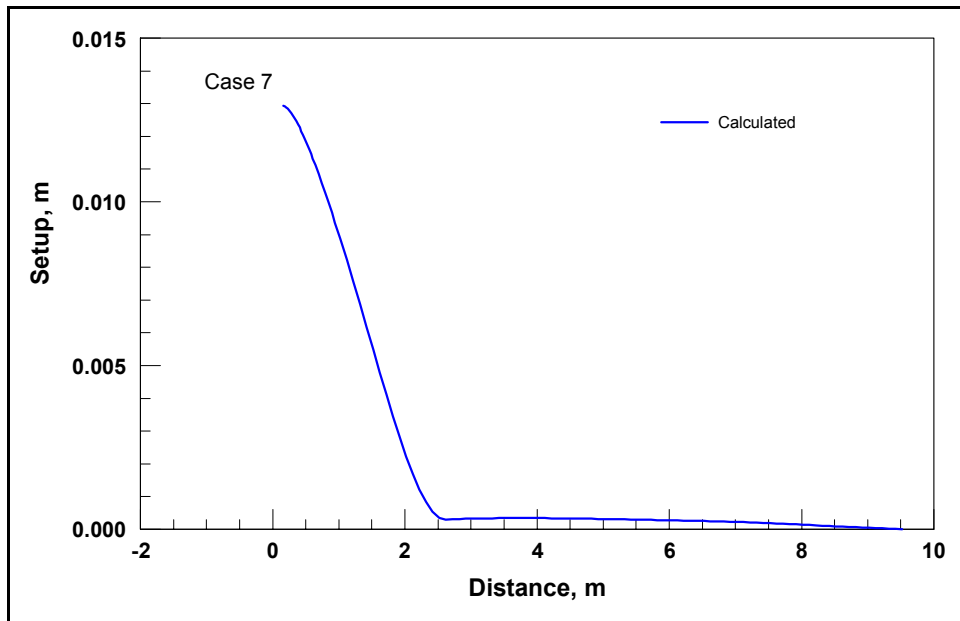


Figure H7. Wave-induced setup calculated by M2D for Case 7

In conclusion, calculations with M2D well reproduced the qualitative and quantitative features of accurate measurements of the longshore current in the laboratory. This test validates the overall equation solution scheme of the model and contributions of several terms, including the radiation stresses, bottom friction, and mixing.



#### **14. (Concluded)**

M2D can be driven by larger-domain circulation models, such as ADCIRC, through boundary specification capabilities contained within the SMS. The Steering Module in SMS provides an automated means of coupling of M2D with STWAVE, which is convenient for projects that require wave-stress forcing for M2D as well as wave friction and mixing owing to breaking waves. The Steering Module allows the user to choose from seven possible coupling combinations, providing flexibility in conducting simulations of wave-driven currents and wave-current interaction.